



City Research Online

City, University of London Institutional Repository

Citation: Jeyarupalingam, N. (1996). Steel, steel/concrete composite and reinforced concrete beams and columns exposed to fire. (Unpublished Doctoral thesis, City University London)

This is the accepted version of the paper.

This version of the publication may differ from the final published version.

Permanent repository link: <https://openaccess.city.ac.uk/id/eprint/7766/>

Link to published version:

Copyright: City Research Online aims to make research outputs of City, University of London available to a wider audience. Copyright and Moral Rights remain with the author(s) and/or copyright holders. URLs from City Research Online may be freely distributed and linked to.

Reuse: Copies of full items can be used for personal research or study, educational, or not-for-profit purposes without prior permission or charge. Provided that the authors, title and full bibliographic details are credited, a hyperlink and/or URL is given for the original metadata page and the content is not changed in any way.

City Research Online:

<http://openaccess.city.ac.uk/>

publications@city.ac.uk

STEEL, STEEL/CONCRETE COMPOSITE AND REINFORCED
CONCRETE BEAMS AND COLUMNS EXPOSED TO FIRE

by

Nadarajah Jeyarupalingam

Thesis submitted in fulfilment of the requirement for the award of
Degree of Doctor of Philosophy in Civil Engineering Structures

Structures Research Centre
Department of Civil Engineering
City University
London EC1V 0HB

February 1996

DEDICATION

To my late parents

SYNOPSIS

This thesis describes the development of a numerical method for the structural analysis of beams and columns subjected to a non-linear variation of temperatures in all three directions. The numerical method allows for analysis of a wide variety of cross sections with a number of materials and members with varying cross section along the length. The member can be subjected to any combination of axial load, end moments, lateral load and bi-axial bending. Any fire temperature characteristic can be specified. The numerical method has been validated by comparing results with a number of experimental results on steel, concrete and composite beams and columns from literature and with the experiments carried out under this research programme.

Experiments were carried out on seven columns with non-uniform temperature distribution along the length and across the depth. The test rig was designed and manufactured at City University. Electrical heating elements were used to heat the specimens. To obtain a comprehensive temperature profile of the test columns several thermocouples were used. Deflection measurements were made using displacement transducers placed at different positions.

Using the new method of analysis a simple design method for steel columns subjected to non-uniform temperature distribution across the depth of the section has been developed. The method has been validated with a number of results on H-section columns from numerical experiments performed using the computer programs developed in this thesis. Another parametric study has been carried out to improve the inherent fire resistance capacity of Slimflor beams. It is concluded that it is possible to design a Slimflor beam with higher fire resistance capacity than the current rating of 60 minutes by introducing steel reinforcing bars at appropriate place.

ACKNOWLEDGEMENT

The author wishes to express his gratitude to Professor K.S.Virdi, Director of Structures Research Centre, for supervising the work described in this thesis and for providing continuous guidance and constructive criticism.

I would also like to thank the technical staff at the Heavy Structures Laboratory, City University for their assistance in carrying out the experiments.

I would also like to thank Dr.G.M.E.Cooke of the Fire Research Station for advice on experimental work and allowing access to the FRS library to carry out literature search. It is gratefully acknowledged that heating elements and thermocouples were provided by the Fire Research Station for experimental work.

British Steel Plc. provided steel for the construction of rig and for test specimens. The author would like to thank Mr.J.Robinson and Mr.J.Dowling of British Steel for organising the supply of steel.

I am grateful to Mr. M.Lascells for patiently going through this thesis and suggesting corrections.

Last, but not least, I would like to thank my wife for her patience and continuous support to complete this work.

DECLARATION

I grant powers of discretion to the University Librarian to allow this thesis to be copied in whole or in part without further reference to me. This permission covers only single copies made for study purposes, subject to normal conditions of acknowledgements.

TABLE OF CONTENTS

Title Page	1
Dedication	2
Synopsis	3
Acknowledgement	4
Declaration	5
Table of Contents	6
List of Tables	12
List of Illustrations	13
1. INTRODUCTION	16
1.0 General	16
1.1 Fire Engineering Design Approach	16
1.1.1 Time - Temperature Response of Fire	17
1.1.2 Thermal Response of Structural Member	19
1.1.3 Structural Response	20
1.2 Objectives	21
1.3 Scope	21
2. REVIEW OF PREVIOUS WORK	24
2.0 Introduction	24
2.1 Mechanical Properties of Steel at Elevated Temperatures	24
2.1.1 Thermal Expansion of Steel With Temperature	24
2.1.2 Stress-Strain-Temperature Relationship of Steel	25
2.1.3 Creep	26

2.2 Mechanical Properties of Concrete at Elevated	27
2.2.1 Thermal Strain	27
2.2.2 Transient Strain	28
2.2.3 Stress-Strain-Temperature Relationship of Concrete	28
2.3 Previous Work on Steel Beams and Columns Exposed to Fire	29
2.3.1 Critical Temperature Method	29
2.3.2 Moment Capacity Method	30
2.3.3 Other Methods of Analysis of Steel Beams	31
2.3.4 Buckling of Steel Columns at Elevated Temperatures	32
2.3.5 Experimental Work on Steel Beams and Columns	33
2.4 Previous Work on Reinforced Concrete Beams and Columns	35
2.4.1 Analysis of Reinforced Concrete Beams	35
2.4.2 Analysis of Reinforced Concrete Columns	37
2.4.3 Experimental Work on Reinforced Concrete Beams and columns	37
2.5 Previous Work on Composite Beams and Columns	39
2.5.1 Analysis of composite Beams	39
2.5.2 Analysis of Composite Columns	40
2.5.3 Experimental Work on Composite Beams and Columns	41
2.6 Numerical Methods and Associated Computer Programs	42
2.7 Summary	46
3. THEORY	54
3.0 Introduction	54
3.1 Description of the Numerical Method	54
3.2 Moment-Thrust-Curvature Relationship	55
3.2.1 Gauss-Quadrature Integration Procedure	57
3.3 Calculation of the Equilibrium Deflected Shape	58
3.3.1 Formation of the Jacobian Matrix	60

3.4 Stability Calculations	64
3.5 Range of Applicability of the Proposed Method	64
3.6 Computer Program	65
3.6.1 Description of Computer Program SOSMEF	65
3.6.2 Capabilities of SOSMEF	66
3.6.2.1 Type of Analysis	66
3.6.2.2 Geometry Idealisation	67
3.6.2.3 End Conditions	68
3.6.2.4 Temperature Distribution	69
3.6.2.5 Material Properties	69
3.7 Summary	69
4. VALIDATION OF THEORY	72
4.0 Introduction	72
4.1 Steel Beams and Columns	73
4.1.1 Comparison With BSC Full Scale Simply Supported Beam Tests	73
4.1.2 Comparison With Model Beam Test By Cooke	74
4.1.3 Comparison With Full Scale Shelf Angle Floor Beam Test By BSC	74
4.1.4 Comparison With Column Tests by Aasen and Larsen	74
4.1.5 Comparison With Column Tests by Vandamme and Janss	75
4.1.6 Comparison with Arbed Column Test	76
4.2 Reinforced Concrete Beams and Columns	77
4.2.1 Comparison With Normal Weight Concrete Slab Tests	77
4.2.2 Comparison With Column Tests by Lie, Lin, Allen and Abrams	77
4.3 Steel/Concrete Composite Beams and Columns	78
4.3.1 Comparison With ARBED Composite Beam Test	78
4.3.2 Comparison With ARBED Composite Column Test	79
4.4 Summary	79

5. EXPERIMENTS ON STEEL COLUMNS WITH TEMPERATURE GRADIENTS	91
5.0 Introduction	91
5.1 Test Rig	92
5.2 Test Specimens and Preparations	92
5.3 Electrical Heating Elements and Thermal Insulation	93
5.4 Temperature Profile Measurement	94
5.5 Deflection Measurements	94
5.6 Loading Equipment and Axial Load Measurement	95
5.7 Data Recording	95
5.8 Test Procedure	95
5.9 Material Properties Test	99
5.10 Results	100
5.10.1 General Observations	100
5.10.2 Comparison of Computed and Experimental Results	100
5.11 Conclusions	103
6. APPLICATIONS	130
6.0 Introduction	130
6.1 Design of Steel Columns Subjected to Non-uniform temperature Distributions Across the Cross Section	130
6.1.1 Introduction	130
6.1.2 Design Method at Room Temperature	131
6.1.3 Design Method at Elevated Temperature	132
6.1.3.1 Proposed design method for buckling about the minor axis	134
6.1.3.2 Proposed design method for buckling about major axis	135
6.1.3.3 Validation of the design methods	137
6.1.4 Conclusions	138
6.2 Enhancement of Inherent Fire Resistance capacity of Slimflor Beams	139

6.2.1 Introduction	139
6.2.2 Proposed Method to Enhance Inherent Fire Resistance	140
6.2.3 Parametric Study	140
6.2.4 Calculations	141
6.2.5 Conclusions	144
7. CONCLUSIONS	149
7.0 Introduction	149
7.1 Review of Previous Work	149
7.1.1 Material Properties	149
7.1.2. Structural Analysis - Simple Calculation Models	150
7.1.3. Structural Analysis - Rigorous Calculation Models	150
7.1.4 Experimental Work	150
7.2 Numerical Method	151
7.2.1 Idealisation of Geometry	151
7.2.2 Material Properties	151
7.2.3 End Conditions	152
7.3 Validation and Experimental Work	152
7.3.1 Heating Arrangements	153
7.3.2 Instrumentation and Data recording	153
7.3.3 Results	153
7.4 Parametric Studies	154
7.4.1 1Design Method for Steel Columns	154
7.4.2 Parametric Study on Slimflor Beams	154
7.5 Summary	155
7.6 Further Research	155

REFERENCES	156
APPENDIX 1 -Example Output from Programs VIEW DATA and POSTPROCESSOR	167
APPENDIX 2 - Raw Experimental Data	173

LIST OF TABLES

Table 4.1	Comparison of Limiting Temperatures - Simply Supported Beam Tests	73
Table 4.2	Comparison of Limiting Temperatures - Column Tests by Aasen and Larsen	75
Table 4.3	Comparison of Limiting Temperatures - Column Tests by Vandamme and Janss	76
Table 5.1	Eccentricities of Test Columns	99
Table 5.2	Mid Span Initial Imperfection of Test Columns	99
Table 5.3	Material Property Test Results	99
Table 5.4	Comparison of Axial Load Capacities of Tested Columns	102
Table 6.1	Cross sectional and Buckling Length details of Columns Analysed	138
Table 6.2	Calculated Temperatures at Points 1 to 4	138
Table 6.3	Different Types of Slimflor Beams	139
Table 6.4	Results of Type 2 Slimflor Beams	143
Table 6.5	Results of Type 3 Slimflor Beams	144

LIST OF ILLUSTRATIONS

Figure 1.1	Standard Fire Curve	23
Figure 1.2	Time - Temperature Curves for Different Fire Loads	23
Figure 2.1	Thermal Elongation of Steel	48
Figure 2.2	General Stress-Strain Diagram of Steel	49
Figure 2.3	Vraiation of Parameters with Temperature	49
Figure 2.4	Comparison of Stress-Strain Curves-Grade 50 Steel	50
Figure 2.5	Components of Total Strain of Concrete	50
Figure 2.6	Thermal Expansion of Concrete	51
Figure 2.7	General Stress-Strain Diagram of Concrete	51
Figure 2.8	Reduction of Ultimate strength with Temperature	52
Figure 2.9	Comparison of Eurocode and NRCC Model	52
Figure 2.10	Types of Composte Beam Cross Sections	53
Figure 2.11	Types of Composte Column Cross Sections	53
Figure 3.1	Cross Section	69
Figure 3.2	Natural Co-ordinate System of a Quadrilateral	70
Figure 3.3	Idealisation of a Member	70
Figure 3.4	Idealisation of Different Cross sections	71
Figure 4.1	Comparison of Results - Model Beam Test	80
Figure 4.2	Comparison of Results - Shelf Angle Floor Beam Test	80
Figure 4.3	Comparison of Results - Arbed Column Test	81
Figure 4.4	Cross Section and Test Arrangement Details of Slabs	81
Figure 4.5	Comparison of Temperatures	82
Figure 4.6	Comparison of Deflections - Non-loaded Slab	83
Figure 4.7	Comparison of Deflections - Loaded Slab	84
Figure 4.8	Cross Section and Test Arrangement Details	85
Figure 4.9	Comparison of Temperatures - 305x305 mm Column	86
Figure 4.10	Comparison of Temperatures - 203x203 mm Column	87

Figure 4.11	Comparison of Deflections - 305x305 mm Column	88
Figure 4.12	Comparison of Deflections - 203x203 mm Column	88
Figure 4.13	Comparison of Results - ARBED Composite Beam	89
Figure 4.14	Comparison of Results - ARBED Composite Column	90
Figure 5.1	Schematic Diagram of Test Rig	103
Figure 5.2	Electrical Heating Element	104
Figure 5.3	Arrangement of Heating Element and Insulation	104
Figure 5.4	Thermocouple Positions	104
Figure 5.5	Device to hold Thermocouples in Position	105
Figure 5.6.	Displacement Transducer Positions	105
Figure 5.7	View of the Deflection Transducers	106
Figure 5.8	View of Hydraulic Jack End of the Rig	106
Figure 5.9	View of Load Cell End of the Rig	107
Figure 5.10	General View of the Experimental Rig	107
Figure 5.11	Cross Section Dimensions of Test Columns	108
Figure 5.12	Variation of Axial Load With Time For Test 1	108
Figure 5.13	Temperature Distribution of Columns at Failure	109
Figure 5.14	Failed Columns - View 1	110
Figure 5.15	Failed Columns - View 2	111
Figure 5.16	Variation of End Rotations With Time For Test 1	112
Figure 5.17	Variation of End Rotations With Time For Test 2	112
Figure 5.18	Variation of End Rotations With Time For Test 3	113
Figure 5.19	Variation of End Rotations With Time For Test 4	113
Figure 5.20	Variation of End Rotations With Time For Test 5	114
Figure 5.21	Variation of End Rotations With Time For Test 6	114
Figure 5.22	Variation of End Rotations With Time For Test 7	115
Figure 5.23	Comparison of Deflected Shape - Test 1	116
Figure 5.24	Comparison of Axial Deflection - Test 1	117
Figure 5.25	Comparison of Central Deflection - Test 1	117
Figure 5.26	Comparison of Deflected Shape - Test 2	118

Figure 5.27	Comparison of Axial Deflection - Test 2	119
Figure 5.28	Comparison of Central Deflection - Test 2	119
Figure 5.29	Comparison of Deflected Shape - Test 3	120
Figure 5.30	Comparison of Axial Deflection - Test 3	121
Figure 5.31	Comparison of Central Deflection - Test 3	121
Figure 5.32	Comparison of Deflected Shape - Test 4	122
Figure 5.33	Comparison of Axial Deflection - Test 4	123
Figure 5.34	Comparison of Central Deflection - Test 4	123
Figure 5.35	Comparison of Deflected Shape - Test 5	124
Figure 5.36	Comparison of Axial Deflection - Test 5	125
Figure 5.37	Comparison of Central Deflection - Test 5	125
Figure 5.38	Comparison of Deflected Shape - Test 6	126
Figure 5.39	Comparison of Axial Deflection - Test 6	127
Figure 5.40	Comparison of Central Deflection - Test 6	127
Figure 5.41	Comparison of Deflected Shape - Test 7	128
Figure 5.42	Comparison of Axial Deflection - Test 7	129
Figure 5.43	Comparison of Central Deflection - Test 7	129
Figure 6.1	Column Exposed to Fire on One Flange	145
Figure 6.2	Idealisation of Section	145
Figure 6.3	Variation of Failure Load With Eccentricity	146
Figure 6.4	Comparison of Results - Minor Axis Buckling	146
Figure 6.5	Comparison of Results - Major Axis Buckling	147
Figure 6.6	Different Types of Slim Floor Construction	147
Figure 6.7	Types of Slimflor Beam	148
Figure 6.8	Cases Analysed	148

CHAPTER 1

INTRODUCTION

1.0 General

Landmarks in the history of structural fire protection, start with the Great Fire of London in 1666^[1]. However, according to Malhotra^[1], the scientific approach to research into structural fire resistance began with the establishment of the British Fire Protection committee at the end of the 19th century. The first British Standard (BS476), aimed at standardising fire resistance tests, was published in 1932^[2]. BS476 was then revised in 1953^[3], 1972^[4] and in 1987^[5] based on research in the UK and other countries.

The traditional way of establishing the fire resistance of a structural member is to perform an expensive full scale test according to BS476:Part 20^[5] or a similar standard such as ISO 834^[6]. Recently, British standard BS5950:Part 8^[7], describing calculational methods for the fire engineering design of steel structural members, was published. European codes for concrete members^[8], steel members^[9] and composite members^[10] are still in the form of draft documents. These documents describe simple methods of assessing the fire resistance of a structural member by calculation. Compared to the methods available for the design of structural members at room temperature, these methods are elementary. This shows the need for further development in this field.

1.1 Fire Engineering Design Approach

The term Fire Engineering Design may be defined as solving a design problem in the event of a fire by means of established methods of calculations. This is an alternative to the way of solving the problem by expensive full scale tests. In this sense, this approach to the design of structures for the fire limit state aims to achieve the same level of sophistication, as the current methods for the design of structures for ultimate limit state.

The procedure for the fire engineering design of structures may be divided into three major stages as follows.

- ✘ Time - Temperature response of fire.
- ✘ Thermal response of structural elements.
- ✘ Structural response of structural elements.

These three stages of calculations can be considered independently. In other words, the second stage of calculations only needs the final result of the first stage, the third stage of calculations only needs the final results of the second stage. The term *fire engineering* might be interpreted differently by different people related to their expertise in the above three subjects^[11]. However, to understand the behaviour of a structure in the event of a fire, it is necessary to solve all three stages of the problem.

1.1.1 Time - Temperature Response of Fire

International standards for fire resistance tests give a standard fire curve for the Time-Temperature response of a fire. BS476:Part 20^[5], ISO 834^[6] and European codes^[8,9,10] define the standard fire curve by the following equation.

$$T - T_0 = 345 \log_{10}(8t+1) \quad (1.1)$$

where,

t = Time from the start of the test in minutes

T = Temperature of fire at time t in °C

T₀ = Initial temperature in °C

Graphical representation of Equation 1.1 is shown in Figure 1.1.

It is well known that a natural fire rarely follows a standard fire curve. A natural fire depends on many factors, some of which are:

- ✘ Fire load density
- ✘ Size of compartment
- ✘ Size of ventilation openings
- ✘ Thermal properties of surrounding material.

A detailed review of how these factors affect the fire severity in a compartment can be found in literature^[1,12,13,14,15]. Pettersson, Magnusson and Thor^[15] have provided tables and equations to calculate the Time-Temperature response of a fire, based on specified fireload. A typical set of such fire curves is shown in Fig. 1.2.

The *Equivalent fire severity* concept was developed to relate the behaviour of a natural fire to an equivalent period of the standard fire curve. Kirby^[12] gives an empirical formula for the equivalent fire resistance period which is given in equation 1.2.

$$t_e = 0.067q \left[\frac{A_t}{A_v \sqrt{h}} \right]^{1/2} \text{ minutes} \quad (1.2)$$

where,

t_e = Equivalent fire resistance period

q = Fire load density of bounding surface (MJ/m²)

A_v = Area of vertical openings (m²)

A_t = Area of walls and ceiling excluding the openings (m²)

h = Height of the opening (m)

The value of q may be calculated by considering all the combustible materials in the compartment or may be obtained from statistical data^[16]. Values of A_v , A_t and h can be calculated from the geometry of the compartment.

Although it is impossible to predict each and every possible fire in a compartment, it can be said that a reasonable estimate can be made, for design purposes, by either predicting the natural fire Time-Temperature response or an equivalent fire resistance period using available empirical formulae.

1.1.2 Thermal Response of Structural Member

Calculation of the thermal response of structural elements exposed to fire is essentially a solution of the heat transfer problem. The three types of heat transfer are:

- ✘ Conduction
- ✘ Convection
- ✘ Radiation

In general, the heat transfer from hot gas to structural elements is a combination of all three types of heat transfer. Data needed for a heat transfer calculation are material properties such as conductivity, specific heat and the convection and radiation boundary conditions. Guidance on these data may be obtained from Parts 10 of draft Eurocodes 2^[8] and 3^[9].

An alternative approach to solving the heat transfer problem is to do a rigorous analysis such as a finite element analysis. There are computer programs available based on finite element methods such as TASEF-2^[17], FIRES-T3^[18], TEMP^[19], CEFFICOS^[20]. Hertz^[21] developed an analytical method for the calculation of temperature profiles in reinforced concrete cross sections, but this method is limited to rectangular cross sections. There are other solutions^[22,23] available using the finite element and finite difference methods for the temperature calculation problem.

In addition to the rigorous analytical methods and computer programs, there are several simple calculation methods^[9,14,24,25,26] available for calculating the temperature distribution in steel members exposed to fire. In these methods, it is generally assumed that the steel has infinite conductivity so that the temperature across the whole cross section will always be uniform. Although this assumption is not strictly correct, it yields reasonable results for both protected steel members and for bare steel members exposed to fire on all four sides.

Draft Eurocode 2:Part 10^[8] provides temperature profiles of standard concrete cross sections, in tabular form, at specified times (e.g.. 30,60,90 minutes etc.) when exposed to a standard fire.

From the above discussion, it is clear that there are rigorous and simple models available for the calculation of temperatures in a structural member exposed to fire. However, there are still uncertainties in assuming the boundary condition values for emmissivity, conduction coefficient and convection parameters. A detailed study of these is beyond the scope of this thesis.

1.1.3 Structural Response

Once the temperature distribution history of the structural element is calculated, the next step is to calculate the structural response. Structural response calculations may be carried out in two ways, which are:

- ✘ Calculate the failure time for a given fire load.
- ✘ Calculate the failure load for given time (Temperature distribution).

In structural response calculations, as in the room temperature calculations, the equilibrium of the structure must always be satisfied at any statge. Change in material properties, such as thermal strain and stress-strain relationship, with temperature also should be taken into account.

A comprehensive review of the available methods for calculating structural response is given in Chapter 2. A new method of analysis for columns and beams exposed to non-uniform heating under fire forms the key part of this thesis.

1.2 Objectives

The objectives of this research are:

- ✎ To develop a rigorous numerical method for the structural analysis of beams and columns subjected to elevated temperature distributions such as encountered in the event of a fire.
- ✎ To develop a user friendly computer program based on the above mentioned numerical method.
- ✎ To obtain experimental data on the behaviour of pin-ended steel columns subjected to temperature variation across the depth and along the length.
- ✎ To verify the numerical method developed and the associated computer program, using the experimental data obtained, and using other experimental data available in literature.
- ✎ To demonstrate the applications of the numerical method in developing design aids.

1.3 Scope

A critical review of the literature on the subject is presented in Chapter 2. The new numerical method developed is described in Chapter 3. Capabilities and limitations of the associated computer program are also discussed in that chapter. Validation of the new numerical method is given in Chapter 4. In this chapter, comparison of computed results with a number of experimental data available in literature is presented.

Chapter 5 describes the details of seven experiments performed at the Structures Laboratory of City University. Electrical heating elements were used to heat the test specimen. A number of thermocouples were used to obtain accurate temperature profiles across the depth and along the length of all the test specimens. Results of the experiments and a comparison of experimental and computed results are also presented in this chapter.

Chapter 6 describes the applications of the numerical method and its associated computer program. A study on the Slimflor floor system aimed at improving its inherent fire resistance capacity is presented. A simple design method for the analysis of steel columns subjected to a non-uniform temperature distribution across the section is also presented in this chapter. Conclusions with recommendations for future research work are presented in Chapter 7.

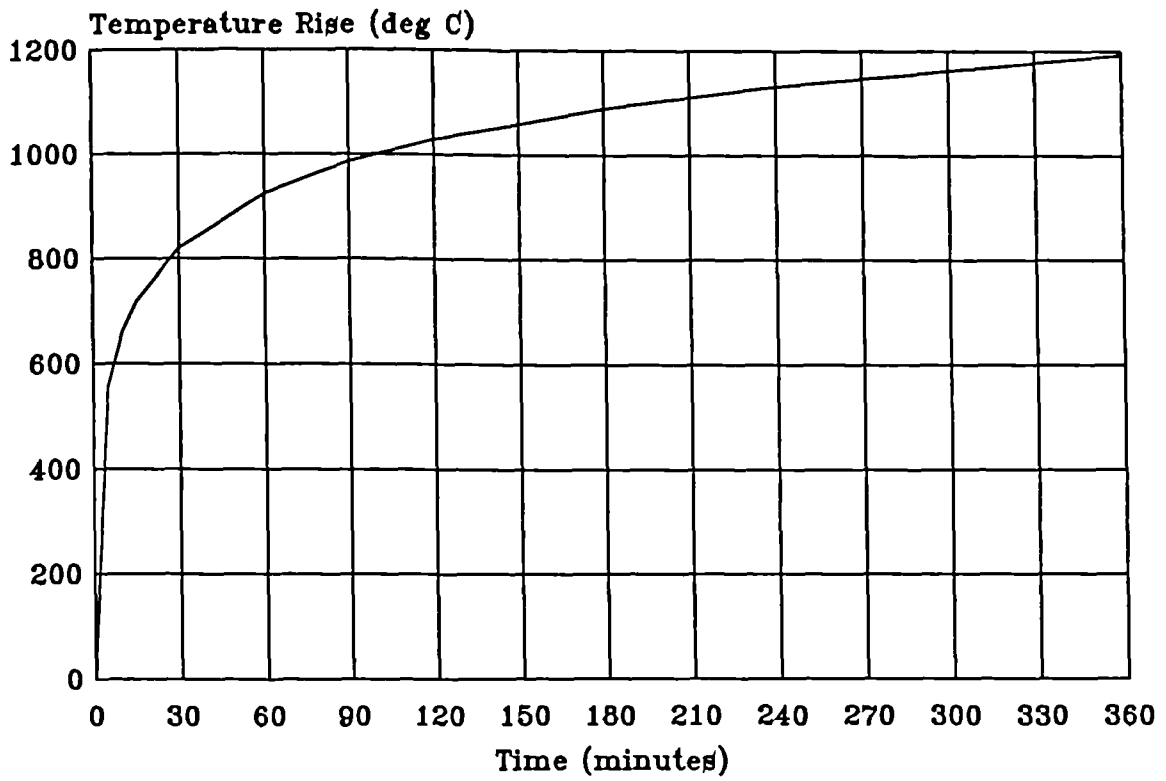


Figure 1.1 Standard Fire Curve

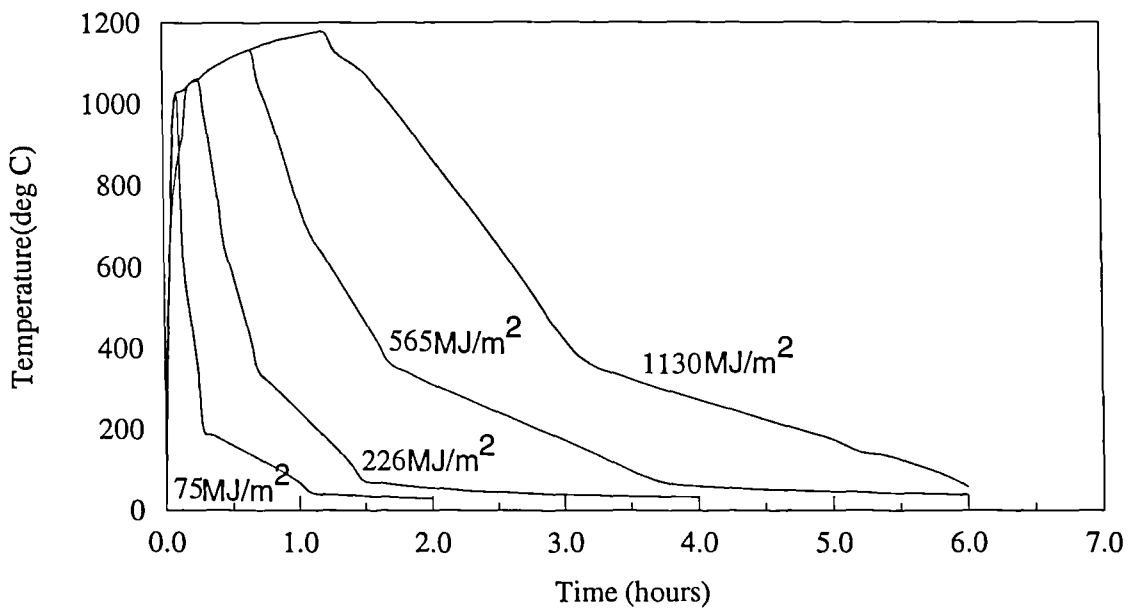


Figure 1.2 Time-Temperature Curves for Different Fire Loads

CHAPTER 2

REVIEW OF PREVIOUS WORK

2.0 Introduction

In this chapter, previous studies on structural response calculation methods are reviewed. To understand the structural response, it is essential to have a clear understanding of the mechanical properties of the materials used. Therefore, studies on material properties at elevated temperatures are reviewed before the studies on structural response calculation methods.

2.1 Mechanical Properties of Steel at Elevated Temperatures

Mechanical properties of steel at room temperature are well understood. However, with the increase of temperature, steel loses both its strength and its well defined yield point at room temperature. In addition, thermal and creep strains also occur.

2.1.1 Thermal Expansion of Steel With Temperature

When a material is heated, its length increases. It is usually assumed that for metals the increase in length is directly proportional to the increase in temperature. It can be written in mathematical form as follows.

$$L_T = L_o(1+\alpha T) \quad (2.1)$$

where,

L_T = Length after temperature rise of T

L_o = Initial length

α = A constant

The coefficient α is called the *Coefficient of Thermal Expansion* of the material. Equation 2.1 represents the thermal expansion behaviour of steel with reasonable accuracy up to approximately 700°C. In the region of approximately 700 - 800°C shrinkage in steel instead of expansion with an increase of temperature can be observed. Expansion continues after approximately 800°C. This sudden change in behaviour is explained by the Phase Transformation phenomenon^[27]. Phase Transformation is the process of change in the atomic structure of the steel. From experimental data, Cooke^[27] idealised the thermal expansion behaviour of structural steel with a Tri-linear curve. A similar expression for Thermal strain - Temperature relationship is given in Eurocode 3:Part 10^[9]. Both of these relationships are shown in Figure 2.1. For calculation purposes, the expression given by Eurocode 3 has been used in this thesis, unless otherwise stated. Eurocode 3 also gives a constant value to use, as an alternative to the non-linear expression.

2.1.2 Stress-Strain-Temperature Relationship of Steel

At room temperature the stress-strain relationship of steel is usually defined by a bi-linear curve with a clearly defined yield point. As the temperature increases, the stress-strain curve becomes smoother and the well defined yield point vanishes. With no clearly defined yield point, the concept of proof stress is used to define the yield stress at elevated temperatures^[28]. Possible bi-linear and tri-linear idealisations for the stress-strain relationship at elevated temperatures are given by Cooke^[28].

A more precise idealisation of stress-strain curves at elevated temperatures was proposed by Anderberg^[29]. In his analytical model, the curve is divided into three parts. The first and third parts of the curve are linear and the second part is an elliptic curve. This curve represents more accurately the behaviour of steel at elevated temperatures. This model is the basis of the recommended stress-strain-temperature relationship given in Eurocode 3^[9]. Eurocode 3^[9] defines the stress-strain-temperature curves in three parts

as shown in Figure 2.2. The variations in elastic modulus and yield strength recommended by Eurocode 3 are shown in Figure 2.3.

A set of multi-linear stress-strain-temperature curves proposed by Kirby and Preston^[33], based on transient state test results, is recommended in BS5950:Part8^[7]. As these multi-linear stress-strain-temperature data are tabulated in a non-dimensional form, the modulus of elasticity will vary within the elastic range with the yield stress of the material. Although this is not exactly correct, the error in structural analysis calculations is likely to be negligible. A comparison between BS5950 and Eurocode 3 curves at selected temperatures is shown in Figure 2.4. From this figure it can be concluded that both Eurocode 3 and BS5950 recommended curves are effectively the same.

Another analytical model for the stress- strain-temperature relationship is to use a modified form of the Ramberg and Osgood equation^[30]. Olawale and Plank^[31] have given the values of the parameters used to define these curves using the Ramberg and Osgood equation.

For calculation purposes, the stress-strain-temperature relationship recommended in Eurocode 3 has been used in this thesis, unless otherwise stated.

2.1.3 Creep

At elevated temperatures, in addition to thermal strain and stress induced strain, creep strain also occurs. A comprehensive analytical model for creep was proposed by Harmathy^[32]. Including creep in analytical structural analysis models increases the complexity of calculation. As the creep strain is small, it can be included approximately in the stress-strain-temperature relationship without losing accuracy. The stress-strain curves given in Eurocode 3 and BS5950 approximately include the effect of creep at elevated temperatures.

2.2 Mechanical Properties of Concrete at Elevated Temperatures

Mechanical properties of concrete are much more variable than those of steel. Accordingly, there is less agreement as to the characteristics to be adopted in design and analysis. Properties of concrete depend on many factors, such as:

- ✘ Size and type of aggregate
- ✘ Age and curing prior to heating and loading
- ✘ Moisture contents
- ✘ Stress history
- ✘ Temperature history

Total strain of concrete at elevated temperatures may be considered to consist of four components, which are:

- ✘ Thermal strain
- ✘ Transient strain
- ✘ Instantaneous stress related strain
- ✘ Creep strain

Anderberg and Thelandersson proposed a constitutive model for all four components of the total strain, for siliceous concrete, based on their comprehensive experimental and theoretical research work^[34,35]. Figure 2.5 shows the contribution of the above mentioned four components to the total strain with temperature.

2.2.1 Thermal Strain

The thermal strain of concrete depends mainly on the type of aggregate used. Generally, the thermal expansion increases with increasing contents of quartz in the aggregate^[34]. Eurocode 2^[8] classifies concrete into two categories, as siliceous and calcareous, based on the type of aggregate used in the concrete. Graphical representation of the thermal expansion data given in Eurocode 2, for both siliceous and calcareous concrete, is shown in Figure 2.6.

2.2.2 Transient Strain

Thermal expansion of concrete reduces with the increase of compressive stress in the specimen. The difference between the thermal strain of unloaded concrete and the thermal strain of loaded concrete is called Transient strain. The transient strain may be regarded as a hindered part of the thermal strain of the loaded concrete specimens exposed to heating^[36]. The transient strain is found to be proportional to the ratio between the compressive stress and the compressive strength of the concrete at room temperature. Furthermore, it is proportional to the thermal expansion^[35].

2.2.3 Stress-Strain-Temperature Relationship of Concrete

There are a number of stress-strain-temperature relationships for concrete available in the literature^[8,35,36,37,38,39]. Of these relationships, the one specified in Eurocode 2^[8] and the one proposed by Lie, Lin, Allen and Abrams^[37] (hereafter called the NRCC model) include the effect of creep in an approximate way. As this type of relationship is more suitable for incorporating into the numerical method described in Chapter 3, both of these relationships are used in this thesis for calculational purposes.

The general stress-strain diagram at elevated temperature, according to Eurocode 2, is shown in Figure 2.7. The reduction of ultimate strength with temperature, according to Eurocode 2, is shown in Figure 2.8. A comparison of stress-strain curves at selected temperatures, according to Eurocode 2 and the NRCC model, is shown in Figure 2.9. This comparison shows that the ascending parts of the curves of both models are close to each other, but the descending parts of the curves of both models differ greatly. Eurocode 2 permits either the linear or non-linear descending branch but fails to give any specific details of the non-linear relationship.

2.3 Previous Work on Steel Beams and Columns Exposed to Fire

2.3.1 Critical Temperature Method

It is usually assumed, for simplicity, that the temperature distribution across the section and along the length of a steel member is uniform. This assumption is reasonable for protected members and for bare members exposed to fire on all sides. On the basis of the above mentioned assumption, one can calculate the temperature at which the structural member will fail under given loading conditions. This temperature is called the *Critical Temperature*. It is also known as the *Collapse Temperature* or the *Limiting Temperature*. Designers then ensure that the structural element will not experience a temperature greater than the critical temperature during the required fire resistance period, by providing enough protection if necessary. This forms the basis of one of the design methods in Eurocode 3: Part 10^[9].

Although it is possible to calculate the critical temperature by means of structural analysis calculations, it is traditionally assumed to be 550°C. This value of 550°C for critical temperature was deduced from early fire tests which showed that around this temperature beams and columns failed under working load^[27]. Manufacturers of fire protection materials, such as sprayed mineral wool and fire protection boards, specify the thickness of the material required for different fire resistance periods^[40]. These specifications are based on the protected steel reaching the critical temperature of 550°C.

A more scientific approach of determining the critical temperature would be to calculate it using structural analysis principles, rather than assuming a fixed value such as 550°C. Several methods are available to calculate the critical temperature of a steel member. Kruppa^[41] and Rubert and Schaumann^[42] described simple methods of determining critical temperatures of steel beams and columns. BS5950:Part8^[7], AISC Guidelines^[43] and Eurocode 3:Part 10^[9] give expressions for the critical temperature of a steel member as a function of load ratio (i.e., Ratio of applied load to the load capacity of the member at room temperature). All these methods mentioned above do not take into account any

additional loading that the member could be subjected to, arising from restraint from other adjacent structural members.

Bennetts et al. carried out an analytical study on the effect of the restraint of compression members in fire^[44]. An analytical method, based on conservative assumptions, was presented for predicting the restraint forces the member will be subjected to in case of a fire occurring only in the compartment where the member under consideration is situated. It is concluded that a small reduction in critical temperature, calculated considering the member as an isolated member, is necessary to compensate for the presence of restraint forces.

The main problem in using the critical temperature concept is the assumption of uniform temperature distribution. In practice there are many cases in which the temperature distribution will not be uniform in the event of exposure to fire. Some examples of such cases are listed below.

- ✘ Columns partly built in to walls
- ✘ Shelf angle floor beams
- ✘ Columns with blocked webs

In these cases the temperature gradients across the section are significant and the concept of critical temperature becomes invalid.

2.3.2 Moment Capacity Method

The moment capacity method is only applicable to beams. The advantage of this method over the critical temperature concept is that the variation of temperature across the section can be allowed. This method is also applicable to reinforced concrete and steel/concrete composite beams. The method involves calculating the plastic moment capacity of the section and checking whether the capacity is sufficient to support the applied load. As the name implies this method is based on calculating the maximum load carrying capacity of the beam at the fire limit state.

If the temperature distribution is uniform through the cross section the calculation method is similar to the plastic moment capacity calculation at room temperature except that the value of the yield stress to be used has to be related to the relevant temperature.

If the temperature distribution is non-uniform, then the section may be divided into several strips having a uniform temperature within each strip. The moment capacity may be calculated using the applicable yield stress of the strips, corresponding to their temperature. This method is included in BS5950: Part 8^[7]. Newman^[45] has described this method in detail, with examples for composite slabs.

2.3.3 Other Methods of Analysis of Steel Beams

The methods of analysis described in previous sections are easy to use and do not involve any deflection calculations. Methods described in this section are more rigorous and also predict the deformation history of the beam.

When a structural member is subjected to non-uniform heating across its cross section, the member deforms due to differential thermal expansion. This deformation with zero external loads is called *thermal bowing*. Cooke and Morgan^[46] showed the importance of thermal bowing in the design of structures. Cooke^[27] derived a simple formula to calculate the thermal bowing displacement of a member subjected to a linear variation of temperature across the section, based on geometry. Gatewood^[47] derived expressions for thermally induced stresses and displacements. Both of these methods are only applicable within the elastic range.

Harmathy^[48] proposed a numerical technique for the calculation of the creep deflection of beams. Cheng^[49] also placed more emphasis on creep and presented a finite element formulation of thermo-creep deformation and creep buckling analysis of steel structures. As discussed in Section 2.1.2, creep in structural steel is small and can be incorporated approximately into the stress-strain-temperature relationship without much loss of accuracy in structural analysis calculations.

Plank^[50] developed a simple method to determine the deformation history of a steel beam exposed to fire until failure. This method is only applicable for simply supported steel beams. Contro, Poggi and Cazzani^[51] presented a finite element model for the analysis of steel beams exposed to fire. Both of the above mentioned methods allow for a non-linear temperature distribution across the section and assume a simplified bilinear stress-strain relationship for steel at elevated temperatures.

Thor^[52] developed a numerical method which uses a more accurate model for the stress-strain relationship, obtained experimentally. Skowronski^[53] proposed an analytical method to predict the deformation of steel beams exposed to fire, based on the Mohr's integral generalised over non-elastic materials. This method is only applicable to beams with linear variations of temperature across the section. Burgess, El-Rimawi and Plank^[54] proposed a numerical method based on the secant stiffness approach to analyse beams at elevated temperatures. Later, the method was extended to analyse beams subjected to non-linear variations of temperature across the section^[55]. The above mentioned methods^[53,54,55] use a more accurate model for the stress-strain relationship of steel at elevated temperatures by using the Ramberg-Osgood equation. Although these methods allow for a non-linear variation of temperature across the section of the beam, it is assumed that the temperature is constant along the length of the beam.

2.3.4 Buckling of Steel Columns at Elevated Temperatures

An early theoretical treatment of steel columns subjected to elevated temperatures was reported by Culver^[56]. He used the finite difference method to calculate the buckling load of a column. The method allows for a thermal gradient along the length but assumes that the temperature is constant across the section. Culver, Aggarwal and Ossenbruggen^[57] then developed simple approximate formulae to calculate the buckling stresses of steel columns subjected to a uniform temperature distribution. The

same authors^[58] also reported a numerical method for the analysis of steel columns subjected to thermal gradients across the section.

Vandamme and Janss^[59] developed buckling curves for different temperatures up to 600°C based on curve 'c' of the European buckling curves for steel columns at room temperature. These curves were then adopted in ECCS recommendations^[26]. Similar work was also reported by Proe, Bennets and Thomas^[60,61]. These buckling curves were produced on the assumption that the temperature of the column is uniform at any given time. The elastic modulus and yield strength of steel corresponding to the specific temperature is used then in place of the room temperature properties. In other words, this method is the same as the critical temperature method but presented in a different form.

For rigorous analysis of columns finite element methods were used by Bock^[62], Aribert and Abdel Aziz^[63] and Sharples^[64]. Olawale and Plank^[31] proposed a finite strip method for the collapse analysis of steel columns. Another method, utilising the moment-thrust-curvature of the cross section and satisfying the static equilibrium conditions, was developed by Poh et al.^[65,66].

2.3.5 Experimental Work on Steel Beams and Columns

A considerable amount of fire testing of steel beams, columns and frames has been carried out over the past few years in many countries. Almost all of these fire tests were carried out according to ISO 834^[6], BS476:Part 8^[4], BS476: Part 20^[5] or other national standards for fire testing. The definition of failure is mainly based on the maximum central deflection or the rate of deflection as specified in the corresponding standard. The definition of failure based on the maximum central deflection, such as span/30 or span/20, is specified mainly for the purpose of protecting the test furnace and rig from any possible damage. Although this may not necessarily be the failure state of the specimen, the test results provide important data including the deformation and the temperature history of the specimen which can be used to validate numerical models.

British fire tests have been carried out mainly by British Steel Plc(formerly British Steel Corporation)^[67,68]. These include over 100 full scale fire tests aimed at understanding the thermal and mechanical response of steel beams and columns. As these tests were carried out with the assumption of no variation in temperature along the length of the specimen, the temperature measurements are inadequate. For example, in a beam test, the thermocouples are placed at different positions across the section at the centre and at longitudinal positions close to the centre of the beam. Without sophisticated equipment to control the temperature of the gases, it would be difficult to attain a uniform temperature throughout the length and breadth of the furnace. In addition, as a small part of the specimen is outside of the furnace at both ends and is exposed to normal atmospheric conditions, the temperature of the beam is bound to have a non-uniform variation along the length.

In other parts of Europe, Thor^[52] carried out about twenty fire tests on steel beams in Sweden but did not give many details about the tests. Olessen^[69] carried out 15 full scale column tests in Denmark. These columns were tested in a horizontal position in a special furnace. The load was increased until failure while the temperature was kept at a constant value. Vandamme and Janss^[59] reported 29 full scale tests on steel columns in Belgium. All but 2 of these columns had fire protection. All columns were axially loaded and were exposed to a standard fire according to ISO 834. The load was kept at a constant value until failure occurred. Kruppa^[70] reported about 20 tests on external steel columns carried out in France. Only a part of the column was exposed to fire to simulate an external column. As a result, a non-linear temperature variation along the length was obtained. Aasen and Larsen^[71] reported 18 tests of high strength steel columns with pinned and restrained end conditions. Heating in these tests was attained by using electrical heating elements. Saito, Uosugi and Miyamoto^[72] reported about 52 tests on H shaped steel beams and columns carried out in Japan using an electrical furnace.

Witteveen and Twilt^[73] tried to evaluate the possible reasons for scatter in column test results obtained from different furnaces and for the repeatability of a test in the same furnace. It was concluded that apart from the heat flow properties of the individual furnaces other factors responsible for inadequate repeatability are:

- ✘ Variation of temperature distribution along the length
- ✘ Imperfections and variations in material properties
- ✘ End restraint conditions

It was recommended to revise the relevant sections in the standards. In particular restrictions to the temperature distribution and end conditions should be specified.

Apart from the above mentioned full scale tests, some quarter scale model tests were carried out in the UK by Cooke^[27] and Sharples^[64]. These tests were mainly carried out to study the effect of non-uniform temperature distributions across the section of beams and columns. The non-uniform temperature distribution was achieved by heating only one flange of the I section using electrical heating elements. Although these tests do not conform to the fire resistance test standards, the results are useful for verifying numerical models. Poh and Bennets^[74] performed tests on large square steel sections. As the main purpose of the tests was to study the thermal response of the sections, no loading was applied.

2.4 Previous Work on Reinforced Concrete Beams and Columns

2.4.1 Analysis of Reinforced Concrete Beams

Ellingwood and Shaver^[75,76] developed an analytical method to calculate the moment-curvature-time relationship of a reinforced concrete beam cross section. This method takes into account the non-linearity of the material properties at elevated temperatures. It is concluded that the primary factor which affects the calculated fire endurance is the correct prediction of the reinforcing bar temperature and using the

correct material properties. Salse and Lin^[77] described a simple method for the calculation of the fire resistance of reinforced concrete beams. The method only calculates the section capacity and does not predict the deformation of the beam. Tassios and Chronopoulos^[78] analysed reinforced concrete elements using a procedure which is based on simple methods of statics. Very few details of how the method was implemented in their analysis are described. For example, no details are given about the material properties of steel and concrete, at elevated temperatures, used in their analysis.

Malhotra^[1] and Wade^[79] describe a design method to calculate the moment capacity of the cross section of a reinforced concrete beam. This method involves calculating the average temperature of the concrete and reinforcement and then using the reduced strength of the concrete and reinforcement to calculate the moment carrying capacity. The average temperature of the reinforcement is calculated by first calculating the average cover to the reinforcement and then calculating the temperature of the reinforcement using the experimentally obtained data. EC2^[8] describes a slightly different method. In this method the concrete outside the 500°C isotherm is ignored. The strength of the reinforcement is reduced individually according to the temperature of each reinforcing bar. The moment capacity is then calculated in the usual manner. The recently published ASCE manual^[80] also describes a method for the calculation of moment capacity. The method is essentially the same as the methods described above.

Hertz^[36] used a different approach and introduced a parameter called the stress distribution factor. The stress distribution factor is a multiplication factor used to further reduce/increase the concrete strength calculated from the average temperature of the compression zone. It represents the non-linear variation of temperature across the cross section. This approach is more rational than simply taking the average strength or ignoring the concrete outside the 500°C isotherm as used in the other methods mentioned above.

In addition to the simple calculation method, EC2^[8] also provides tabulated design data specifying the minimum sectional dimensions and reinforcement cover for different fire

resistance requirements. A similar approach is also adopted in BS8110^[81] and the FIP/CEB report^[82].

2.4.2 Analysis of Reinforced Concrete Columns

EC2^[8] and BS 8110^[81] only provide tabulated design data for the design of columns. The ASCE manual^[80] gives the minimum section dimensions and cover to the reinforcement in the form of a simple formula, based on the work of Lie, Lin, Allen and Abrams^[37]. Hertz^[36] used the extended Rankine formula, given in equation 2.2, to calculate the buckling load of a column.

$$\frac{1}{F_{cr}} = \frac{1}{F_{cu} + F_{su}} + \frac{1}{F_{ce} + F_{se}} \quad (2.2)$$

where,

F_{cr} = Buckling Load

F_{cu} = Ultimate load capacity of the concrete section

F_{su} = Ultimate load capacity of the steel section

F_{ce} = Euler load of the concrete section

F_{se} = Euler load of the steel section

Ultimate load capacity and Euler loads are calculated using the reduced yield strength and elastic modulus. Even at room temperature, without any complication of temperature dependent material properties, the Rankine formula does not give an accurate estimate of the failure load of intermediate slender columns. It is therefore, unlikely that this approach will give good results for fire exposed columns.

2.4.3 Experimental Work on Reinforced Concrete Beams and columns

There are numerous publications about experimental work on reinforced concrete structural elements to be found in literature. Uddin and Culver^[83] have reviewed most of the early experimental work, some of it dating back to the 1920's.

A recent major experimental programme was carried out by Cooke^[84-97] at Warrington Fire Testing Laboratories. In this programme, 20 precast concrete slab panels were tested under standard and hydrocarbon fire conditions. Some of the specimens were not loaded, others were subjected to a nominal design load. Six of these specimens were subjected to an axial load in addition to the lateral loading. Although they are stated to be slab specimens, they were tested as if they were beam specimens. A major drawback of these tests was the evidence of movement of moisture along the thermo couple wires^[98], resulting in lower than expected temperatures.

A number of fire tests on reinforced concrete columns were carried out at the National Research Council of Canada^[37,99]. All the tests were on columns subjected to concentrically applied axial loads and exposed to a standard fire on all sides. From these tests, it is concluded that increasing the cross section size, even in one direction, or the use of carbonated concrete rather than siliceous concrete, significantly increases fire resistance.

Ng and Mirza^[100] carried out an experimental investigation on 1/2.23 and 1/3 scaled models of square reinforced concrete prototype columns subjected to fire and axial load. The main purpose of these tests was to find out whether it is possible to predict the prototype column's behaviour when exposed to fire, from model test results. It is concluded that, with appropriate care, it is possible to construct and test models subjected to fire up to length scale factors between 1/2 and 1/3.

Haksever and Anderberg^[101] reported results of tests on reinforced columns exposed to fire on only three sides. An axial load was applied at different eccentricities for each column.

2.5 Previous Work on Composite Beams and Columns

2.5.1 Analysis of Composite Beams

Compared to steel beams, composite beams have a superior performance under fire. The efficient use of the low thermal conductivity of concrete and the high strength property of steel can result in a composite beam with very high inherent fire resistance capacities. Several different types of composite beams currently used in the UK are shown in Figure 2.10. Some of these cross sections have only recently been introduced^[102,103,104]. The cross section in Figure 2.10(a), which shows a concrete floor placed on top of an unprotected steel beam and is designed to act compositely by the use of shear connectors, is not very efficient when exposed to fire. As the steel section will be directly exposed to fire on three sides, the temperature of the steel will rise very rapidly and reduce the load carrying capacity of the beam. In other sections shown in Figure 2.10, most of the steel section is protected by concrete, thus making the cross section more efficient when exposed to fire.

The moment capacity method described in Section 2.3.2 is also applicable to composite beams. As the temperature across the section varies significantly in the composite cross section, it is necessary to divide the cross section into a number of strips to perform the moment capacity calculation. This simple method is applicable to all composite beams and is also included in BS5950: Part 8.

ARBED Recherches^[104] provide tabular and graphical design data for ARBED composite beams for different fire resistant classes. These data were obtained by performing a parametric study using the finite element based computer program CEFICOSS). EC4: Part 10^[10] outlines a method for calculating the bending moment capacity of a composite beam. In this method, the effect of temperature is taken into account either by reducing the dimensions of the parts composing the cross section or by multiplying the mechanical properties of the materials by a reduction factor. The reduction factors are supplied in the form of tabulated data. Applying two different types of reduction factors (a section dimension reduction factor and a mechanical property

reduction factor) makes the calculation process more complicated than necessary. A simple method of applying only one reduction factor to modify the mechanical properties of the material, as recommended in BS5950: Part 8, yields results with much the same accuracy but is easier to use. It should be noted that most of the reduction factor tables provided in EC4 are related to ARBED composite beams. For composite beams with cross sections other than those specified in EC4, the tabular design data of reduction factors are not valid.

2.5.2 Analysis of Composite Columns

As in the case of composite beams, the efficient use of steel and concrete can result in composite columns with a very high inherent fire resistance capacity. Different cross sections^[104,105] of the composite columns currently used in UK are shown in Figure 2.11.

ARBED Recherches provide graphical and tabulated data^[104] for their columns as in the case of their beams. EC4^[10] outlines a simple method to calculate the buckling load of a column exposed to fire. Effective rigidity EI_e , and Plastic load N_p are calculated using the reduced dimensions of the different parts of the section (steel flange, web, concrete and reinforcement) and reduced material properties. It is recommended to use the European buckling curve "c" for bare steel columns to calculate the buckling load of the composite column. No explicit guidance is given on how to calculate the reduced dimensions of the different parts of the section. It is perhaps intended that the data supplied for composite beams should be used. Tabulated data for sectional minimum dimensions, cover to reinforcement, and Buckling load diagrams for ARBED columns, concrete encased steel I section and reinforced concrete filled hollow steel tubular columns are also given in EC4. BS5950:Part 8 also gives tabulated design data for concrete filled tubular columns and concrete encased steel I section columns.

A numerical method was developed by O'Meagher et al.^[106] for the analysis of composite columns. This method is similar to their method for steel columns, but

includes the material properties of the concrete, developed at the same institution(BHP Australia)^[65,66].

2.5.3 Experimental Work on Composite Beams and Columns

Tests on four ARBED beams carried out at Gent Laboratories, Belgium were reported by Schleich^[107]. Thor^[102] reported one test on the Swedish composite beam marketed as *Thor Beam* in the UK by ConstrucThor Plc as a patented beam section. British Steel^[103] have carried out a number of tests on a composite beam called *Slimflor Beam*. These test results have not yet been published. The Slimflor beam system was developed by British Steel and the Steel Construction Institute of the UK as a joint venture. There are ongoing research projects on using the Slimflor beam system with different types of floor arrangements.

Extensive experimental work on ARBED columns have been carried out in different European countries^[108]. About 22 tests have been reported. Of these, two were carried out at the Fire Research Station, UK, as part of the appraisal programme to use these columns in UK construction. A review of over 200 tests on different types of composite columns carried out in Europe and Canada is presented in Reference 90. Most of the Canadian work reported in this reference is from a recent extensive experimental programme supported by the National Research Council of Canada.

One test was carried out on a Thor Column (concrete filled tube with a cruciform section in the middle) at the Fire Research Station as part of the appraisal of this construction for use in the UK^[105]. Thor column was developed in Sweden and was introduced in the UK by ConstrucThor Plc as a patented column section.

2.6 Numerical Methods and Associated Computer Programs

Numerical methods and associated computer programs available for structural response calculations of beams and/or columns exposed to fire, are discussed in this section. As most of these computer programs can be used to analyse more than one type of structural element discussed in previous sections, to avoid repetition, they are discussed collectively in this section.

Terro^[39] reported a survey on a number of thermal and structural analysis computer programs dedicated to fire response. In this survey, no computer programs developed in the UK were reported, although many were at the development stage at the time of the survey. Later, Terro carried out a survey including the programs in UK as part of a study commissioned by BRE.

Computer programs discussed in this section are:

- ✘ FIRES-RC (USA)
- ✘ CONFIRE (Norway)
- ✘ STEELFIRE (Norway)
- ✘ STABA-F (Germany)
- ✘ CEFFICOS (Belgium)
- ✘ SAFE-RCC (UK)
- ✘ BFIRE (UK)
- ✘ STRUCT (LUSAS Shell) (UK)
- ✘ NARR2 (UK)
- ✘ FLAMEFIRE (UK)

FIRES-RC

This is the first known fire dedicated structural analysis computer program developed in 1974 at the University of California, Berkeley by Becker and Bresler^[109]. The numerical method employed in this program is the non-linear finite element technique. This program is capable of analysing reinforced concrete frames exposed to fire. The temperature data input of this program is compatible with the output of the thermal analysis computer program FIRES-T, which was also developed at the same institution. This program was later revised by Iding, Nizamuddin and Bresler^[110] and the new version was named FIRES-RC II.

FASBUS

FASBUS^[111] was first developed for the American Iron and Steel Institute by Illinois Institute of Technology in 1975. Later it was revised by Wiss, Janney, Elestner and Associates Inc. The revised version of the program is called FASBUS II. This program was developed for the analysis of steel deck floor systems exposed to fire using a non-linear finite element technique. As in the case of FIRES-RC II the temperature input can be obtained from the output of the thermal analysis computer program FIRES-T3. Material properties (up to a maximum of 3 materials) are input as data by giving the yield stress and elastic modulus for different temperatures. This indicates that the bi-linear stress-strain relationship is used in the program.

CONFIRE

CONFIRE is another finite element computer program developed by Forsen^[112]. This was developed for the analysis of reinforced concrete plane frames exposed to fire. Temperature data obtained from the thermal analysis carried out using the computer program TASEF-2 can be used as input to this program. The material constitutive relationships of steel and concrete developed by Anderberg and Thelandersson^[35] are used in this program.

BFIRE

BFIRE^[117] is a structural analysis software developed at the Steel Construction Institute, UK for the modelling of fire tests. This program is capable of analysing steel and composite beams subjected to non-linear temperature variation across the section and along the length. The material properties used in this program are according to BS5950: Part 8 and Part 10 of Eurocodes 2 and 3. The numerical method employed is based on the calculation of the moment-curvature relationship satisfying static equilibrium at both ends of the longitudinal segments and calculating the deflection profile by integrating curvatures along the length. This program cannot be used for column analysis.

STRUCT (LUSAS Shell)

STRUCT was developed by Terro^[39] at Imperial College London. This program forms a part of the general purpose finite element program LUSAS. Although theoretically this program should be able to analyse any framed and shell structure, the author^[39,118] of the program only validated it against fire tests on reinforced concrete structures despite the availability of numerous test results on steel and composite structures. As part of LUSAS, this program has the advantage of using a massive finite element library and graphical pre and post processor facilities already developed. However, LUSAS is too general and too expensive to run for most design engineers. Although LUSAS can be used as a good research tool, the computer time required to perform any non-linear analysis is prohibitively large.

NARR2

NARR2 is a structural analysis program capable of analysing 2D plane framed structures exposed to fire. This program was developed by El-Rimawi at Sheffield University^[119]. This is an extension of the earlier work^[54,55] done at Sheffield University on steel beams exposed to fire.

FLAMEFIRE

This is also a structural analysis program applicable to steel and composite plane frames exposed to fire, and was developed by Wang^[120] at the Building Research Establishment, UK. This is a non-linear finite element based program. The temperature input can be obtained from the output of the thermal analysis program TEMPCALC. The variation of temperature across the section is accounted for, but no details are given on the ability to take the variation of the temperature along the length.

2.7 Summary

From the review of the material properties of steel and concrete at elevated temperatures presented in Section 2.1 and 2.2 the following conclusions can be drawn.

- ⌘ Material properties of steel at elevated temperatures are reasonably well defined and the data presented in BS5950:Part8 and EC3:Part 10 are acceptable for use in structural analysis calculations.
- ⌘ Material properties of concrete at elevated temperatures are not so well defined as in the case of steel. There is no data available in the British standards. The data given in EC2:part 10 does not have any information on transient strains which is an important part of the total strain of the concrete at elevated temperatures. There is a need for more research in this area to study all the existing constitutive models available and to prescribe the more appropriate ones in European or British codes of practice. As this is beyond the scope of this thesis the properties specified in EC2 are used for the calculations.

From the review of previous work on steel, reinforced concrete and composite beams and columns presented in Sections 2.3-2.6 the following conclusions can be drawn.

- ⌘ Simple analytical methods are available for uniformly heated steel columns and beams.

- ✘ Simple calculational methods are also available for steel, reinforced concrete and composite beams with temperature variations across the section.
- ✘ One simple design method is proposed in EC4:Part 10 for composite columns.
- ✘ Only tabulated data are available for the fire resistant design of reinforced concrete beams and columns.
- ✘ Draft Eurocode, EC4:Part 10, has graphical and tabulated design data for ARBED (Luxemburg) composite beams and columns, clearly showing the lack of research in this field by other European Community countries.
- ✘ Despite the numerous experimental studies, the amount of analytical work on structures exposed to fire is very limited.
- ✘ Of the computer software reviewed, most are very recent. This shows that only recently attention has been given to analytical work in this field. Most of the analytical work reported is finite element based modelling.
- ✘ No computer software available, to the authors knowledge, can analyse all types of steel, reinforced concrete and composite beams or columns subjected to a non-linear variation of temperature in all three dimensions and with axial and lateral loading.
- ✘ Almost all the experimental work to date is based on the assumption that the structural element will be subjected to a uniform heating along the length of the element. Even in carefully controlled laboratory conditions the test specimen does not have perfectly uniform heating along the length of the element.
- ✘ There is a need for experimental and theoretical investigations on structural members subjected to non-uniform temperature distribution across the section and along the length. This is the most likely situation when a beam or column is exposed to real fire.

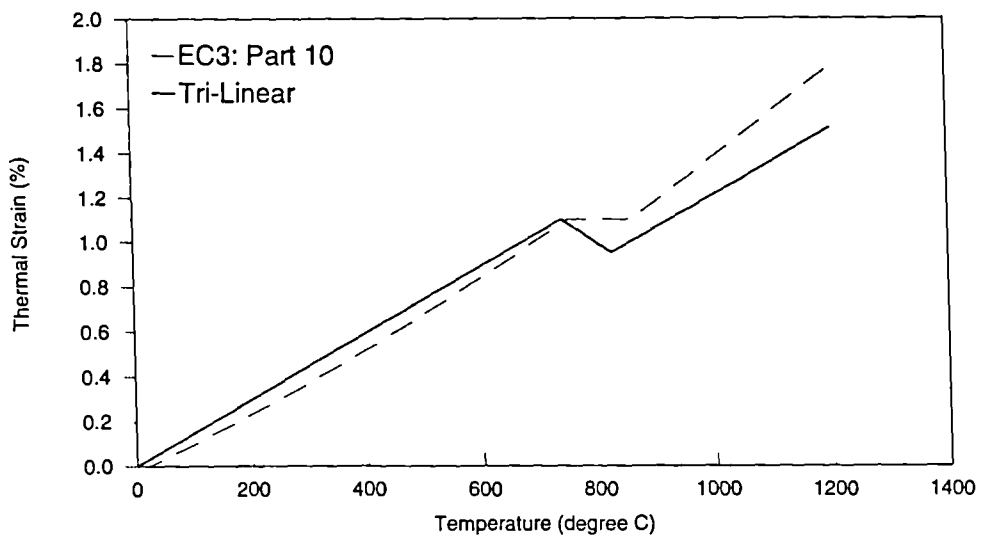


Figure 2.1 Thermal Elongation of Steel

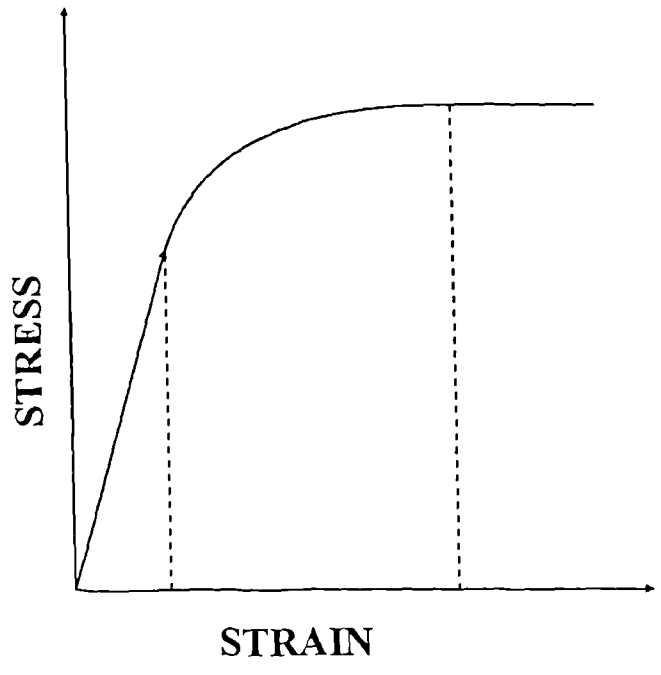


Figure 2.2 General Stress-Strain Diagram of Steel

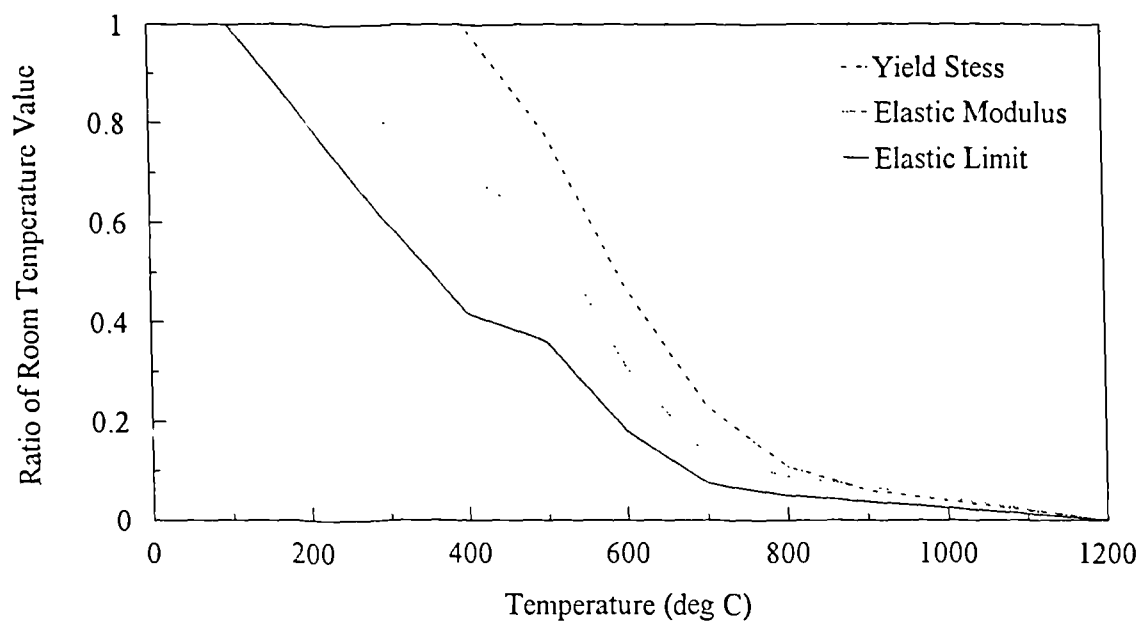


Figure 2.3 Variation of Parameters with Temperature

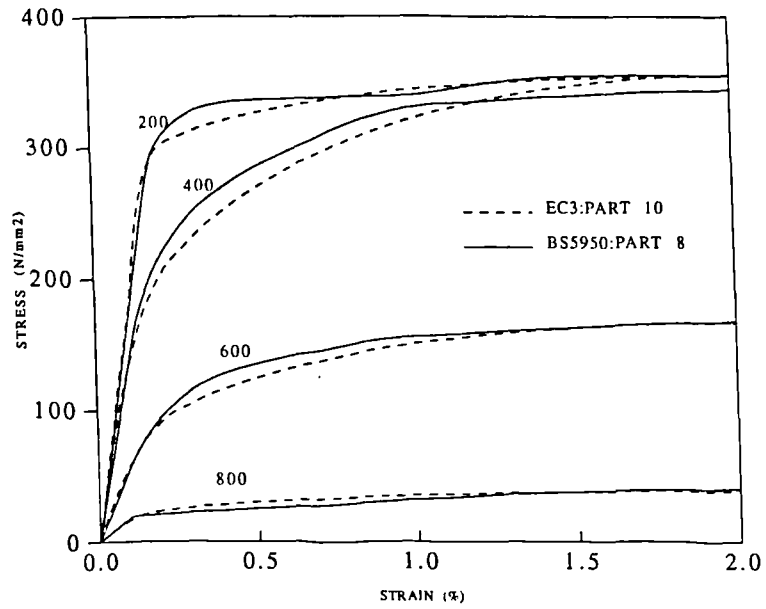


Figure 2.4 Comparison of Stress-Strain Curves-Grade 50 Steel

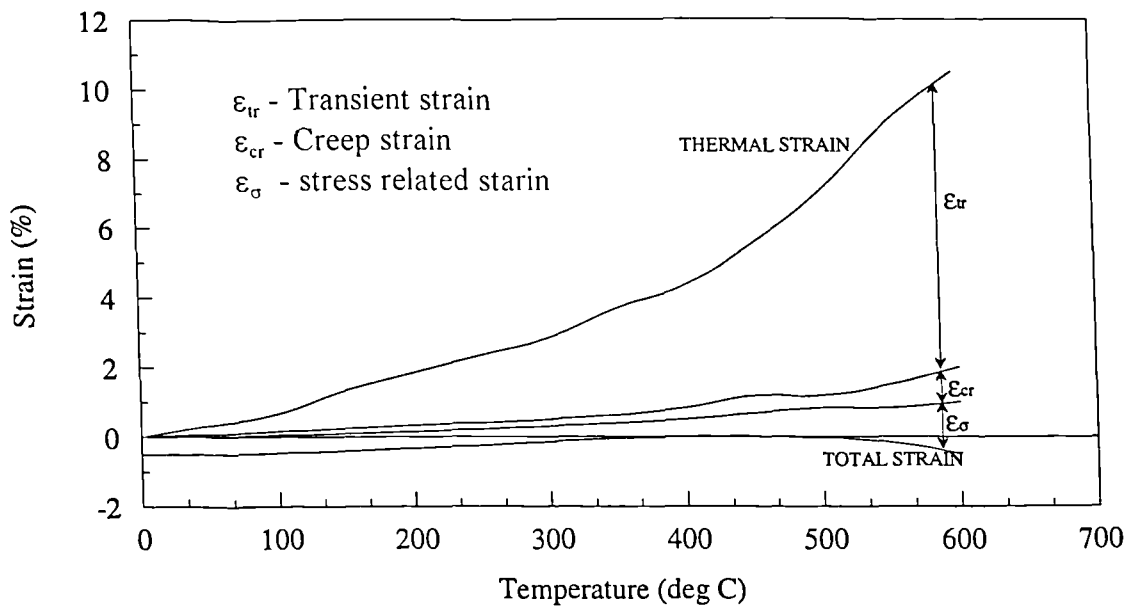


Figure 2.5 Components of Total Strain of Concrete

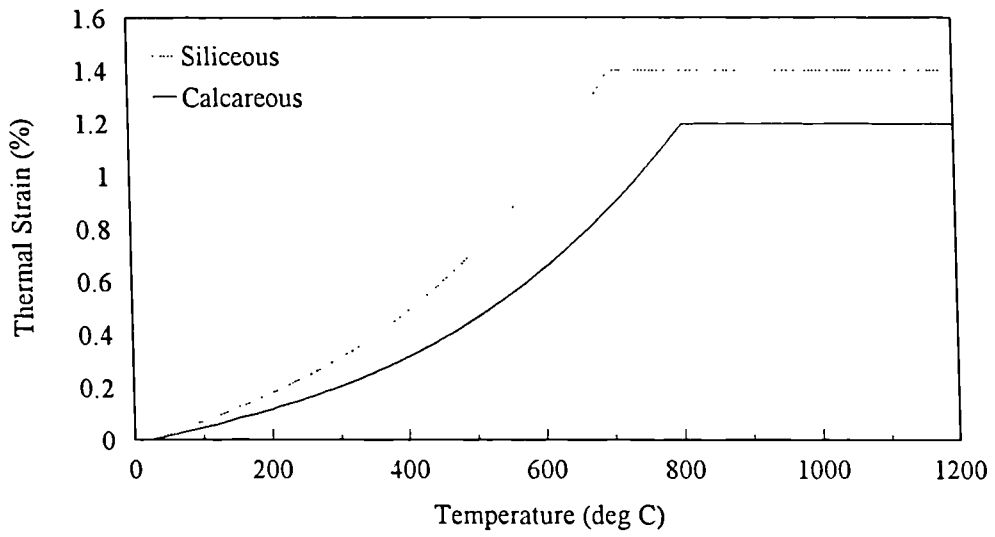


Figure 2.6 Thermal Expansion of Concrete

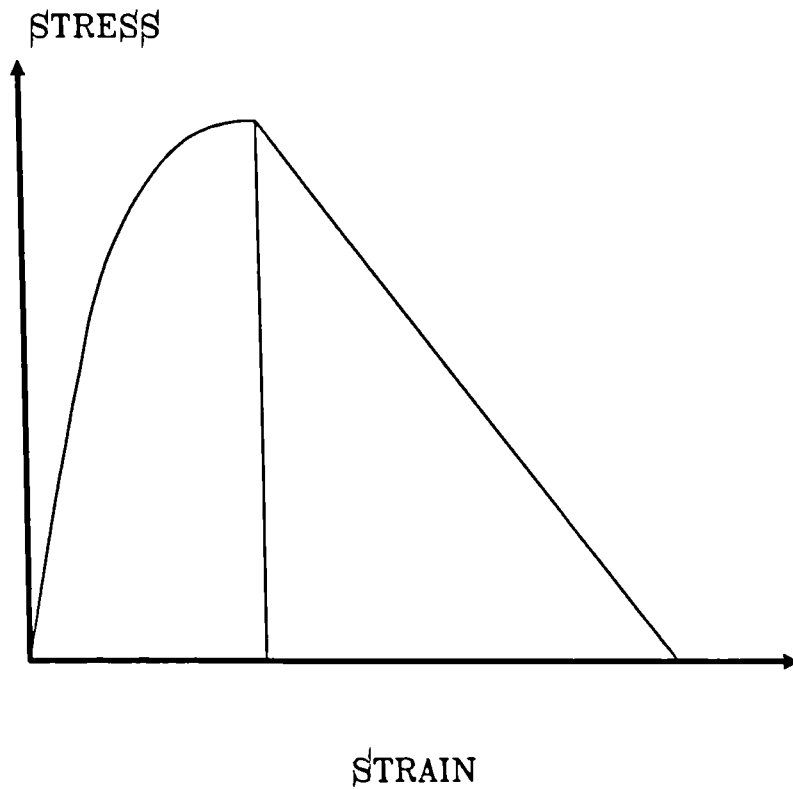


Figure 2.7 General Stress-Strain Diagram of Concrete

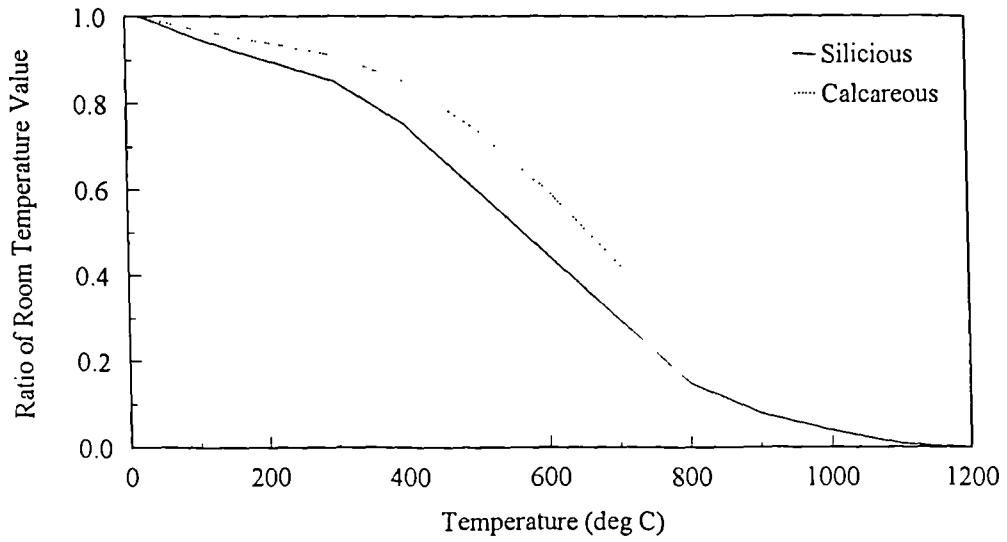


Figure 2.8 Reduction of Ultimate strength with Temperature

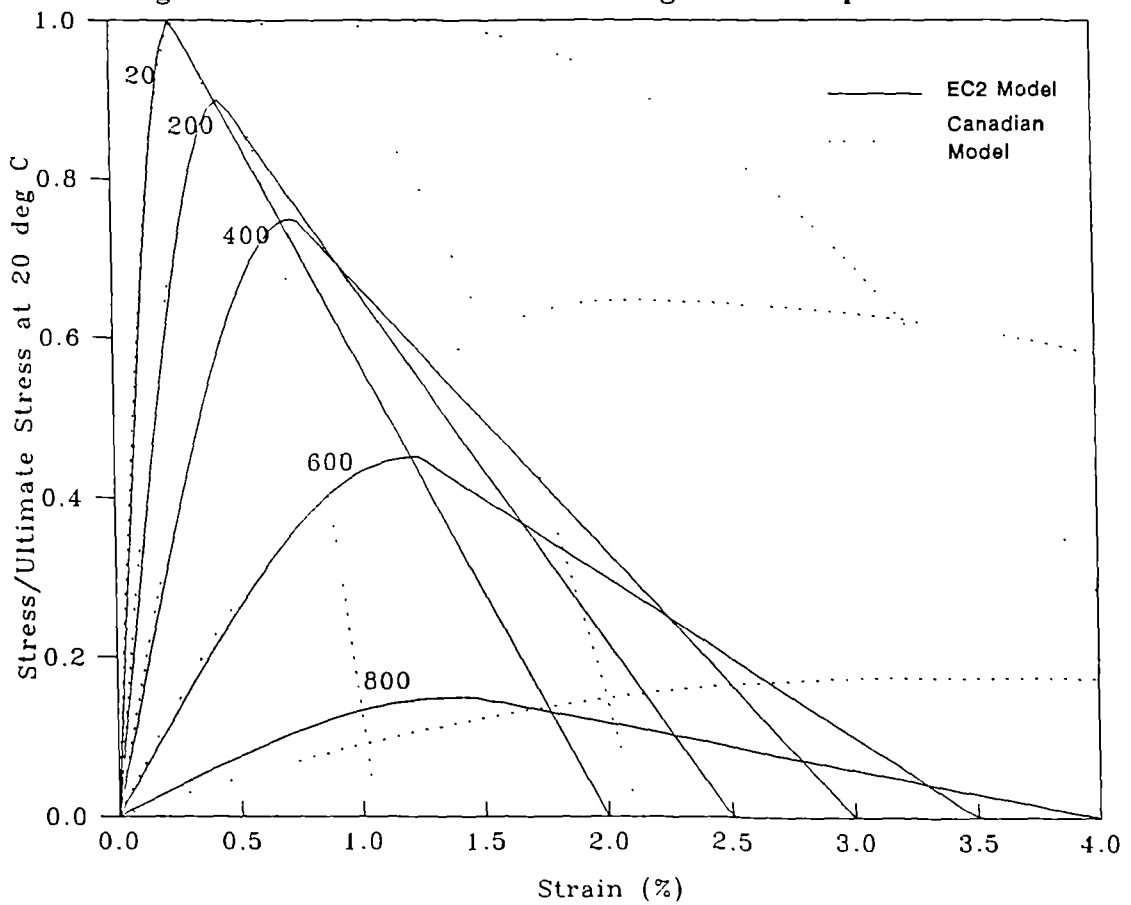


Figure 2.9 Comparison of Eurocode and NRCC Model

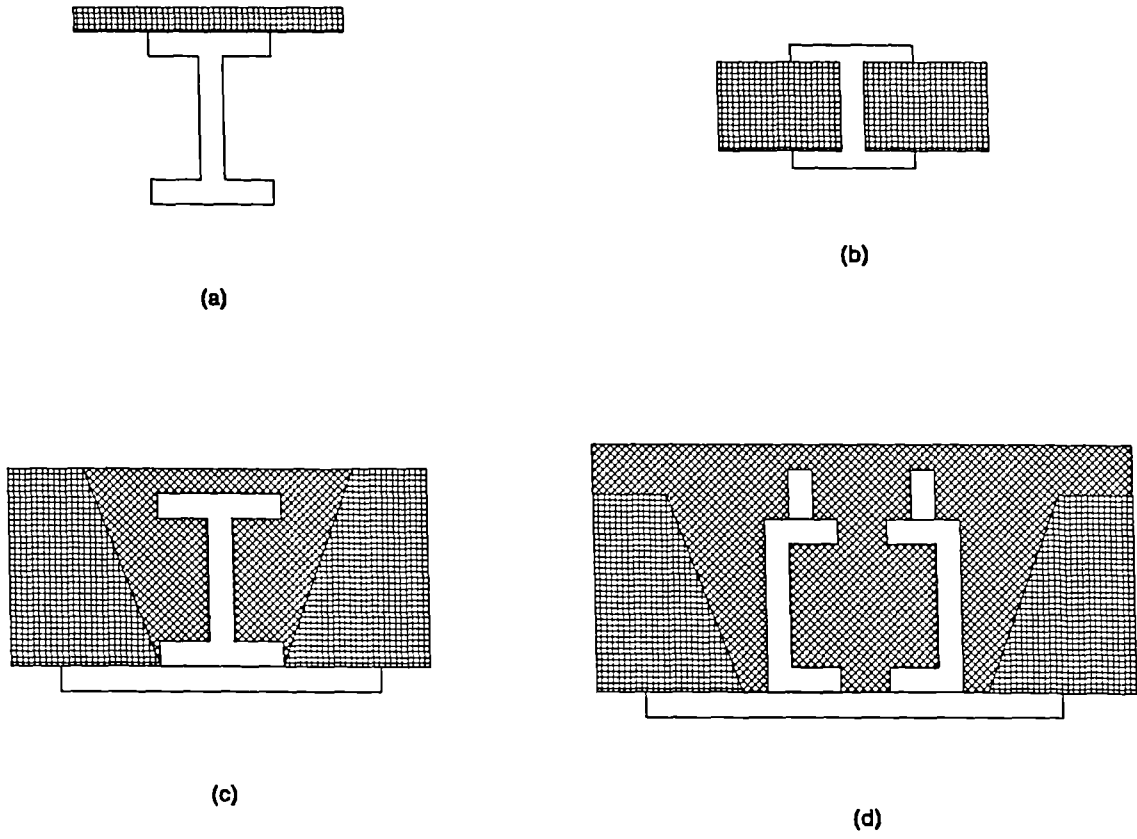


Figure 2.10 Types of Composite Beam Cross Sections

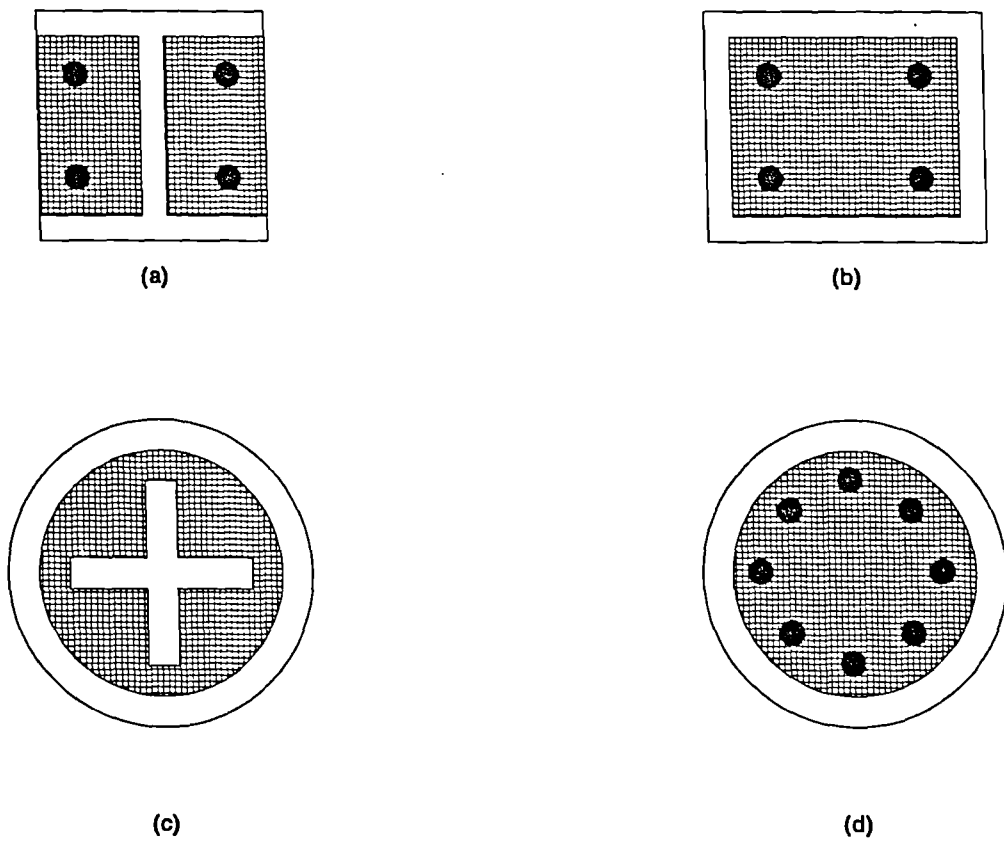


Figure 2.11 Types of Composite Column Cross Sections

CHAPTER 3

THEORY

3.0 Introduction

This chapter describes the numerical method developed in this thesis for the structural analysis of beams and columns subjected to a non-linear variation of temperature in all three directions, axial and lateral loading and external end moments. The method is based on the numerical method developed by Viridi and Dowling^[121,122] and Viridi^[123] for the inelastic analysis of biaxially loaded columns at room temperature. The original method cannot be used to analyse a member with zero axial load as it causes a singularity in the influence coefficient matrix. In this work, the method was first generalised to analyse beams as well as columns by reformulating the equations so that zero axial load will not cause any numerical problem. Then the method was extended to take account of the effect of elevated temperature.

3.1 Description of the Numerical Method

The numerical method is based on finding a deflected shape which satisfies static equilibrium conditions, for each increment of load, time or temperature. The equilibrium conditions are checked at a number of stations along the length of the member, spaced at regular intervals. As in any numerical application, it is necessary to make a few reasonable assumptions.

The following assumptions are made in this method:

- ✕ Plane sections remain plane during bending
- ✕ Torsional effects are negligible
- ✕ High temperature creep effects can be ignored
- ✕ Contribution of shear forces to the deflection is negligible

- ⌘ The stress at any point is independent of the stress and temperature history
- ⌘ The member is free to expand or shorten axially

The calculation procedure can be divided into two major steps,

- ⌘ Calculation of the Moment-Thrust-Curvature relationship, and
- ⌘ Calculation of the equilibrium deflected shape.

3.2 Moment-Thrust-Curvature Relationship

Consider the section subjected to the temperature distribution as shown in Fig. 3.1. Let the axial force and the two biaxial moments be P , M_x and M_y respectively. Let the neutral axis be at a distance d_n from the centroidal axis, and let the curvatures of the section be ϕ_x and ϕ_y in the X and Y directions, respectively.

The total curvature at a point can be expressed as,

$$\phi = \left[\phi_x^2 + \phi_y^2 \right]^{1/2} \quad (3.1)$$

Now consider an arbitrary point Z in the section, at a distance d from the neutral axis. Let the temperature at Z be T . This may be obtained from a temperature analysis such as TASEF-2 as stated earlier, or from experiments.

Under conditions of thermal strain, and ignoring the effect of creep, the strain at point Z at distance d from the neutral axis, can be written in terms of curvature as follows:

$$\varepsilon = \phi d - \varepsilon_t \quad (3.2)$$

where,

ε = strain caused by the imposed stress at the point

ε_t = thermal strain

If the stress-strain relation of the material is known at temperature T , the stress at point Z can be obtained. Internal forces in the section can then be calculated from the following integrals:

$$P = \int \sigma dA \quad (3.3 \text{ a})$$

$$M_x = \int \sigma_x dA \quad (3.3 \text{ b})$$

$$M_y = \int \sigma_y dA \quad (3.3 \text{ c})$$

To perform the above integrations numerically, the cross section is divided into a number of quadrilaterals, and Gauss quadrature formulae are used to calculate the values of P , M_x and M_y . The technique is described in detail in Section 3.2.1

Equations 3.3a-3.3c represent the moment-thrust-curvature relations for the section. The equations involve six variables: d_n , ϕ_x , ϕ_y , P , M_x , and M_y .

where,

d_n = Distance of the neutral axis from the centroid (Reference point)

ϕ_x = Curvature in X direction

ϕ_y = Curvature in Y direction

P = Axial force

M_x = Moment about X axis

M_y = Moment about Y axis

By selecting any three, the other three variables can be determined. Based on the assumption that the member is free to expand or shorten axially without any restraints, the axial force P will be constant at any given time. If we start with an assumed deflected shape, the curvatures ϕ_x and ϕ_y can be calculated. These three variables (P , ϕ_x and ϕ_y) are treated as known variables.

By varying the neutral axis depth d_n , the computed axial force from Equation 3.3a is made to match the externally applied force P iteratively. The iterative procedure used here is the Newton-Raphson iterative scheme for the numerical solution of an equation with a single unknown. This determines the value of d_n . The corresponding moments M_x and M_y are then obtained from the above integrations.

3.2.1 Gauss-Quadrature Integration Procedure

The Gauss-Quadrature integration scheme is the most efficient numerical procedure available to perform a multi dimensional integration. In this case the problem is two dimensional. The idealisation of the cross section is done by dividing it into a number of quadrilaterals, enabling the idealisation of a wide variety of cross sections. Integration is performed in each quadrilateral using the Gauss-Quadrature formulae.

Gauss quadrature formulae enable the evaluation of a definite integral between the limits -1 and $+1$ by a process of weighted summation of the values of the integrand at prescribed points. Thus:

$$\int_{-1}^{+1} f(\xi) d\xi = \sum_{i=1}^m H_i f(\xi_i) \quad (3.5)$$

where,

H_i are the weighting coefficients and ξ_i are the specified points.

The higher the value of m , the more accurate is the integral obtained. For a polynomial of degree $(2r-1)$, the selection of $m = r$ points leads to an exact integral, and no benefit accrues by adopting a higher value of m . Tabulated values of H_i and ξ_i are available for values of m ranging from 2 to 10^[124].

Equation 3.5 can be extended for a double integral over the square area implied by the limits -1 and $+1$ in both directions as follows.

$$\int_{-1}^{+1} \int_{-1}^{+1} f(\xi, \eta) d\xi d\eta = \sum_{i=1}^m \sum_{j=1}^m H_j H_i f(\xi_i, \eta_j) \quad (3.6)$$

The problem of evaluating an arbitrary quadrilateral can be solved by mapping the quadrilateral area to the required square area by the following transformation:

$$x = \frac{1}{4}[(1-\xi)(1-\eta)x_p + (1+\xi)(1-\eta)x_q + (1-\xi)(1+\eta)x_r + (1+\xi)(1+\eta)x_s] \quad (3.7a)$$

$$y = \frac{1}{4}[(1-\xi)(1-\eta)y_p + (1+\xi)(1-\eta)y_q + (1-\xi)(1+\eta)y_r + (1+\xi)(1+\eta)y_s] \quad (3.7b)$$

Fig. 3.2 illustrates the manner in which the transformation is affected. It is clear that at the sides of the quadrilateral $pqsr$, the natural co-ordinates have the limits of -1 and +1. The elemental area $dx dy$ can now be transformed to the area $d\xi d\eta$ by the following relation.

$$dx dy = |J| d\xi d\eta \quad (3.8)$$

where $|J|$ is the determinant of the Jacobian matrix J given by

$$J = \frac{1}{4} \begin{bmatrix} -a & a-c & c \\ -b & d & b & d \\ \begin{matrix} x_p & y_p \\ x_q & y_q \\ x_r & y_r \\ x_s & y_s \end{matrix} \end{bmatrix} \quad (3.9)$$

where, $a = (1-\eta)$, $b = (1-\xi)$, $c = (1+\eta)$ and $d = (1+\xi)$

3.3 Calculation of the Equilibrium Deflected Shape

Let the column AB be divided into n equal segments, each of length h , and let the stations be numbered from 1 to $n+1$ from end A to end B as shown in Fig. 3.3. Let the lateral deflections of the centroid of the station i be denoted by u_i and v_i in the X and Y directions respectively. The external moments at station i can be written as,

$$M_{xi} = Pv_i + \left[1 - \frac{(i-1)}{n}\right]M_{xA} + \frac{(i-1)}{n}M_{xB} + M_{exi} \quad (3.10a)$$

$$M_{yi} = Pu_i + \left[1 - \frac{(i-1)}{n}\right]M_{yA} + \frac{(i-1)}{n}M_{yB} + M_{eyi} \quad (3.10b)$$

where, M_{exi} and M_{eyi} are free moments due to lateral loads at station i .

The biaxial curvatures ϕ_{xi} and ϕ_{yi} at station i , can be expressed in finite difference form using the central difference formula as follows,

$$\phi_{xi} = \frac{\partial^2 u}{\partial x^2} = \frac{u_{i-1} - 2u_i + u_{i+1}}{h^2} \quad (3.11a)$$

$$\phi_{yi} = \frac{\partial^2 v}{\partial y^2} = \frac{v_{i-1} - 2v_i + v_{i+1}}{h^2} \quad (3.11b)$$

The internal moments M_{ixi} and M_{iyi} at station i can be calculated using the moment-thrust-curvature relationship described earlier. Since the curvatures at station i are functions of $\{u\}$ and $\{v\}$, the internal moments can be rewritten in terms of unbalanced moments at station i as follows:

$$M_{uxi} = M_{xi} - M_{ixi} = f\{u\} \quad (3.12a)$$

$$M_{uyi} = M_{yi} - M_{iyi} = f\{v\} \quad (3.12b)$$

For equilibrium, the unbalanced moments M_{uxi} and M_{uyi} must vanish. The above two equations can be combined and rewritten in matrix form as follows:

$$f w = 0 \quad (3.13)$$

where,

$$w = \begin{Bmatrix} u \\ v \end{Bmatrix}$$

Equation (3.13) represents a system of non-linear equations, the solution of which requires an iterative procedure. In the present work, the well known generalised

Newton-Raphson iterative scheme is used. In this approach, given a trial value at iteration k, a better approximation can be obtained as follows:

$$f(w^{k+1}) = f(w^k) - [K]^{-1} f(w^k) \quad (3.14)$$

where [K] is a Jacobian matrix, and could be interpreted as a matrix of influence coefficients. When using the finite difference approximation for curvatures, most of the elements of the Jacobian matrix will be zero. An efficient procedure for the formation of the Jacobian matrix is described in detail in Section 3.3.1.

The procedure is continued, until two successive iteration values are within the required tolerance, or the number of iterations reaches a specified number. If the two successive values are within the specified tolerance, then the calculated deflected shape is assumed to be the equilibrium deflected shape. If after the specified number of iterations, the two successive values are not within the specified tolerance, then it is assumed that convergence is not achieved and the load/time/temperature step is reduced by half and the procedure is repeated. Once the load/time/temperature step value has reached a value which is less than the specified tolerance for the load/time/temperature step, the calculation is terminated with the output of the last load/time/temperature, for which the equilibrium is achieved, as the failure load/time/temperature.

3.3.1 Formation of the Jacobian Matrix

Referring to Equation 3.13, the Jacobian matrix [K] can be expressed as:

$$[K] = \begin{bmatrix} \frac{\partial f_1}{\partial w_1} & \frac{\partial f_1}{\partial w_2} & \frac{\partial f_1}{\partial w_{2n}} \\ \frac{\partial f_2}{\partial w_1} & \frac{\partial f_2}{\partial w_2} & \frac{\partial f_2}{\partial w_{2n}} \\ - & - & - \\ - & - & - \\ \frac{\partial f_{2n}}{\partial w_1} & \frac{\partial f_{2n}}{\partial w_2} & \frac{\partial f_{2n}}{\partial w_{2n}} \end{bmatrix} \quad (3.15)$$

Equation 3.13 can be written in expanded form as follows:

$$f \{w\} = f \begin{Bmatrix} u \\ v \end{Bmatrix} = \begin{Bmatrix} M_x - M_{ix} \\ M_y - M_{iy} \end{Bmatrix} = \{0\}$$

Differentials of the calculated internal moments may be written as:

$$\begin{aligned} \frac{\partial M_{ixi}}{\partial u_j} &= \frac{\partial M_{ixi}}{\partial \phi_{x_i}} \frac{\partial \phi_{x_i}}{\partial u_j} & \text{and} & \quad \frac{\partial M_{ixi}}{\partial v_j} = \frac{\partial M_{ixi}}{\partial \phi_{y_i}} \frac{\partial \phi_{y_i}}{\partial v_j} \\ \frac{\partial M_{iyi}}{\partial u_j} &= \frac{\partial M_{iyi}}{\partial \phi_{x_i}} \frac{\partial \phi_{x_i}}{\partial u_j} & \text{and} & \quad \frac{\partial M_{iyi}}{\partial v_j} = \frac{\partial M_{iyi}}{\partial \phi_{y_i}} \frac{\partial \phi_{y_i}}{\partial v_j} \end{aligned}$$

From equation 3.11 the following can be derived.

$$\frac{\partial \phi_{x_i}}{\partial u_j} = 0 \quad \text{for } j < i-1 \text{ and } j > i+1$$

$$\frac{\partial \phi_{x_i}}{\partial u_{i-1}} = \frac{\partial \phi_{x_i}}{\partial u_{i+1}} = \frac{1}{2} \frac{\partial \phi_{x_i}}{\partial u_i} = \frac{1}{h^2}$$

$$\frac{\partial \phi_{y_i}}{\partial v_j} = 0 \quad \text{for } j < i-1 \text{ and } j > i+1$$

$$\frac{\partial \phi_{y_i}}{\partial v_{i-1}} = \frac{\partial \phi_{y_i}}{\partial v_{i+1}} = \frac{1}{2} \frac{\partial \phi_{y_i}}{\partial v_i} = \frac{1}{h^2}$$

To calculate the contribution of M_{ix} and M_{iy} to the Jacobian matrix, the moment thrust curvature calculations should only be performed three times, with $\{\phi_x \text{ and } \phi_y\}$, $\{\phi_x + \Delta\phi_x \text{ and } \phi_y\}$ and $\{\phi_x \text{ and } \phi_y + \Delta\phi_y\}$, at each station.

For simply supported members, $M_{xA}, M_{xB}, M_{exi}, M_{yA}, M_{yB}, M_{eyi}$ are of constant values.

Thus:

$$\frac{\partial M_{y_i}}{\partial u_j} = P \quad \text{for } i=j \quad \text{and} \quad \frac{\partial M_{y_i}}{\partial u_j} = 0 \quad \text{for } i \neq j$$

$$\frac{\partial M_{x_i}}{\partial v_j} = P \quad \text{for } i=j \quad \text{and} \quad \frac{\partial M_{x_i}}{\partial v_j} = 0 \quad \text{for } i \neq j$$

$$\frac{\partial M_{x_i}}{\partial u_j} = 0 \quad \text{and} \quad \frac{\partial M_{y_i}}{\partial v_j} = 0$$

From the above described expressions for the differentials, one can note that most of the elements of the Jacobian matrix becomes zero. The non zero components of the Jacobian matrix for a simply supported member are given below

For $i \leq n$

$$\frac{\partial f_i}{\partial w_j} = \frac{-2.}{h^2} \frac{\partial M_{iyi}}{\partial \phi_{yi}} + P \quad \text{for } i=j$$

$$\frac{\partial f_i}{\partial w_j} = \frac{1.}{h^2} \frac{\partial M_{iyi}}{\partial \phi_{yi}} \quad \text{for } i=j-1 \text{ and } i=j+1$$

$$\frac{\partial f_i}{\partial w_j} = \frac{-2.}{h^2} \frac{\partial M_{iyi}}{\partial \phi_{xi}} \quad \text{for } i=j-n$$

$$\frac{\partial f_i}{\partial w_j} = \frac{1.}{h^2} \frac{\partial M_{iyi}}{\partial \phi_{xi}} \quad \text{for } i=j-1-n \text{ and } i=j+1-n$$

For $i > n$

$$\frac{\partial f_i}{\partial w_j} = \frac{2.}{h^2} \frac{\partial M_{ixi}}{\partial \phi_{xi}} + P \quad \text{for } i=j$$

$$\frac{\partial f_i}{\partial w_j} = \frac{-1.}{h^2} \frac{\partial M_{ixi}}{\partial \phi_{xi}} \quad \text{for } i=j-1 \text{ and } i=j+1$$

$$\frac{\partial f_i}{\partial w_j} = \frac{2.}{h^2} \frac{\partial M_{ixi}}{\partial \phi_{yi}} \quad \text{for } i=j+n$$

$$\frac{\partial f_i}{\partial w_j} = \frac{-1.}{h^2} \frac{\partial M_{ixi}}{\partial \phi_{yi}} \quad \text{for } i=j-1+n \text{ and } i=j+1+n$$

Modification of the Jacobian Matrix for Fixed End Condition

If the end at A is fixed, then the curvatures at end 1 becomes

$$\phi_{x1} = \frac{\partial^2 u}{\partial x^2} = 2 \frac{u^2}{h^2}$$

$$\phi_{y1} = \frac{\partial^2 v}{\partial x^2} = 2 \frac{v^2}{h^2}$$

and the end moments M_{xA} and M_{yA} become a function of the curvatures at the end, and hence the function of the displacement vector $\{w\}$. As a result, the Jacobian matrix will have two additional columns of non-zero elements as given below.

For $i \leq n$

$$\frac{\partial f_i}{\partial w_2} = \left[1 - \frac{(i-1)}{n}\right] \frac{2}{h^2} \frac{\partial M_{xA}}{\partial \phi_{x2}}$$

$$\frac{\partial f_i}{\partial w_{n+2}} = \left[1 - \frac{(i-1)}{n}\right] \frac{2}{h^2} \frac{\partial M_{xA}}{\partial \phi_{y_{n+2}}}$$

For $i > n$

$$\frac{\partial f_i}{\partial w_2} = \left[1 - \frac{(i-1)}{n}\right] \frac{2}{h^2} \frac{\partial M_{xA}}{\partial \phi_{y2}}$$

$$\frac{\partial f_i}{\partial w_{n+2}} = \left[1 - \frac{(i-1)}{n}\right] \frac{2}{h^2} \frac{\partial M_{xA}}{\partial \phi_{x_{n+2}}}$$

Similarly, if the end B is fixed another two columns ($n-1$ and $2n-1$) of the Jacobian matrix will become non-zero.

Modification of the Jacobian Matrix for Spring Supported End Conditions

If the end A is spring supported, then the end moments M_{xA} and M_{yA} become a function of the rotational angles (θ_x and θ_y) at the end A. The following expressions for the rotational angles, in terms of displacements, are used:

$$\theta_x = (4u_2 - u_3) / h$$

$$\theta_y = (4v_2 - v_3) / h$$

Based on the above expressions and the Moment-Rotation data supplied, the Jacobian matrix can be modified. Columns 2,3,n+2 and n+3 will have non-zero elements as a result of this modification. A Similar approach can be applied to the end B.

3.4 Stability Calculations

The above procedure for the determination of the equilibrium deflected shape is carried out starting with an initial level of applied load, time duration of fire, or a specified temperature. In the event convergence is obtained, the next load, time or temperature increment is applied, and the above procedure is repeated. The maximum value of the load, time or temperature for which an equilibrium deflected shape is obtained, is adopted as the failure load, time or temperature. It will be seen that the above procedure for stability analysis closely resembles the approach adopted in physical testing.

3.5 Range of Applicability of the Proposed Method

The numerical method described above is a general method so that its applicability is not restricted to steel members. The method has been programmed so that it is possible to analyse beams or columns of a range of materials, including reinforced concrete or steel/concrete composite beams or columns.

3.6 Computer Program

3.6.1 Description of Computer Program SOSMEF

A user friendly computer program called SOSMEF (Strength Of Structural Members Exposed to Fire) has been developed based on the numerical method described in the previous section. The program consists of four modules:

- | | |
|--------------------------------|---|
| SOSMEF - Data Edit | This program is used for data preparation, or for editing the data file for the main program. This is a text based menu driven program. |
| SOSMEF - View Data | This program shows the data in graphical form on the screen. It is also possible to get hard copies of the graphics on a colour PostScript printer or on a Plotter which uses the HPGL graphic language. Some examples printed on a colour PostScript printer are given in Appendix A. |
| SOSMEF - Main Program | This is the main program which performs the structural response calculations in accordance with the method outlined above. The results are stored in a file with suitable annotation to make them easily understood. The program also creates two additional files which contain information for use with the graphical Post processor. |
| SOSMEF - Post processor | This program can be used to display the results in a graphical form on the screen. It is also possible to get hard copies on a colour PostScript printer or on a Plotter. Some examples printed on a colour PostScript printer are given in Appendix A. |

All four modules are independent programs, coded in standard FORTRAN 77. This makes the programs portable between different types of machines with minimum amounts of modification. View Data and Post processor programs use the GINO-F graphical libraries to produce graphical output. The complete software is currently

installed on Sun Sparc+1 work stations under the Unix operating system environment. The main program has also been installed on an IBM compatible PC under the MSDOS operating system environment with the DBOS DOS extender.

3.6.2 Capabilities of SOSMEF

3.6.2.1 Type of Analysis

The four types of analysis which can be performed using SOSMEF are:

- ✧ Ultimate Axial Load capacity
- ✧ Ultimate Lateral Load Factor
- ✧ Failure Temperature
- ✧ Failure Time

Ultimate Axial Load Capacity

This analysis will calculate the ultimate axial load capacity of the given member for a given temperature distribution and lateral loading condition.

Ultimate Lateral Load Factor

This analysis will calculate the ultimate load factor relating to the lateral load, for the given axial load and temperature distribution conditions.

Failure Temperature

This analysis will calculate the failure temperature for the given loading conditions. It should be noted that, in this case, it will be assumed that the temperature distribution throughout the member is uniform. No temperature distribution data will be prompted for. For cases of a non-uniform temperature distribution, the Failure Time option should be used.

Failure Time

This analysis will calculate the failure time of the member for given loading conditions for the specified time-temperature distribution data. It is necessary to provide temperature distribution data at intervals after the initial time. The temperature distribution data for intermediate times will be linearly interpolated from the temperature distribution data for two adjacent times. If the program reaches the maximum time for which the temperature data is given, it will print a message that the maximum time has been reached, implying that the structure has not failed.

For this option, it is possible to vary the axial load with time. This is allowed to simulate the increase in axial force due to restraints. Although the program would not calculate the increase or decrease in axial force due to restraints, as it assumes that the member is free to expand or contract, if experimentally obtained data is available, the test can be fully simulated by providing the measured axial force-Time data.

3.6.2.2 Geometry Idealisation

The cross section of the member is idealised using a number of quadrilaterals, enabling the analysis of a wide variety of cross sectional shapes. A cross section can consist of quadrilaterals of different materials. This allows for the analysis of reinforced concrete and steel/concrete composite sections. Reinforcing bars can be specified as concentrated areas by defining the cross sectional area, co-ordinates of the position and the material properties of the bar(steel) and the material(concrete) it is replacing. The temperature of the reinforcing bar will be taken as that at the centre of the bar. Some examples of how to idealise different cross sections are shown in Figure 3.4. It is also possible to analyse a beam or column with a varying cross section along its length such as tapered members. Any initial imperfection of the member can be defined either by the central amplitude, if sinusoidal, or by providing the values at each station.

3.6.2.3 End Conditions

Provision has been made for three types of end condition for any member.

- ⌘ Simply supported (Pinned end)
- ⌘ Rotationally restrained (Fixed end)
- ⌘ Rotationally flexible (Spring supported end)

For the rotationally flexible support condition, it is necessary to provide the moment-rotation relationship data for the end restraint.

It is assumed that the member is free to expand or shorten axially. In other words, no catenary action is considered.

3.6.2.4 Temperature Distribution

Non-linear variation of temperature in all three directions can be specified. The data needed has been made compatible with the TASEF-2 temperature output so that the results of a temperature analysis carried out using TASEF-2 can be used as the temperature distribution input data for SOSMEF. Of course, it is possible to use any other means of establishing temperature distributions, including experimentally observed temperature distribution data.

Temperature distribution data is supplied in a rectangular grid across the section and along the length at a number of points. Spacing along the length or across the section need not necessarily be uniform. If there is a symmetry in temperature distribution pattern across the section, only the temperature data of the positive half or positive quarter of the section needs to be supplied. During the calculations, the temperature at any arbitrary point is calculated using the linear transformation function of eight nodal solid elements. Although this is the general format for catering for a variation of temperature in all three directions, for simple cases, such as the temperature variation in

only one direction, the user need " define the temperature at various points in the specific direction only.

3.6.2.5 Material Properties

Stress-Strain-Temperature properties and Thermal expansion properties of steel and concrete according to Parts 10 of Eurocodes 3 and 2, respectively, are included in the program. An option to define any other material properties as a set of multilinear curves is also available. This gives great flexibility in the use of the analysis.

3.7 Summary

A new numerical method for structural analysis of beams and columns exposed to fire has been described in this chapter. The numerical method is validated with number of experimental data available in literature in the next Chapter.

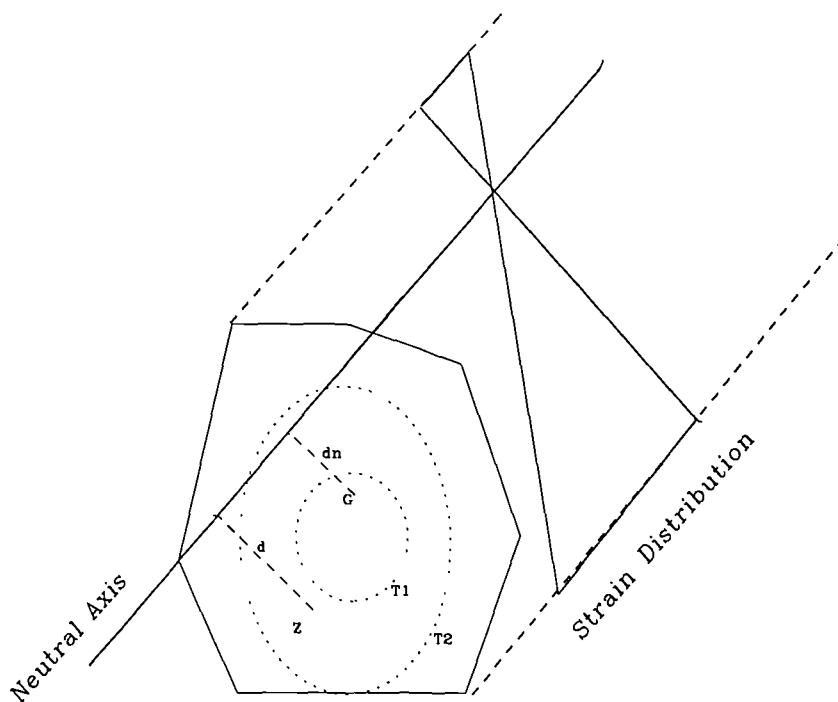


Figure 3.1 Cross Section

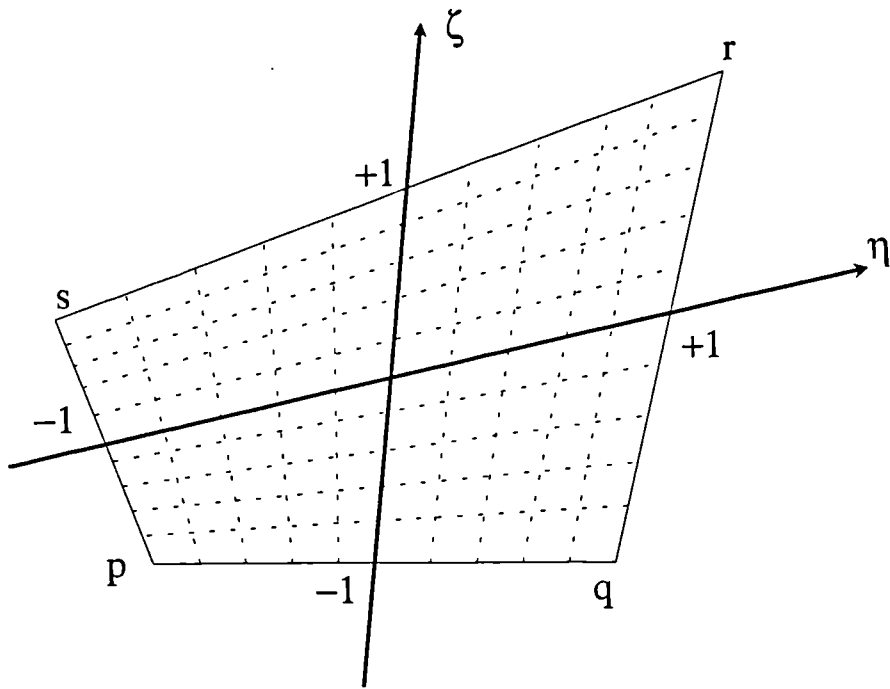


Figure 3.2 Natural Co-ordinate System of a Quadrilateral

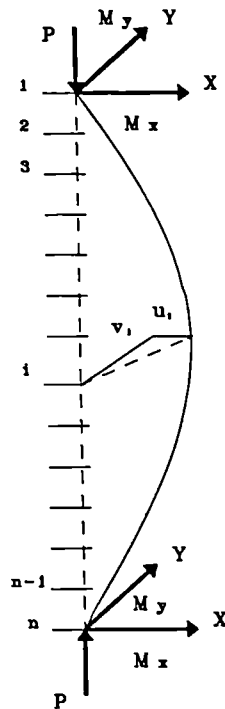
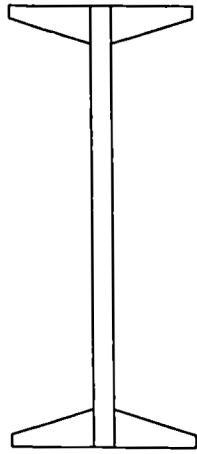
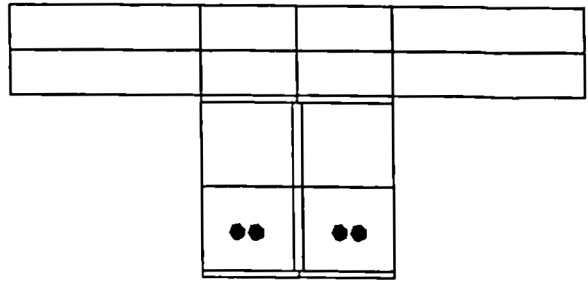


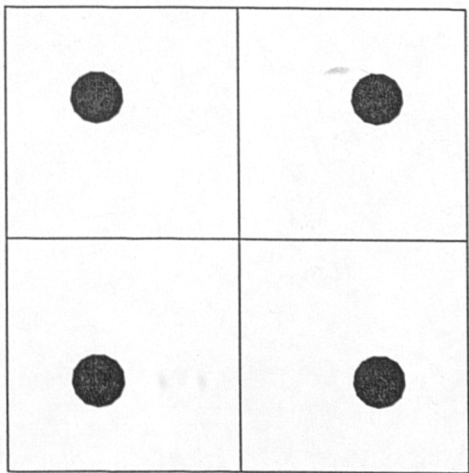
Figure 3.3 Idealisation of a Member



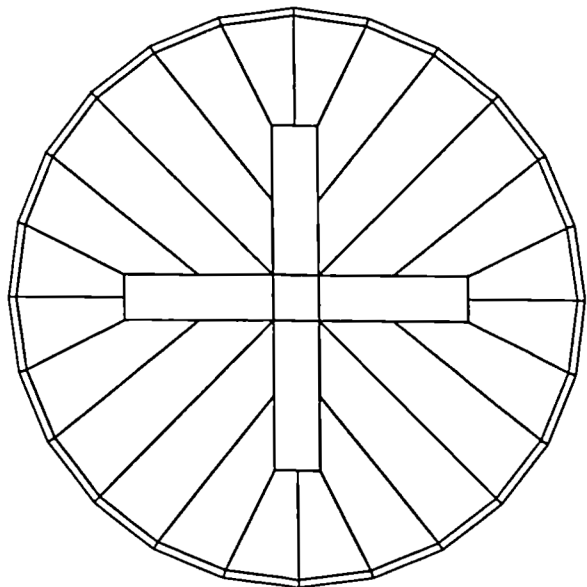
(a)



(b)



(c)



(d)

Figure 3.4 Idealisation of Different Cross sections

CHAPTER 4

VALIDATION OF THEORY

4.0 Introduction

In this Chapter, the analytical method developed in Chapter 3 is validated by comparing the computed results with a number of experimental results. In numerically simulating the experimental behaviour of a structural member accurately, it is necessary to have a good understanding of material properties at elevated temperatures. However, such data is extremely difficult to generate. Most of the experimental results reported in literature provide only the room temperature properties of the material used. The only alternative is to compare the experimental and computed results, using standard material properties. The stress-strain-temperature relationship and the thermal strain-temperature relationship of steel are assumed to be as given in the draft Eurocode3:Part10^[9]. The Material properties of steel at elevated temperatures have been discussed in detail in Section 2.1. Figure 2.1. shows the thermal elongation of steel and Figure 2.4 shows the stress-strain relationship of steel at different temperatures. For concrete two different constitutive models are used. One is according to Eurocode2:Part10^[8], referred to hereafter as the EC model, and the other one is according to Lie,Lin, Allen and Abrams^[37], referred to hereafter as the NRCC model. These two different formulations were discussed in Section 2.2. Figure 2.10 shows the stress-strain relationship of concrete at different temperatures according to the EC and NRCC model.

Stress-Strain relationships of steel and concrete at elevated temperature are defined as functions of their room temperature properties. In all the comparisons, the actual room temperature properties measured are used, if available. In the case of room temperature properties data not being available, nominal values are assumed.

4.1 Steel Beams and Columns

4.1.1 Comparison With BSC Full Scale Simply Supported Beam Tests

Experimental data for 14 simply supported floor beams, supporting concrete slabs exposed to fire on three sides, are reported by Wainman and Kirby^[67]. The comparison of experimental results, computed predictions and temperatures calculated according to BS5950:Part 8^[7] is given in Table 4.1. The limiting temperature for a beam is taken as the hot flange temperature at failure. An experimentally obtained temperature distribution is used in the computer analysis. It was assumed that there is no variation of temperature along the length of the beam. The limiting temperatures in accordance with BS5950:Part 8 were calculated using the actual yield stress of the specimens, that is, with the material partial safety factor as 1.0.

From Table 4.1, it is evident that a good three way agreement has been obtained between tests, computed results from SOSMEF, and from the code.

Table 4.1 Comparison of Limiting Temperatures - Simply Supported Beam Tests

Data Sheet Number	Limiting Temperature in °C			Ratios	
	Test (1)	SOSMEF (2)	BS5950 (3)	(2)/(1) (4)	(3)/(1) (5)
1	682	642	672	0.941	0.985
2	660	633	654	0.959	0.991
3	634	622	637	0.981	1.005
4	701	680	703	0.970	1.003
5	647	597	630	0.923	0.974
6	737	677	697	0.919	0.946
7	731	676	704	0.925	0.963
8	705	685	701	0.972	0.994
9	714	671	698	0.940	0.978
10	655	622	659	0.950	1.006
11	683	634	657	0.928	0.962
12	681	626	647	0.919	0.950
13	727	664	689	0.913	0.948
14	745	737	759	0.989	1.019
Mean				0.945	0.980
Standard Deviation				0.024	0.023

4.1.2 Comparison With Model Beam Test By Cooke^[27]

A small scale laterally loaded steel I-beam was tested by Cooke^[27]. The beam was heated using electrical heating elements along the bottom flange to obtain a non-uniform temperature distribution across the section. The span of the test beam was 1500mm. The test load was applied at 4 points using load spreaders to simulate a uniformly distribution load. Section details and the comparison of experimental and computed central deflections are shown in Figure 4.1. It can be seen that the computed and experimental central deflections are in excellent agreement. Also the duration to failure is computed very accurately.

4.1.3 Comparison With Full Scale Shelf Angle Floor Beam Test By BSC^[125]

A full scale test on a shelf angle floor beam was carried out by British Steel in 1991. The material properties of the beam and the shelf angles at elevated temperatures are also reported for this test. The main purpose of this test was to find out whether there is any significant difference between computed results using standard material properties of steel according to BS5950: Part 8 or Eurocode 3: Part 10 and that of using actual material properties at elevated temperature. Details of the test specimen, loading and the comparison of computed results using different material properties with the experimental central deflection of the beam are shown in Figure 4.2. It can be seen that there is no significant difference between the computed results when different curves to represent the material properties were used.

4.1.4 Comparison With Column Tests by Aasen and Larsen^[71]

Aasen and Larsen^[71] reported tests on steel columns. The columns were of the European IPE 160 section. Limiting temperatures for these columns, when subjected to ISO fires, were recorded. Table 4.2 shows the comparison between computed and experimental results, as well as values calculated from BS5950:Part 8. Overall the results are in good agreement.

Table 4.2 Comparison of Limiting Temperatures - Column Test by Aasen and Larsen

Column Number	Limiting Temperature in °C			Ratios	
	Test (1)	SOSMEF (2)	BS5950 (3)	(2)/(1) (4)	(3)/(1) (5)
2	471	400	465	0.849	0.987
5	527	526	540	0.998	1.025
6	460	402	466	0.874	1.013
10	481	403	470	0.838	0.977
12	351	397	477	1.131	1.359
13	461	526	549	1.141	1.191
14	473	397	477	0.839	1.008
16	679	629	635	0.926	0.935
19	575	629	635	1.094	1.104
20	520	629	635	1.210	1.221
Mean				0.990	1.082
Standard Deviation				0.136	0.128

4.1.5 Comparison With Column Tests by Vandamme and Janss^[59]

The limiting temperatures of column tests reported by Vandamme and Janss^[59] are compared in Table 4.3. The end conditions of the columns were assumed fixed at both ends. In calculating the limiting temperatures according to BS5950:Part 8, a slenderness ratio was calculated using an effective length of 0.5xColumn Length, to enable a direct comparison with theoretical values. Table 4.3 shows a good agreement between the test and computed results, although the code values are somewhat non-conservative.

Table 4.3 Comparison of Limiting Temperatures - Column Tests by Vandamme and Janss

Column Number	Limiting Temperature °C			Ratios	
	Test (1)	SOSMEF (2)	BS5950 (3)	(2)/(1) (4)	(3)/(1) (5)
2.1	588	544	576	0.925	0.980
2.2	564	581	585	1.030	1.037
2.3	486	540	528	1.111	1.086
2.4	559	561	587	1.004	1.050
2.5	394	512	530	1.299	1.345
2.6	519	508	564	0.979	1.087
2.7	551	557	613	1.011	1.113
2.8	616	572	621	0.929	1.008
2.9	560	494	552	0.882	0.986
2.10	565	488	562	0.864	0.995
2.11	561	533	571	0.950	1.018
2.12	502	409	*	0.815	-
2.13	549	428	594	0.780	1.082
2.14	250	415	467	1.660	1.868
2.15	516	416	516	0.806	1.000
2.16	576	534	592	0.927	1.028
2.17	522	513	563	0.983	1.079
2.18	508	397	512	0.781	1.008
Mean				0.985	1.104
Standard Deviation				0.205	0.207

Note * Outside the range given in BS5950:Part 8.

4.1.6 Comparison with Arbed Column Test

A comparison of experimental and computed results for a column with a typically heavy ARBED section is shown in Figure 4.3. The figure also includes the section dimensions. This test result was reported in Reference [67], Data sheet 43. The length of the column was 3890 mm, both ends were pinned, and the axial load of 3400 kN was applied at an eccentricity of 180 mm. The figure shows a very good agreement between the experimental and computed deflections for the entire duration of the fire. The error in calculated fire duration is less than 5 minutes.

4.2 Reinforced Concrete Beams and Columns

4.2.1 Comparison With Normal Weight Concrete Slab Tests

The test results of two 150 mm thick and 930 mm wide normal weight reinforced concrete slabs exposed to a standard BS476 : Part 8 fire are reported in Reference [85]. Although these two specimens are reported as slabs, these tests can be modelled as two simply supported beams. One of the slabs was subjected to an imposed load of 1.5kN/m^2 and the other was subjected to no imposed load. In the analysis, the dead load of the specimens has been taken into account. Figure 4.4 shows the cross section details and the test arrangement. The comparison of measured and calculated temperatures using TASEF-2, at different depths from the exposed surface, is shown in Figure 4.5. The agreement between the calculated and measured temperatures is generally poor. However, one can notice some irregularities in the measured temperatures. Due to these irregularities the measured temperatures have not been used in the analysis. Although the computed and measured temperatures are not in good agreement, the calculated temperatures are higher than the measured temperatures and hence by using the calculated temperatures a conservative structural response is obtained.

Figures 4.6 and 4.7 compare the calculated and measured deflections. Reasonably good agreement can be noticed in these comparisons. The use of different material models was not very significant. However, the NRCC material model shows a better agreement with the experimental results.

4.2.2 Comparison With Column Tests by Lie, Lin, Allen and Abrams

Lie, Lin, Allen and Abrams^[37] reported 12 tests on reinforced concrete columns with variation in size, load and aggregate. The comparison between calculated and experimental results for Test 2 and Test 6 are given in this section. Both columns were made of Siliceous aggregate concrete. The length of the columns was 3810 mm with both ends rotationally restrained. The size of the column for Test 2 was 305mm x305mm and that of Test 6 was 203mm x203mm. The axial load in both cases was applied

concentrically. Any initial imperfection was taken into account in the calculations by introducing a 2.5 mm eccentricity to the axial load as recommended in the original report. All four sides of both columns were exposed to an ISO 834 standard fire. Cross section details of both columns and the test arrangement details are shown in Figure 4.8. Figure 4.9 shows the comparison of measured temperatures and calculated temperatures using TASEF-2 at different points of Test Column 2. Figure 4.10 shows the comparison of temperatures for Test Column 6. The agreement between measured and calculated temperatures is good.

Figures 4.11 and 4.12 compare the computed and measured axial deflection of Test2 and Test6 respectively. Computed deflections are given for both EC2 and NRCC material models. The difference in failure time calculated using the different material models in both cases is not significant. The difference in axial deflection was significant and the NRCC material model shows a better comparison with the measured axial deflections in both cases. Calculated failure times using both material properties are conservative.

4.3 Steel/Concrete Composite Beams and Columns

4.3.1 Comparison With ARBED Composite Beam Test

The section details and a comparison of the results are shown in Figure 4.13. This test was reported in Reference [107] as Composite Beam Test 2.11. As it is difficult to get a comprehensive temperature distribution profile from measurements at a limited number of thermocouple positions, the temperature distribution was calculated using the TASEF-2 computer program. A comparison between the calculated and measured temperatures at two different points is also shown in Figure 4.13. The agreement between measured and calculated temperatures is very good. The computed and experimental central deflections are also in good agreement. These comparisons show that using both computer programs TASEF-2 and SOSMEF, the fire test of a composite structural element can be simulated with confidence.

4.3.2 Comparison With ARBED Composite Column Test

Section details and a comparison of the results are shown in Figure 4.14. This test was reported in Reference [107] as Composite Column Test 1.3. As in the case of the composite beam described above, the temperature distribution was calculated using the computer program TASEF-2. The experimental and computed results, both for temperature distribution and for the central deflection, are again in good overall agreement. The discrepancy for times around 30 min and 80min, of an opposing nature, is attributed to the uncertainty in modelling the concrete material properties at high temperatures.

4.4 Summary

In this Chapter, it has been shown that the structural response of beams and columns can be predicted using the computer program SOSMEF with reasonable accuracy. Generally, the computed results were conservative. Average limiting temperatures calculated for steel beams (Table 4.1) were about 5% lower than the experimental values. For steel columns (Table 4.2 and Table 4.3), average calculated limiting temperatures were about 1.5% lower than those of experimental values.

Computed and experimental deflection histories also are in good agreement for all steel, reinforced concrete and steel/concrete beams and columns. Predicted temperature distributions for reinforced concrete and steel/concrete composite cross sections, using the computer program TASEF-2, were in good agreement with the measured temperature data.

It can be concluded that the computer programs TASEF-2 and SOSMEF can be used as an alternative to performing expensive fire tests on isolated structural members. Furthermore, the computer program SOSMEF is validated against the experimental data on steel columns subjected to nonlinear temperature distribution along the length and across the section, obtained in the present work and detailed in the next Chapter.

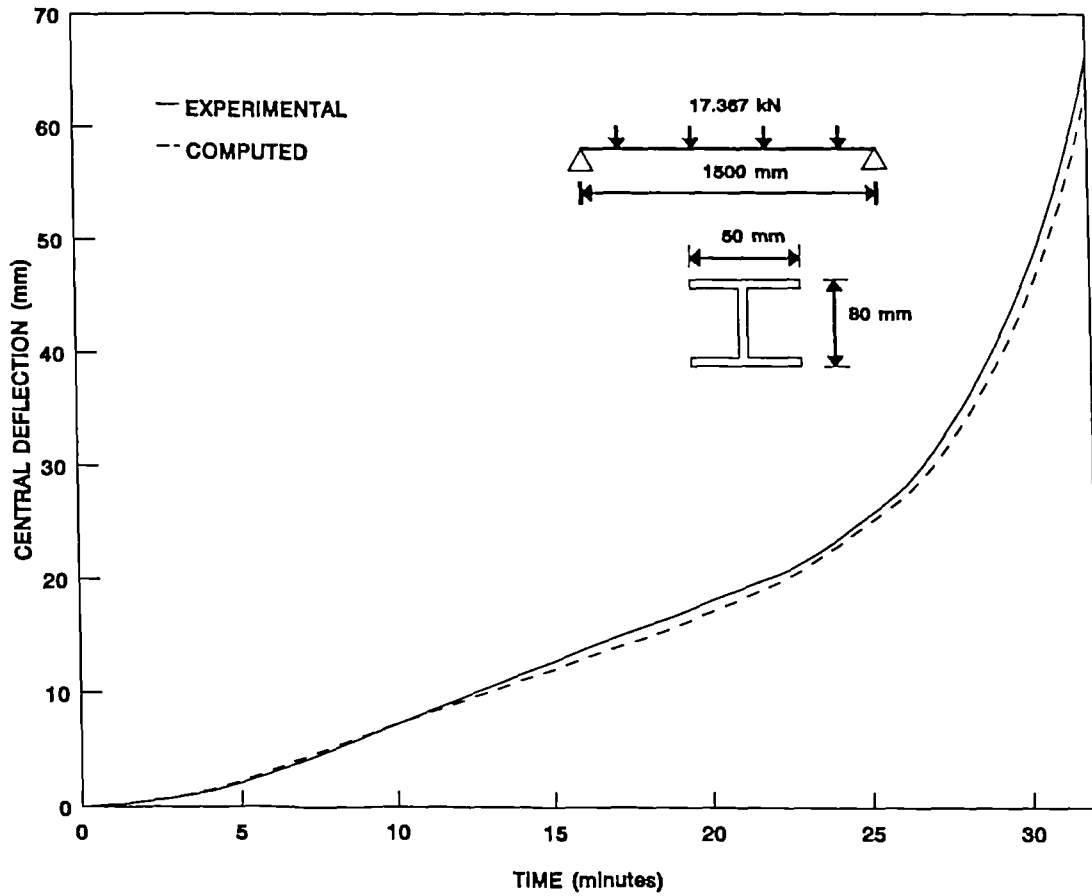


Figure 4.1 Comparison of Results - Model Beam Test

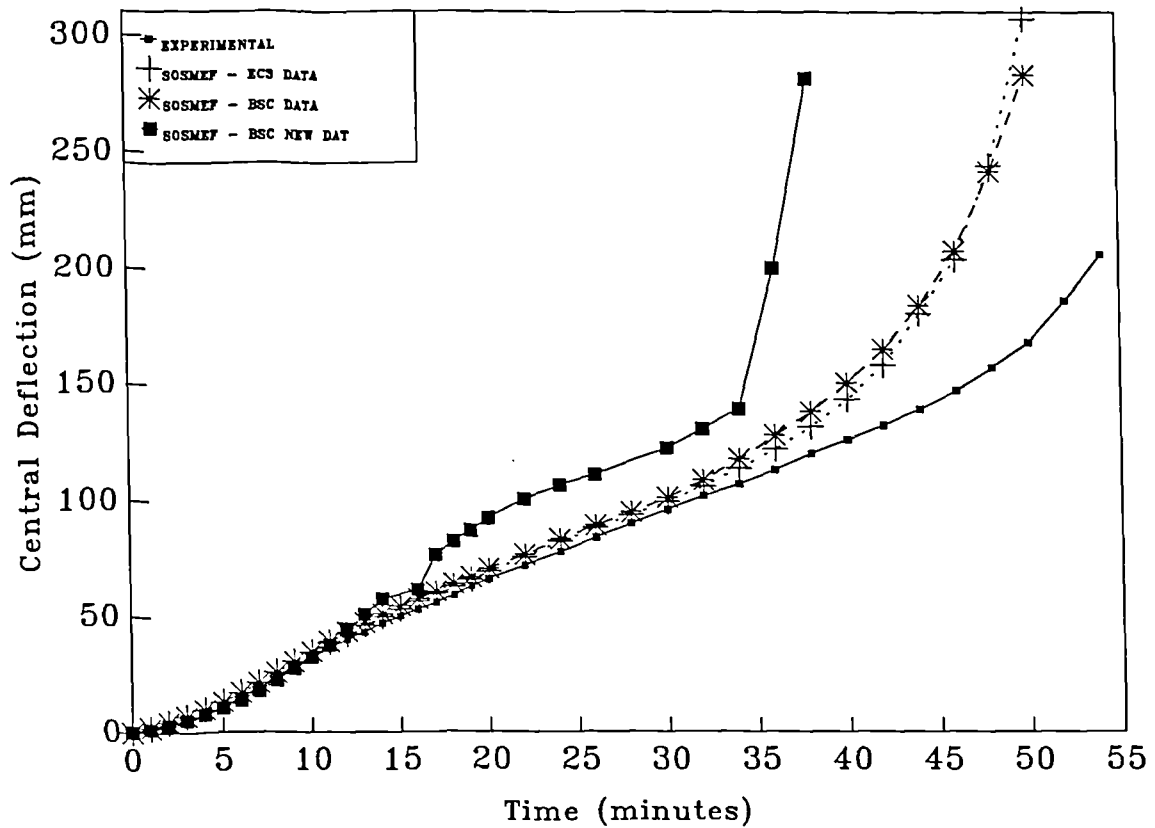


Figure 4.2 Comparison of Results - Shelf Angle Floor Beam TestZ_LABEL CAP

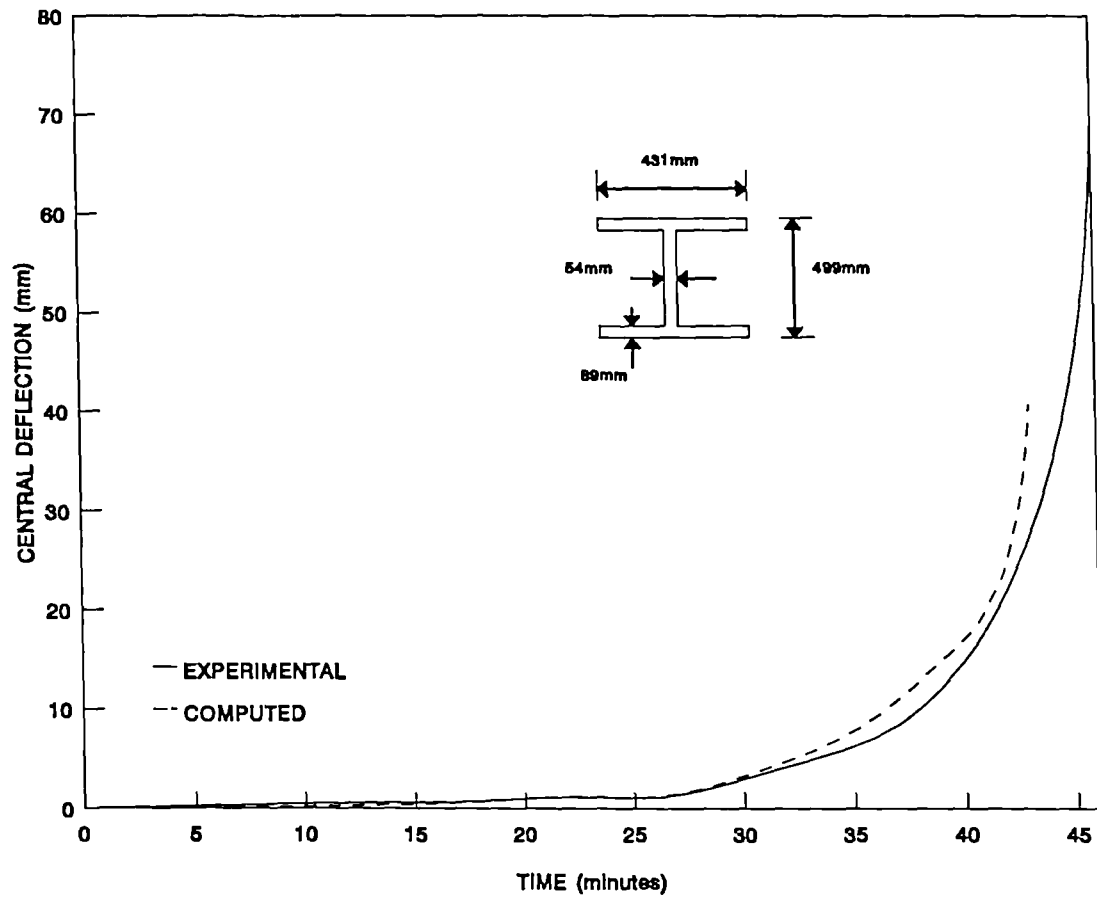


Figure 4.3 Comparison of Results - Arbed Column Test

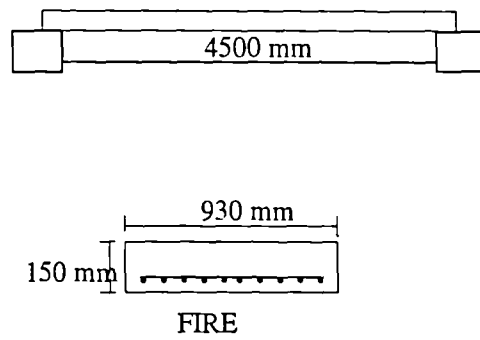
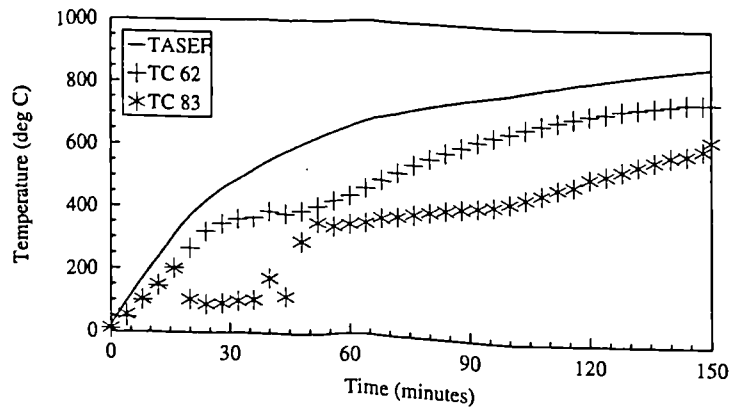
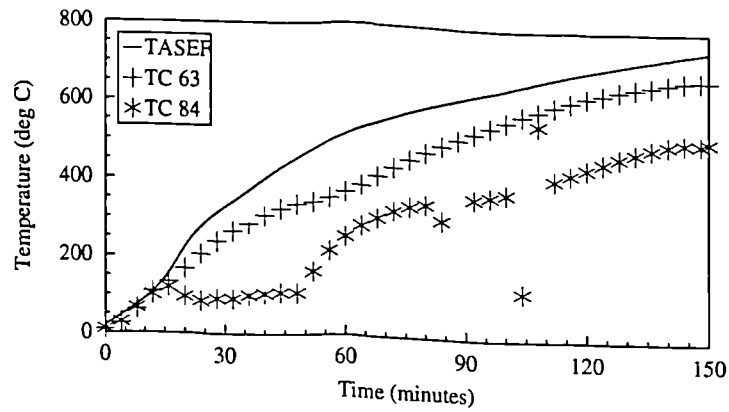


Figure 4.4 Cross Section and Test Arrangement Details of SlabsZ_LABEL CAP

Comparison of Temperatures at 10 mm From Exposed Face



Comparison of Temperatures at 20 mm From Exposed Face



Comparison of Temperatures at 40 mm From Exposed Face

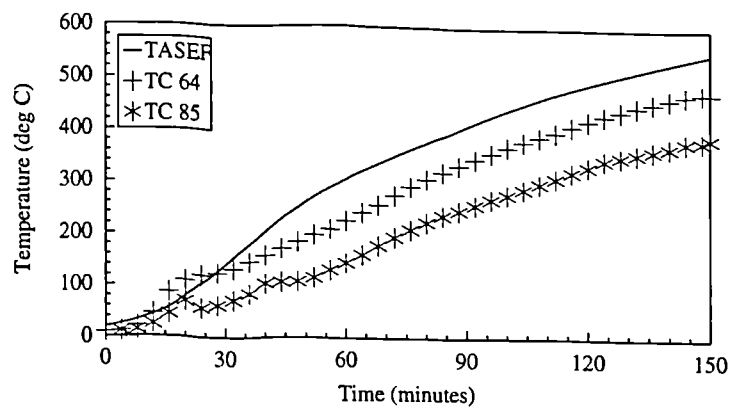


Figure 4.5 Comparison of Temperatures

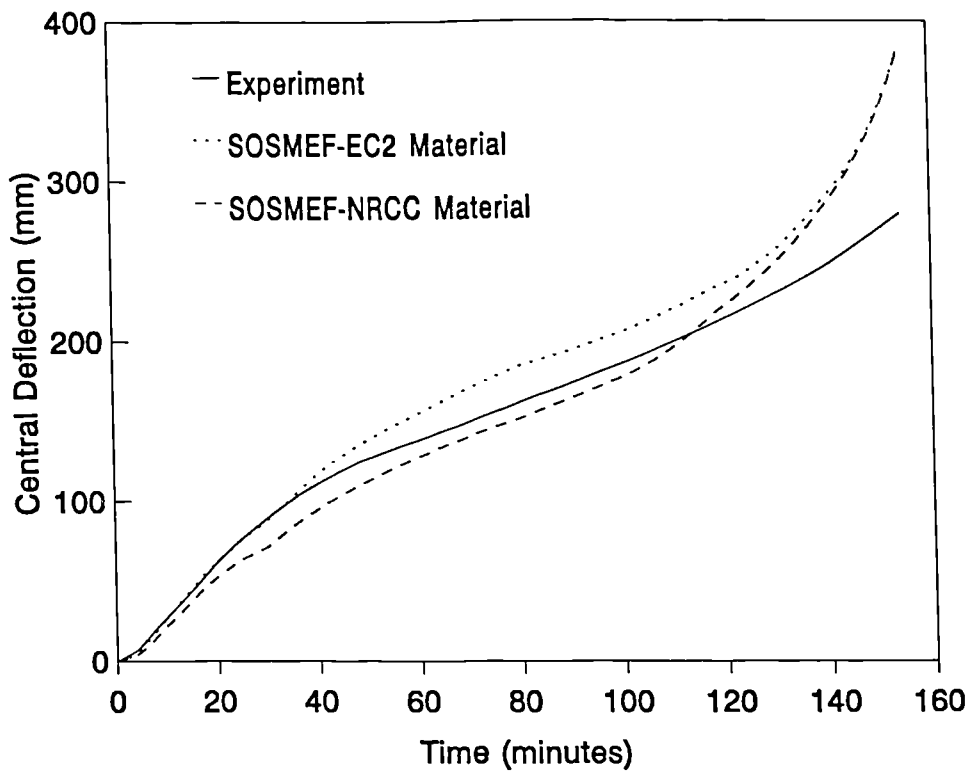
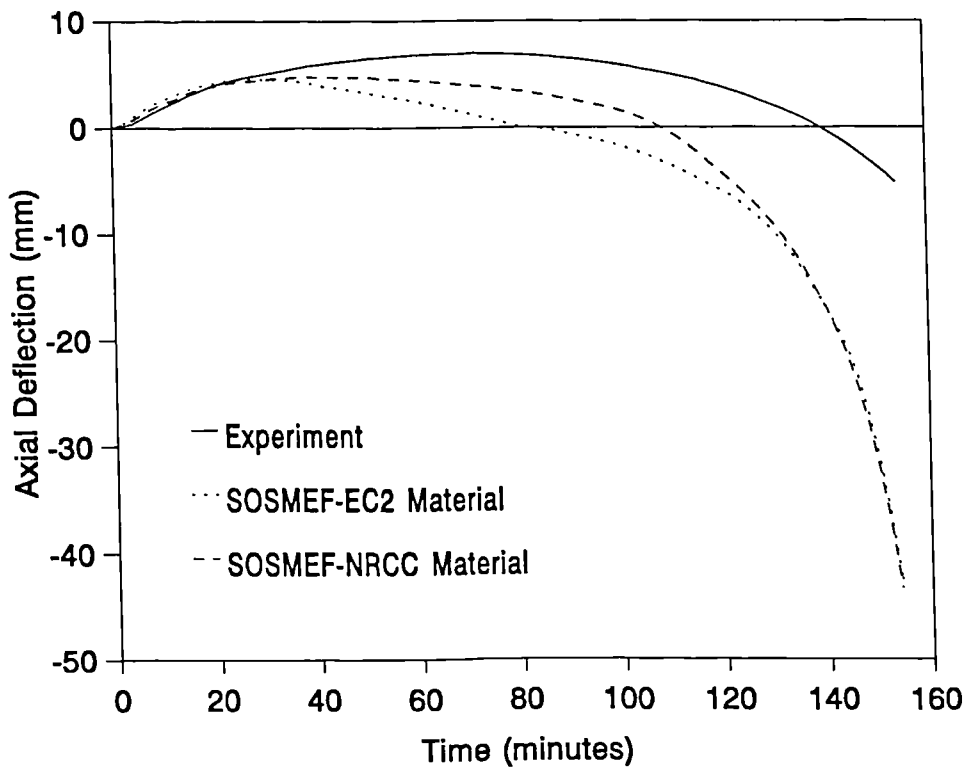


Figure 4.6 Comparison of Deflections - Non-loaded Slab

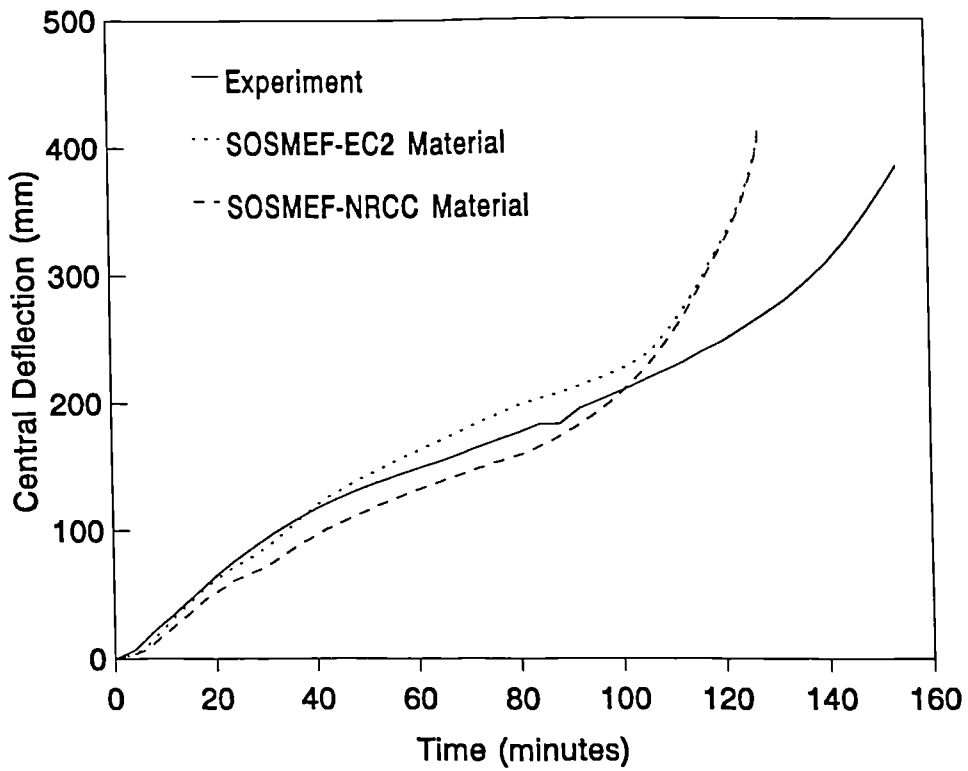
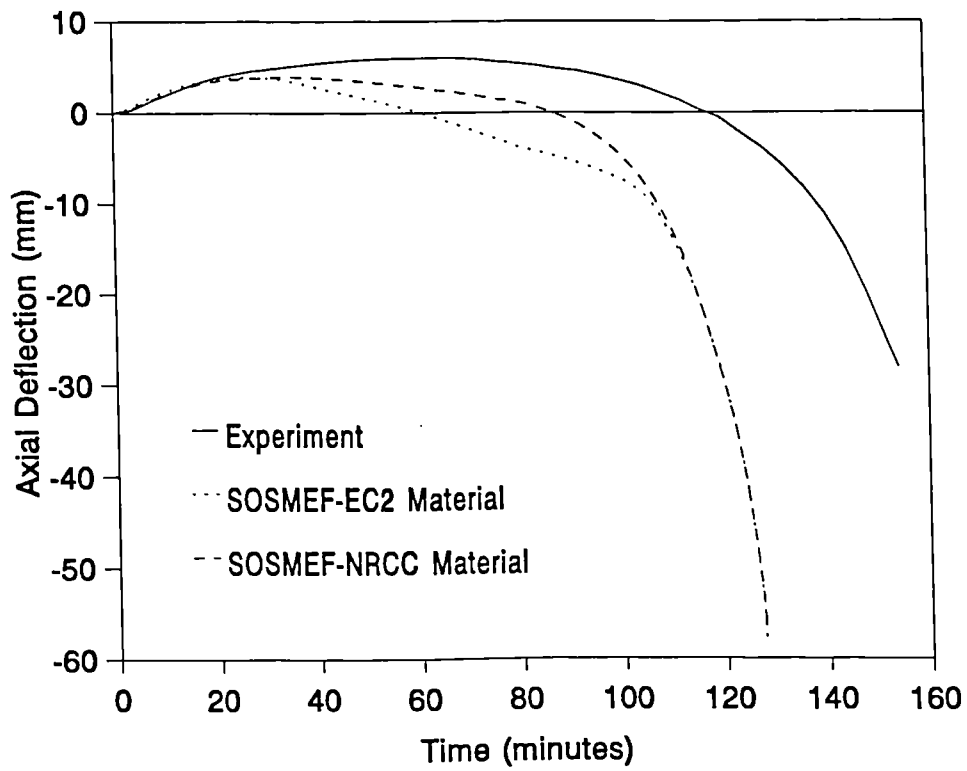


Figure 4.7 Comparison of Deflections - Loaded Slab

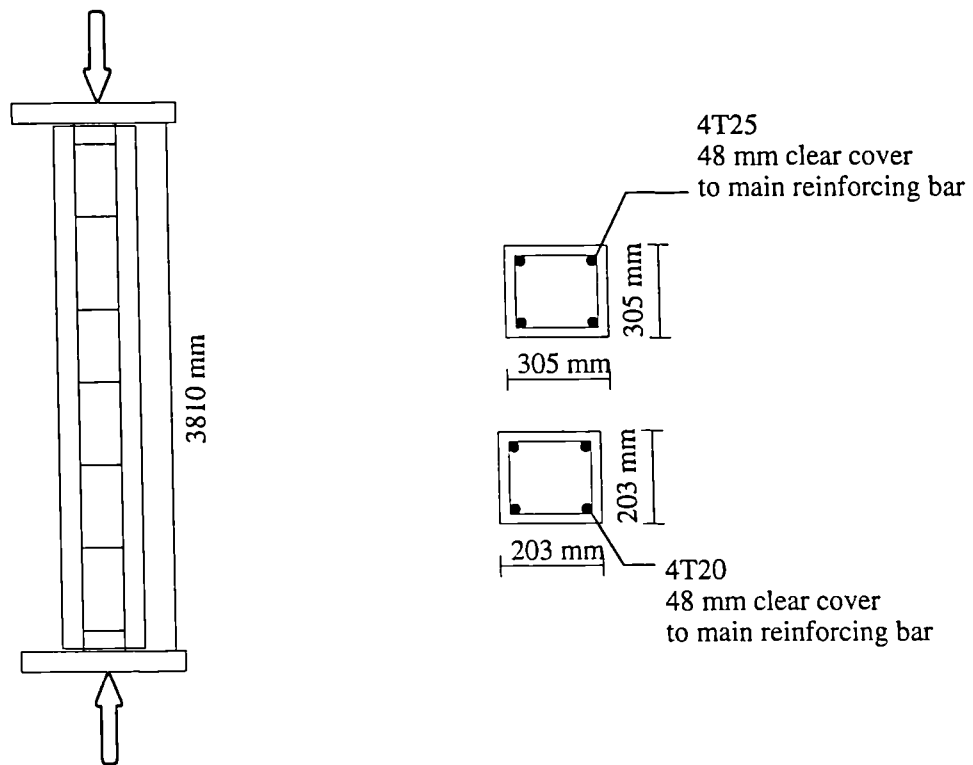
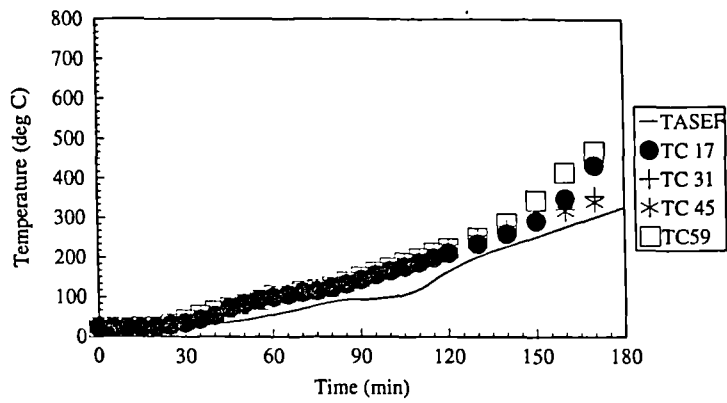
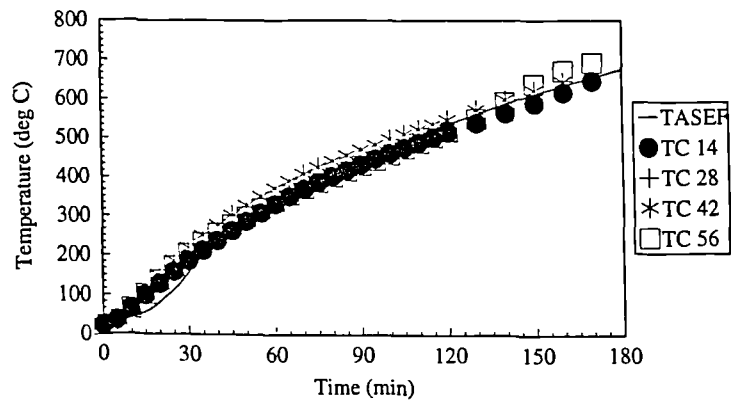


Figure 4.8 Cross Section and Test Arrangement Details

Comparison of Temperatures At Centre



Comparison of Temperature at 114 mm from Centre



Comparison of Temperatures at Reinforcement

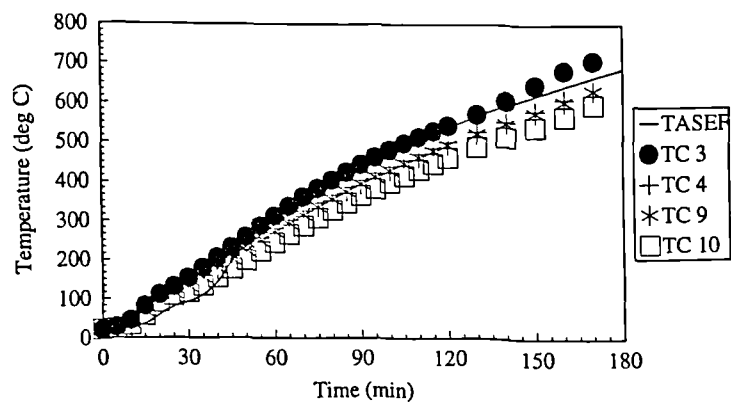
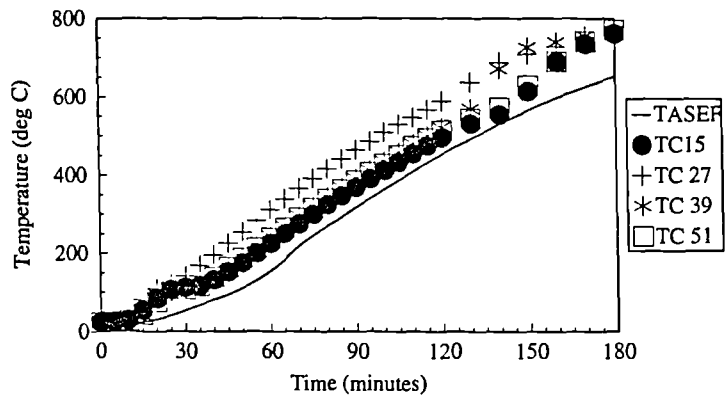
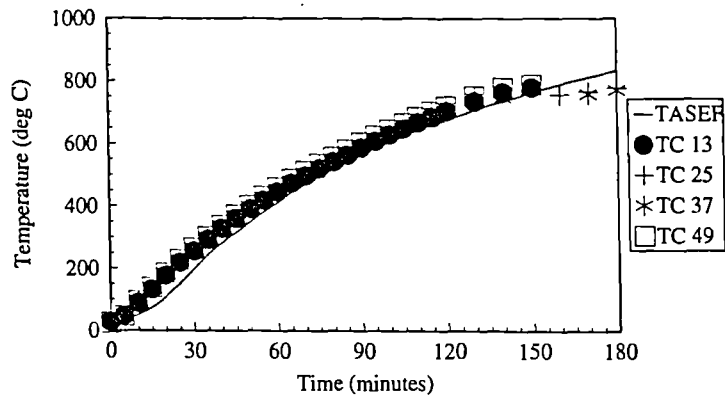


Figure 4.9 Comparison of Temperatures - 305x305 mm Column

Comparison of Temperatures at Centre



Comparison of Temperatures at 69 mm from Centre



Comparison of Temperatures at Reinforcement

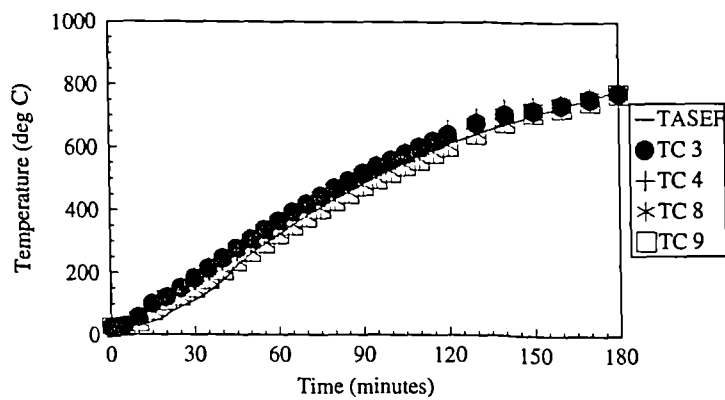


Figure 4.10 Comparison of Temperatures - 203x203 mm Column

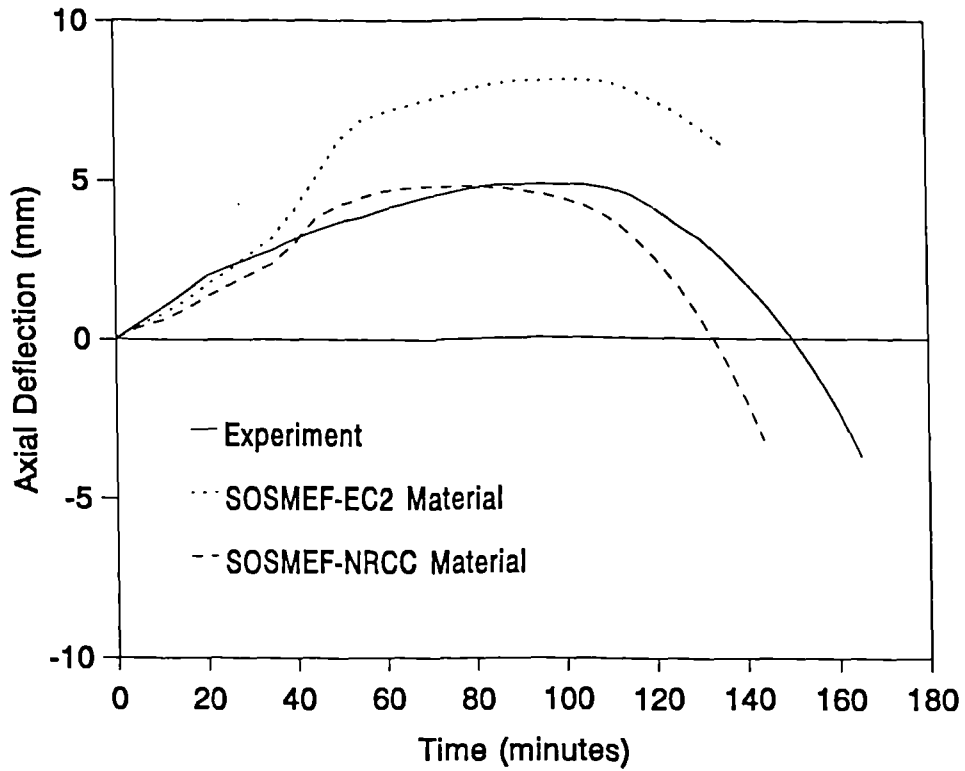


Figure 4.11 Comparison of Deflections - 305x305 mm Column

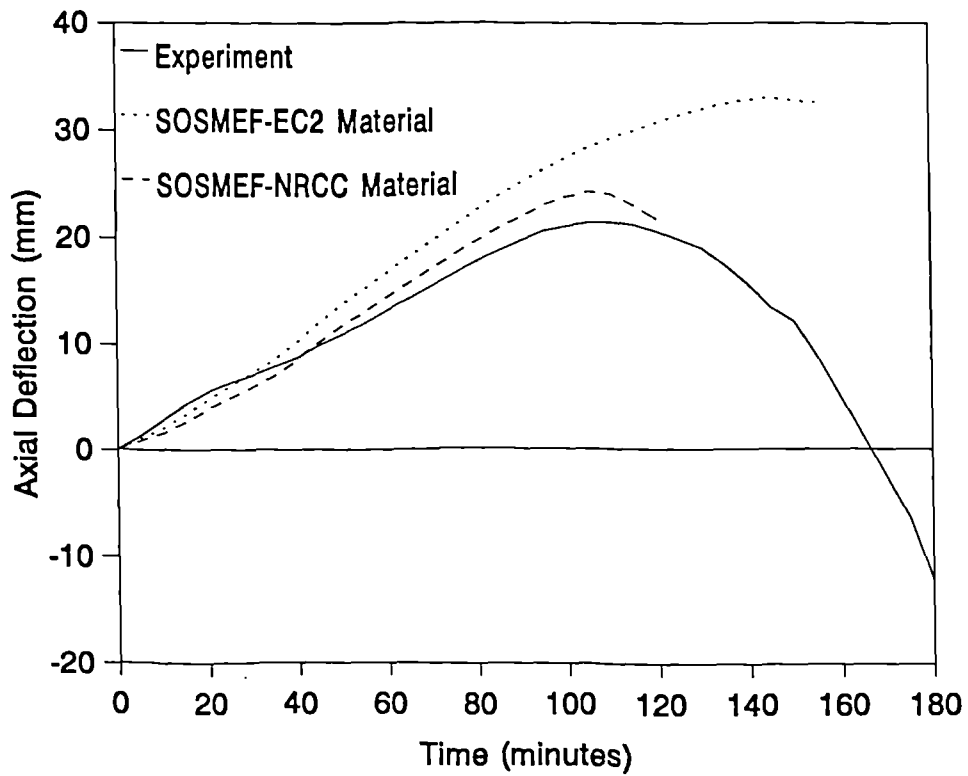
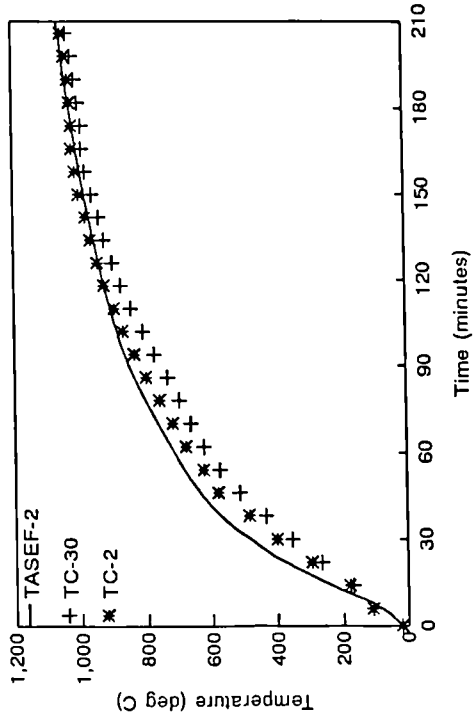
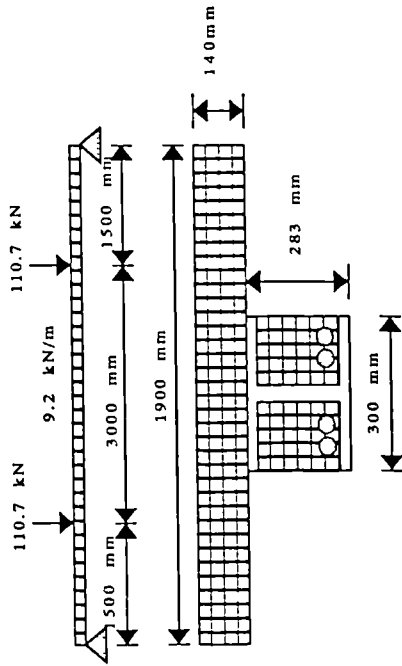
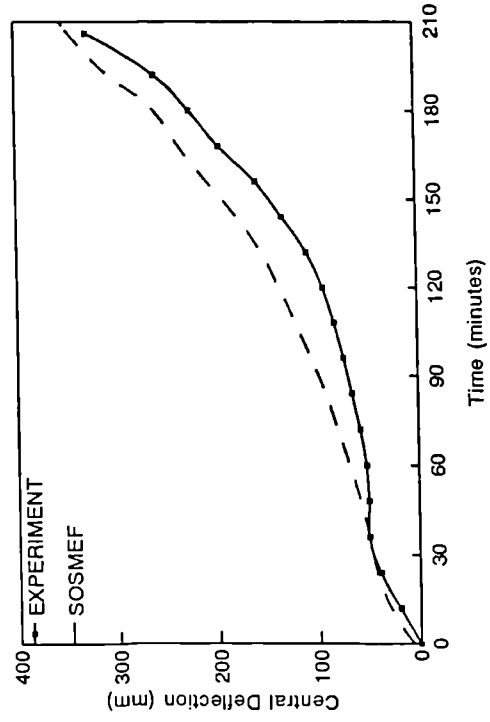


Figure 4.12 Comparison of Deflections - 203x203 mm Column

Comparison of Temperature at Hot Flange and Web Junction



Comparison of Central Deflection



Comparison of Temperature at Web

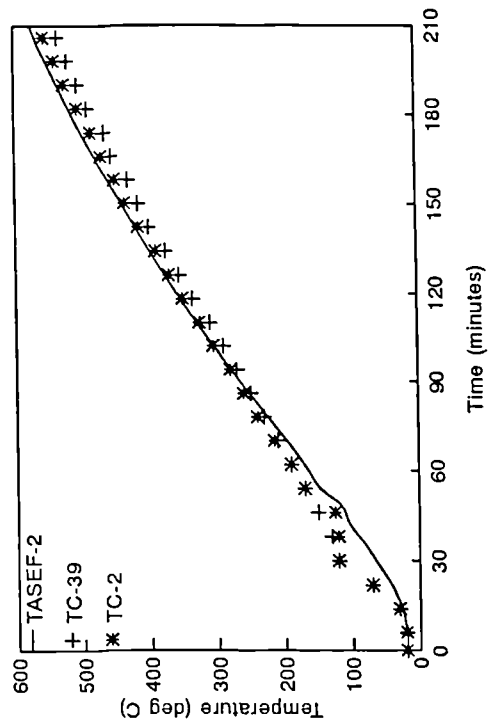
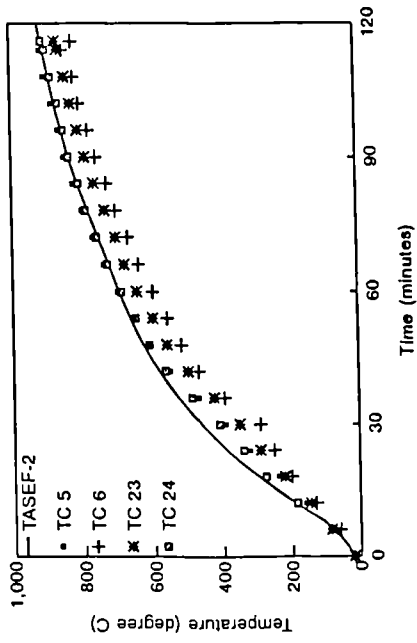
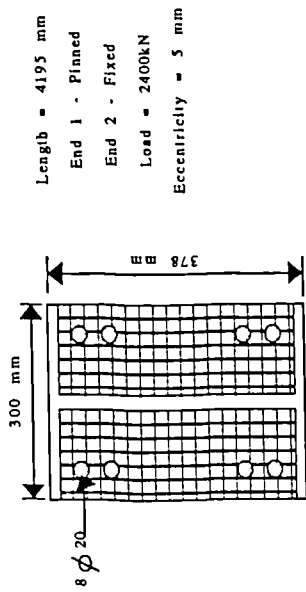
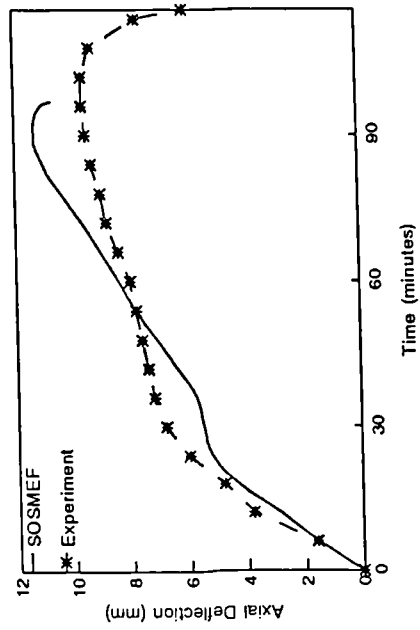


Figure 4.13 Comparison of Results - ARBED Composite Beam

Comparison of Web-Flange Junction Temperature



Comparison of Axial Deflection



Length = 4195 mm
 End 1 - Pinned
 End 2 - Fixed
 Load = 2400kN
 Eccentricity = 5 mm

Comparison of Web Temperature

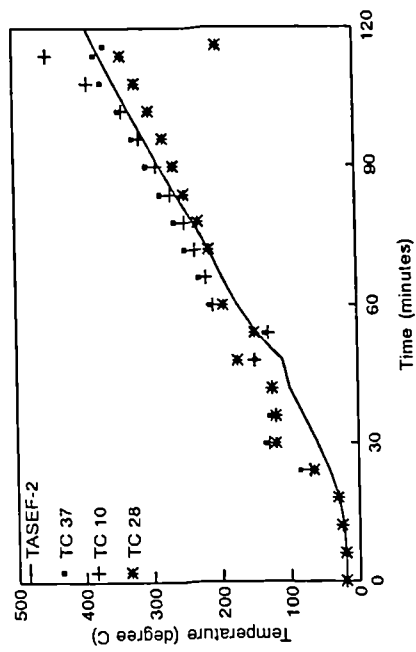


Figure 4.14 Comparison of Results - ARBED Composite Column

CHAPTER 5

EXPERIMENTS ON STEEL COLUMNS WITH TEMPERATURE GRADIENTS

5.0 Introduction

There are several full scale and model scale fire tests on steel columns reported in literature, conducted in the UK and other countries. The majority have the test specimen exposed to fire from all sides and along the full length of the column. There is little data available on the behaviour of steel members with a non-uniform temperature distribution along the length of the member and across the depth of the cross section. In a realistic situation, especially for columns, temperatures may vary not only through the depth but also along the length. This represents a situation where in the event of a fire in a compartment, the column is heated from one or two faces, and due to the accumulation of heat near the top of the compartment, temperatures are higher at the top than at the lower end. The numerical method, described in Chapter 3, is capable of modelling these variations in temperature. To validate the method of analysis and the associated computer program SOSMEF it was decided to perform a number of tests on steel columns with non-uniform temperature distribution along the length as well as across the depth of the cross section. Since it is difficult to control heating in this manner in traditional fire test rigs with burning gas, electrical heating elements were used as the source of heat.

5.1 Test Rig

Initially it was proposed to use an existing test rig at the Fire Research Station, previously used for model scale column tests. Since the maximum load capacity of this existing test rig was 100 kN, it was deemed to be inadequate for any rolled section columns. It was decided to design and manufacture a new test rig with a somewhat higher load capacity. The new test rig has a load capacity of 600kN and was fabricated at City University's Heavy Structures laboratory. The schematic diagram of the test rig is shown in Figure 5.1.

The rig is an assembly of two end blocks bolted to a strong beam. The strong beam was part of a large test frame already available at the Heavy Structures Laboratory. The strong beam had holes drilled through the top flange at regular intervals typical for this type of construction of test rig. The end blocks were made of 20 mm thick steel plates. Each end block was bolted on to the strong beam with 12 No 20 m, bolts. A hydraulic jack was connected to one of the end blocks and a load cell was connected to the other. To restrain any large movements of the end blocks when loaded, both end blocks were connected by two 20mm steel bars at the top.

5.2 Test Specimens and Preparations

It was decided to use the smallest rolled section available for the columns. This ensured the test was full scale. A larger section would have required greater electrical power for heating. The smallest section available was a 76x76x12.65kg joist section. This section is available in 12m lengths. One length of the section was cut into 8 specimens of 1.5m each. One of the 8 specimens was allocated for material property tests. The other seven specimens were tested with varying eccentricities of axial load and with different heating arrangements.

The end conditions at both ends were designed to represent pinned supports. To achieve this, ball and socket bearings were used at both ends. The test specimen was welded to 300mmx300mmx20mm plates at both ends. The eccentricity of loading was achieved by welding the specimen off centre to the end plate. Each end plate was connected to another plate of the same size, permanently connected to the sockets of the bearing. A 25mm New Tacfire board, manufactured by Eternit, Promat Fire Protection Division, Meldreth, Herts SG8 5RL, was placed in between the pairs of plates at each end to avoid any heat being conducted to the Load cell at one end or the Hydraulic Jack at the other end. This material had the required low conductivity together with compressive strength to withstand the maximum expected stress.

5.3 Electrical Heating Elements and Thermal Insulation

Two heating elements with transformers supplied by the Fire Research Station were used. Heating elements were manufactured by Electrothermal Engineering Ltd., Southend-on-Sea, Essex. The size of the elements was 67mm wide by 30mm thick by 680mm long. A photograph of the heating element is shown in Figure 5.2. For the first test, only one heating element was used. However, it became clear during the test that a single element was not capable of heating the specimen to temperatures exceeding 500°C. For all other tests, therefore, two heating elements were used. To obtain a non-uniform temperature distribution across the depth of the section and along the length of the column, both elements were tied together and held against the bottom flange, either approximately at the middle of the column or nearer one end of the column, depending upon the location of maximum heat desired in the experiment.

To reduce heat loss from the heating elements, 25mm thick New Tacfire insulation boards were used to insulate the heating elements from the atmosphere. A schematic diagram of the arrangements is shown in Figure 5.3.

5.4 Temperature Profile Measurement

To obtain a comprehensive temperature profile of the test columns, 48 thermocouples were used. The thermocouples were K type 1.0mm diameter and 3m long, with stainless steel sheathing, and with extension cables insulated with TEFLON. The thermocouples were purchased from ARI industries (UK) Ltd. Unit 2F, Albany Park, Frimley Road, Camberley, Surrey GU15 2GL. Thermocouples were installed into 1.2mm diameter and 3mm deep holes drilled at the positions shown in Figure 5.4. To avoid the thermocouples from becoming accidentally dislodged because of deformations during the test, a special mounting device was used. This consisted of a 90° bent steel plate fixed to the test specimen. Thermocouple wires were passed through holes in the bent plate and their ends were fixed to the test specimen. This ensured that the ends experienced no pull as the column deformed. A photograph of the device and thermocouples attached to a specimen is shown in Figure 5.5.

5.5 Deflection Measurements

To obtain a measure of the deflected shape of a test column in the horizontal and vertical directions, as well as to measure the axial displacement and end rotations about the major axis, 14 displacement transducers were used (except for Test1 and Test2 which had 8 and 13 transducers respectively). The positions of the transducers are shown in Figure 5.6. To avoid heating the transducers due to conductive heat transfer, 10mm diameter Vitreous rod extensions, purchased from Heraeus Silica and Metals Ltd., 1 Craven Court, Canada Road, Byfleet, Weybridge, Surrey KT14 7JL, were used. The vitreous rods were supplied in 1m lengths. The rods were then cut into 150mm pieces. Connectors, to join the end of the transducer shaft and one end of the extension rod, were manufactured from aluminium rods, to suit individual transducers. The other end of the extension rod was tapered to approximately 2mm diameter, to minimise the contact area with the specimen. A view of the deflection transducers is shown in Figure 5.7

5.6 Loading Equipment and Axial Load Measurement

A hydraulic jack of 50 tonnes capacity was used to apply the axial load. For Test 1, the load was applied using a manually operated pump. It was found that maintaining the constant axial load using this pump was very difficult. For all other tests an electronically operated pump was used. A load cell with a range of up to 50 tonnes was used to monitor the axial load applied. Figures 5.8 and 5.9 show views of the hydraulic jack end and the load cell end of the test rig, respectively. The applied load was recorded, however, along with other measurements throughout the tests.

5.7 Data Recording

All thermocouples and displacement transducers were connected to an Intercole data logger which was controlled by a BBC Microcomputer. During the test, the data is displayed on screen, printed on a dot matrix printer and recorded on to a floppy disk. Figure 5.10 shows a general view of the complete experimental setup

5.8 Test Procedure

The following procedure was adopted in preparation for the experiments

- ✘ After welding the end plates, measure the initial imperfections of the specimen in both the X and Y directions (see Figure 5.11).
- ✘ Place the specimen in the rig and connect the heating elements, thermocouples and displacement transducers.

The following procedure was used in conducting the experiments:

- ✘ Record initial measurements
- ✘ Apply a pinch load and record the measurements
- ✘ Apply the full test load and record the measurements
- ✘ Start the heating and start the automatic time based data logging to record the data at 2 minute intervals.

- ⌘ Load cell readings were also taken at 2 minute intervals . Maximum effort was applied to keep the axial load at a constant value. However, there were small unavoidable variations in the value of the axial load during all the tests.
- ⌘ If the specimen did not fail when the rate of increase in the temperature of the steel reached a very small value, then the axial load was increased slowly until the failure occurred.

Eccentricity in the X direction was measured positively in the downward direction, i.e. the positive eccentricity will result in the specimen bending upwards, towards the transducers. Eccentricity in the Y direction is measured towards the top flange, i.e. the positive eccentricity will result in bending towards the heating element. Figure 5.11 shows the cross section of the test columns and defines the directions of axes X and Y referred to in this Section.

Test 1

This was a learning test. The displacement transducer arrangement was slightly different from the other tests shown in the Figure 5.6. Only one transducer was used to measure the central deflection in the Y direction instead of transducers 6&9 as shown in Figure 5.6. Transducer 14 was not used. Axial displacement and end rotation measurements were taken using manually read dial gauges. Reading all four dial gauges at the same time from beyond the safety net was found to be very difficult. As mentioned in Section 5.6, in this test, the axial load was applied using a manually operated pump. Maintaining the constant axial load using this pump was also found to be very difficult. The load was applied concentrically at both ends.

The heating element was placed approximately at the centre of the element. The test load applied was 17.6 tonnes (approximately 173 kN). Load cell and dial gauge readings were taken at 2 minutes intervals. At 98 minutes the rate of increase in the temperature of the specimen was found to be very small. The axial load was then increased at the

rate of approximately 1.0 tonne per minute. The specimen failed at 104 minutes. The failure load was 24.0 tonnes (235.4 kN).

Test 2

The lessons learnt from Test 1 were adopted in this and subsequent tests. Loading was applied using an electronically controlled pump. The displacement transducer arrangement was as shown in Figure 5.6 except that transducer 14 was not used. The Heating elements were placed near the jack end. The end of the heating element was at 75 mm from the end plates. Except for the load cell readings all the other measurements were automatically made using the data logger. As a result of non-uniform heating, the maximum vertical deflection occurred between the transducer positions 2 and 3. From the experience of this test, for all other tests, displacement transducer 14 was used to record the deflection in the vertical direction at a point half way between transducers 2 and 3.

The test load applied was 10.5 tonnes (103.0 kN). Eccentricities of 10 mm in the X direction and 25 mm in the Y direction were introduced at both ends. The load was kept constant until failure occurred at 54 minutes.

Test 3

The displacement transducer arrangement for this test was as shown in Figure 5.6. The heating elements were placed at the jack end of the specimen. There were no eccentricities in the X direction. Eccentricities of 25 mm were introduced in the Y direction at both ends. The test load applied was 12.5 tonnes (122.6 kN). As the rate of increase in temperature of the specimen at 104 minutes became very small, it was decided to increase the load at the rate of 0.25 tonnes per minute. The specimen failed at 112 minutes at a failure load of 14.5 tonnes (142.2 kN).

Test 4

For this test, heating elements were placed approximately at the centre of the specimen. There were no eccentricities in the X direction. Eccentricities of 25 mm were introduced in the Y direction at both ends. The test load applied was 14.0 tonnes (137.3 kN). This load was kept constant until failure occurred at 50 minutes.

Test 5

For this test, the heating elements were placed near the jack end of the specimen. There were no eccentricities in the X direction. Slightly higher eccentricities of 35 mm were introduced in the Y direction at both ends. The applied axial load for this test was 11.5 tonnes (112.8 kN). The load was kept constant throughout the test until failure occurred at 62 minutes.

Test 6

This test was identical to test 5 except for the applied axial load, which was 10 tonnes (98.1 kN). The axial load was maintained at a constant value throughout the test. The failure time for this test was 70 minutes, which is higher than that of test 5, as expected.

Test 7

Once again, the heating elements were placed at the jack end of the specimen. The test load applied was 8.0 tonnes (78.1 kN). Eccentricities of 5 mm in the X direction and 30 mm in the Y direction were introduced at both ends. The load was kept constant until failure was obtained at 78 minutes.

Details of the eccentricities of all the test columns are summarised in Table 5.1. The measured mid span initial imperfections of all the specimens are given in Table 5.2.

Table 5.1 Eccentricities of Test Columns

Column Number	Eccentricity (mm)	
	X Direction	Y Direction
1	0	0
2	10	25
3	0	25
4	0	25
5	0	35
6	0	35
7	5	30

Table 5.2 Mid Span Initial Imperfection of Test Columns

Column Number	Initial imperfection(mm)	
	X Direction	Y Direction
1	*	*
2	0.000	0.000
3	0.125	-0.150
4	0.010	-0.015
5	0.555	-0.040
6	0.560	-0.350
7	0.050	-0.025

* - No measurement was made

5.9 Material Properties Test

Three specimens were made for material property tests. The specimens were cut one from each flange and one from the web. These specimens were tested using a Schand tensile testing machine, to obtain yield stress and ultimate stress at room temperature. The results of these tests are given in Table 5.3

Table 5.3 Material Property Test Results

Sample No.	Yield Stress (N/mm ²)	Ultimate Stress (N/mm ²)
Flange 1	329.42	480.2
Flange 2	333.33	477.8
Web	329.58	504.0
Average	330.78	487.3

5.10 Results

Figure 5.12 shows the variation of the applied axial load with time for all seven tests. Apart from tests 1 and 3, where the load was slightly increased towards the end to induce failure, it will be seen that the applied load was kept almost constant in all the tests. Figure 5.13 shows the temperature distribution across the depth and along the length of all seven test columns at failure. The contours have been plotted from the observed thermocouple readings. The maximum temperature attained was 700°C which shows the effectiveness of using electrical heating elements. Figures 5.14 and 5.15 show the permanently deflected shape, about the major axis and the minor axis respectively, of all seven test columns after the experiment. Figures 5.16-5.22 show the variation of measured end rotations with time for all seven test columns. Deflections in the X, Y and axial directions are compared with the computed values in Section 5.10.2, which also gives a comparison of the computed and experimental failure loads.

A sample set of raw experimental data is given in Appendix 2. Complete experimental data is given in a separate report^[127].

5.10.1 General Observations

Although only two columns (columns 2 and 7) were subjected to biaxial eccentricities, all seven columns failed in a biaxial mode. It was also noticed that the deflection about the minor axis was almost non-existent up to the failure time and then sudden bending about the minor axis occurred. This behaviour indicates that the failure was mainly due to buckling. Maximum deflection was always observed to be approximately at the location where the column was experiencing maximum temperature.

5.10.2 Comparison of Computed and Experimental Results

The main objective of the test programme was to obtain data to validate the numerical method and its associated computer program SOSMEF described in Chapter 3. For calculation purposes, the Stress-Strain-Temperature relationship of steel as

recommended in Eurocode 3: Part 10, was used. The only variable used is the yield stress at room temperature. The average measured yield stress of 330.78 N/mm^2 given in Table 5.3 was used. In the analysis, all columns were allowed to bend biaxially. It is assumed that the initial imperfection of all the columns was sinusoidal in both directions with the midspan amplitude of the measured values given in Table 5.2. For Test 1 the midspan initial imperfection was not measured. For this test, a value of $L/1000$ as specified in codes of practice was used.

Two types of analysis were carried out.

- ✘ Calculation of the failure load
- ✘ Structural response of the column with time

Calculation of failure load

The purpose of this analysis is to find out the load carrying capacity of a member subjected to a given temperature distribution. For this calculation, the measured temperature distributions of the specimens at the failure time shown in Figure 5.13, were used. The axial load was increased in steps until the failure was predicted. The computed failure load is defined as the last load at which an equilibrium deflected shape was obtained and the load increment has reached a value which is less than the value of the accuracy specified in the data.

The comparison between the computed and experimental axial loads at failure is given in Table 5.4. An examination of the last column in the table shows excellent agreement between the calculated and experimental values of failure loads. Not only is the mean value of the ratio between computed and experimental failure loads close to unity, but the standard deviation is also very small.

Table 5.4 Comparison of Axial Load Capacities of Tested Columns

Column Number	Axial Load at Failure (kN)		Ratio (2)/(1) (3)
	Test (1)	SOSMEF (2)	
1	235.4	228.8	0.972
2	103.0	107.5	1.044
3	142.2	128.6	0.904
4	137.3	146.2	1.065
5	112.8	107.1	0.949
6	98.1	94.6	0.964
7	78.1	81.9	1.043
		Mean	0.992
		Standard Deviation	0.055

Structural response of column with time

The objective of this analysis is to predict the structural response of the test columns for a given time-temperature distribution and loading data. Experimental values of the applied load and thermocouple readings were used for all the columns. The variation of the applied load was also modelled as it was measured in the test. Analysis was carried out up to the time failure is predicted or up to the time the test was terminated. The failure time was defined as the time at which an equilibrium deflected shape was obtained and the time increment has reached a value which is less than the value of the accuracy specified in the data.

The comparison of the computed and experimental deflected shapes at different times, and the comparison of computed and experimental central and axial deflections for all the tests are shown in Figures 5.23-5.43.

Figures 5.23-5.43 show that the program SOSMEF computes the deflections very accurately up to just before collapse. For each test, two types of graphs are presented. One set of graphs shows the deflections along the length at selected events. The other set of graphs shows the development of axial deflections, and lateral deflections at midspan. The graphs show that the numerical method gives good results for the case with variations in temperature both across the depth of the column and along its length.

It should be emphasised that the good comparison with these tests shows that the proposed method is capable of dealing effectively with concurrent fire and instability conditions.

5.11 Conclusions

Seven experiments have been conducted, on columns with non-uniform temperature distributions both along their length and across their depth. This type of variation is more realistic for steel columns exposed to fire. The main purpose of these experiments is to provide data to validate the numerical method developed in Chapter 3. The comparison of results shown in Table 5.4 and Figures 5.23-5.43 shows an excellent agreement between computed and experimental results covering failure loads as well as deflection profiles for the full duration of the tests. From these results, it can be concluded that the numerical method is capable of accurately predicting the behaviour of steel columns subjected to non-uniform temperature distributions along the length and across the depth, accurately.

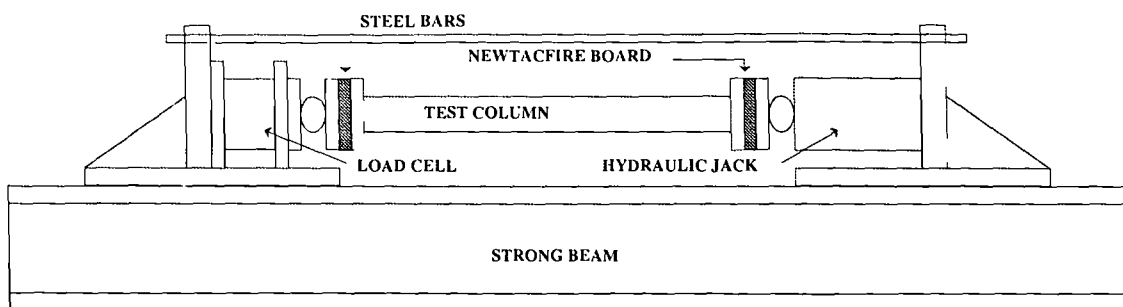


Figure 5.1 Schematic Diagram of Test Rig

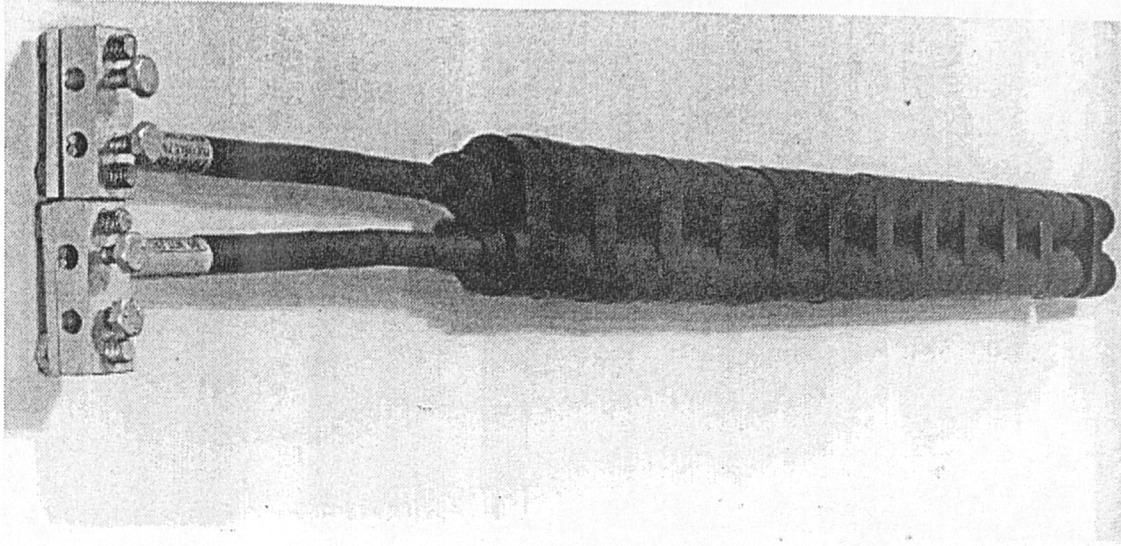


Figure 5.2 Electrical Heating Element

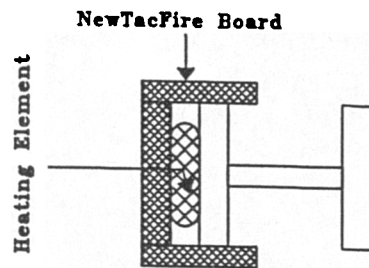


Figure 5.3 Arrangement of Heating Element and Insulation

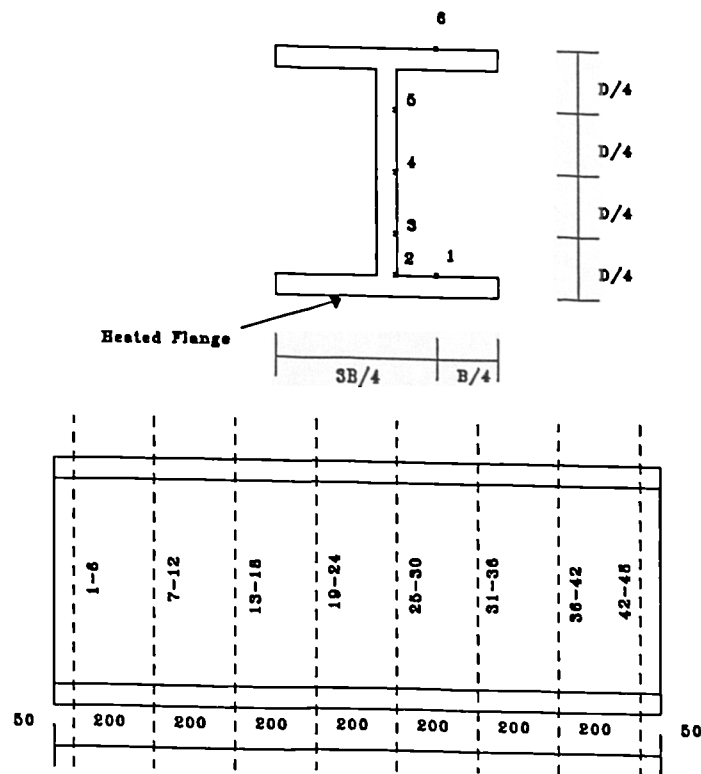


Figure 5.4 Thermocouple Positions

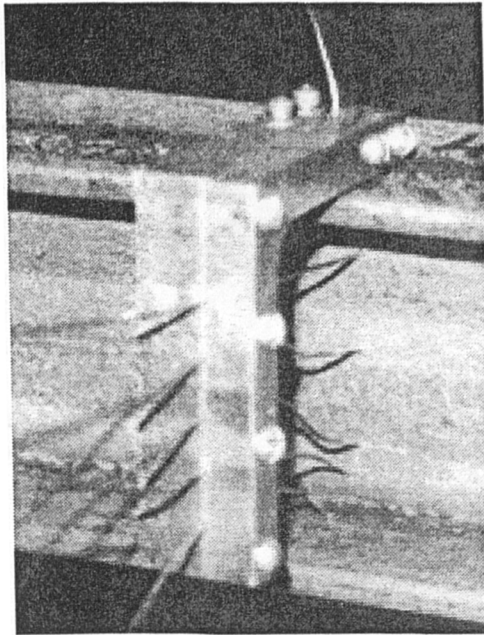


Figure 5.5 Device to hold Thermocouples in Position

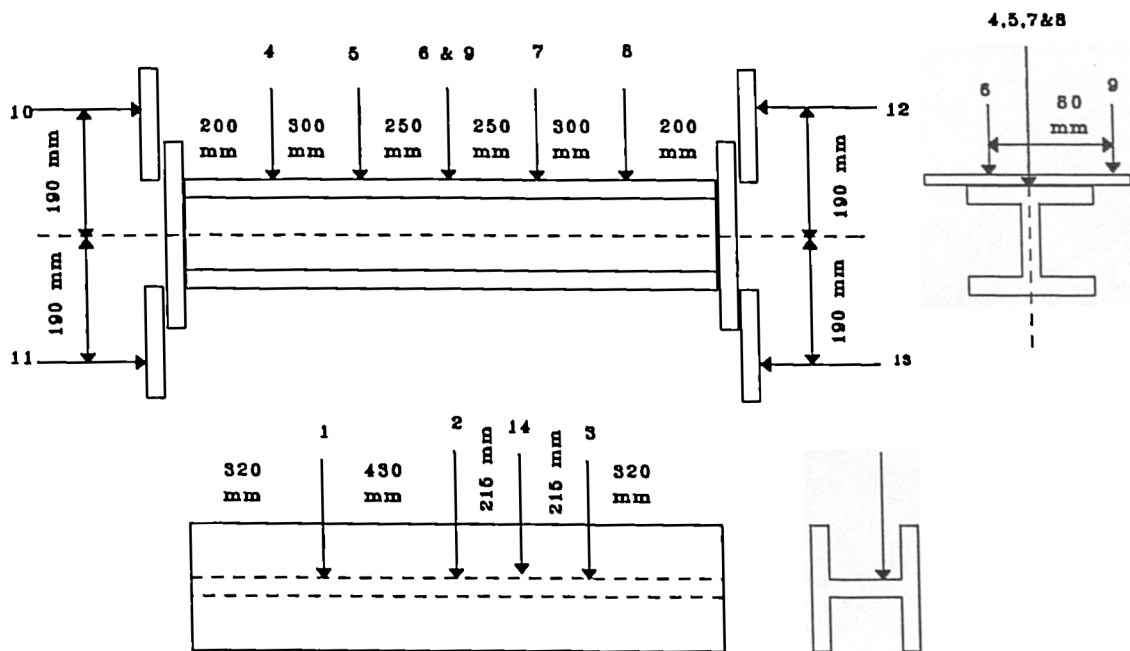


Figure 5.6. Displacement Transducer Positions

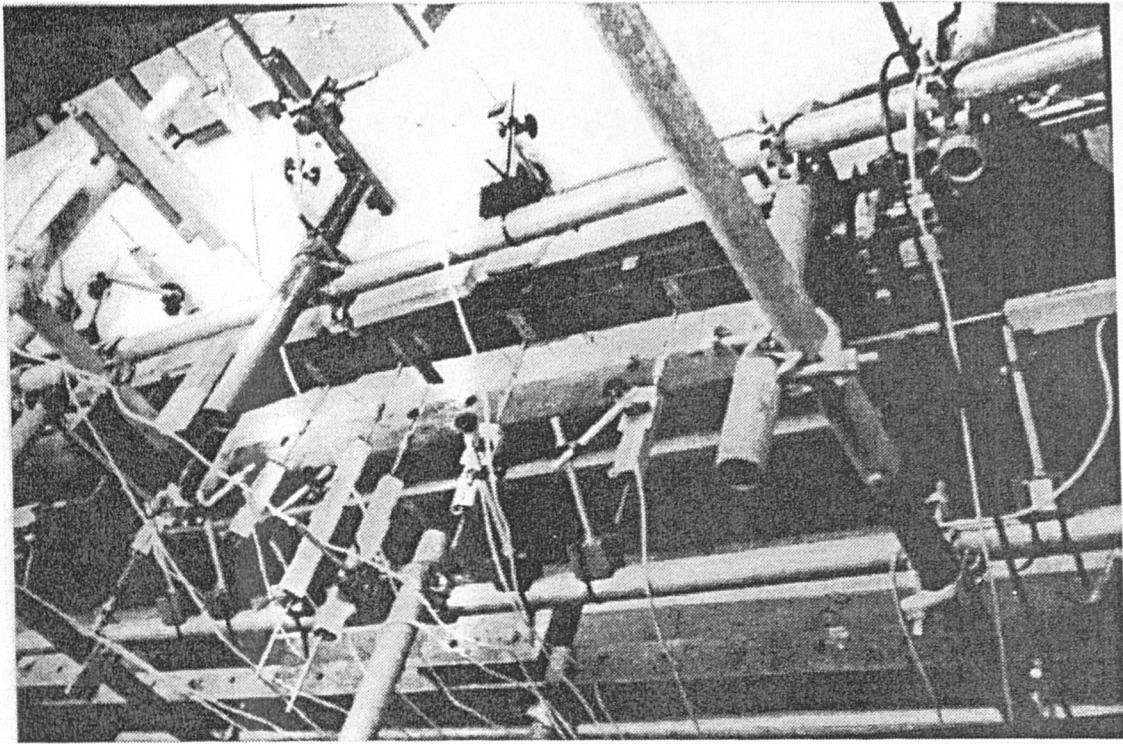


Figure 5.7 View of the Deflection Transducers

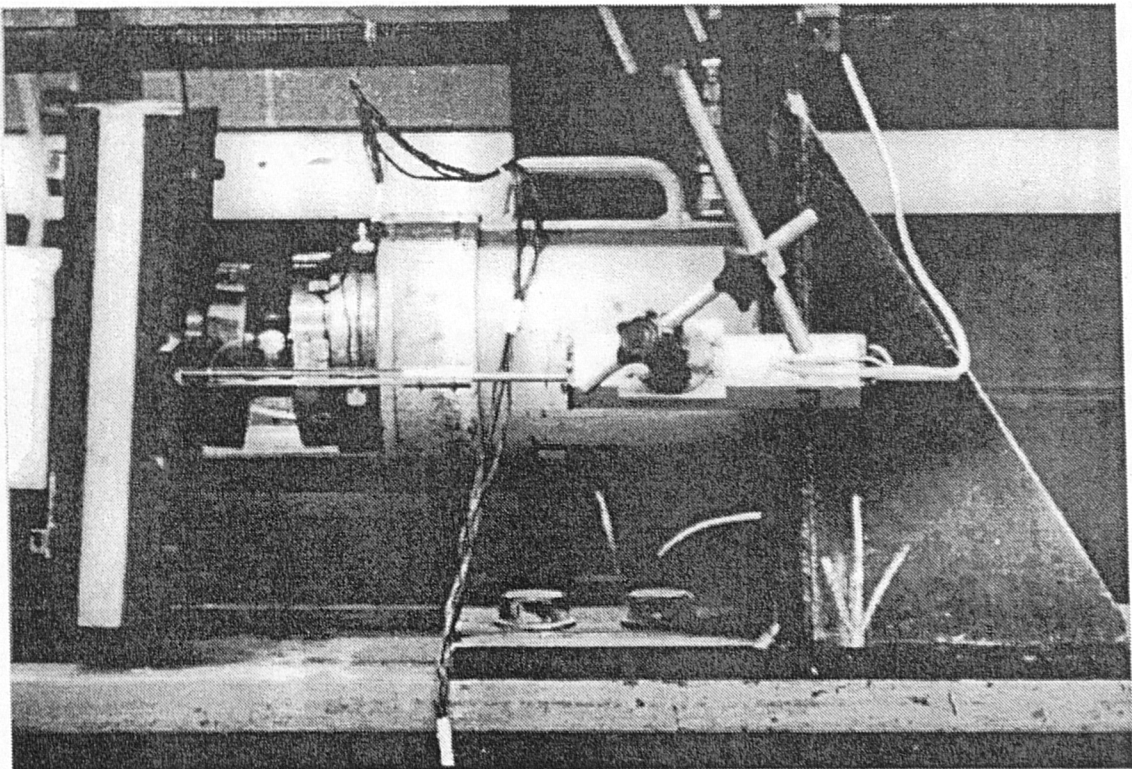


Figure 5.8 View of Hydraulic Jack End of the Rig

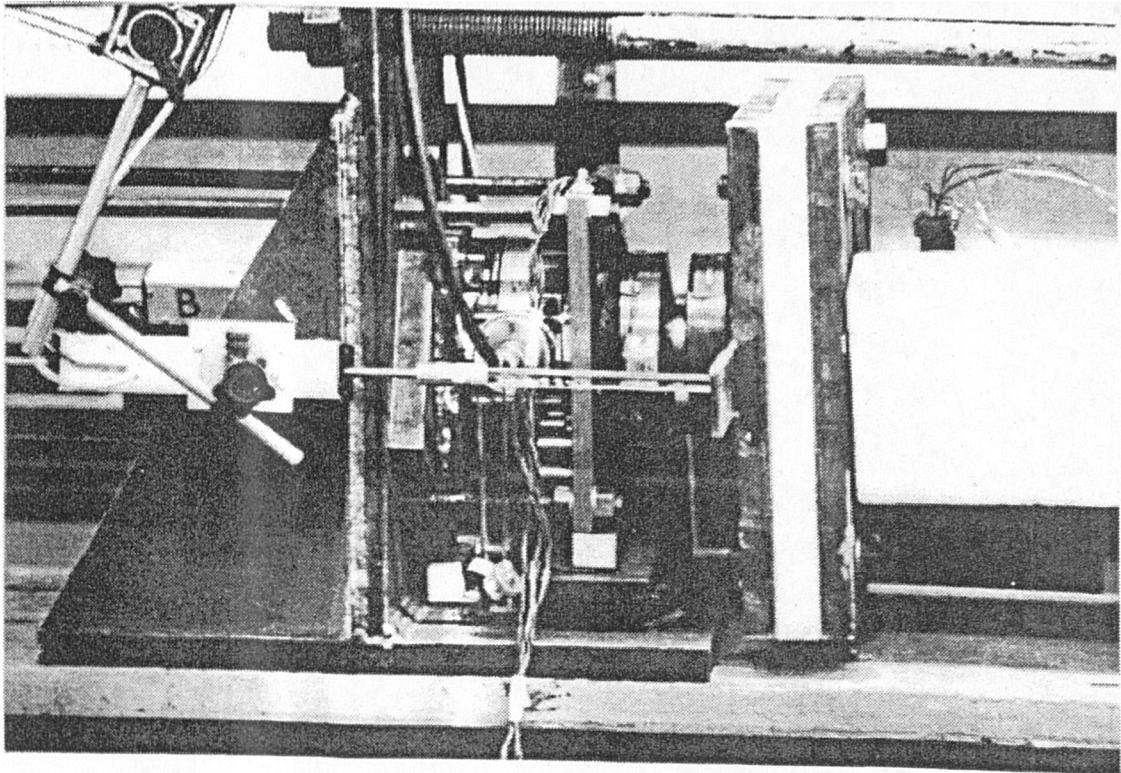


Figure 5.9 View of Load Cell End of the Rig

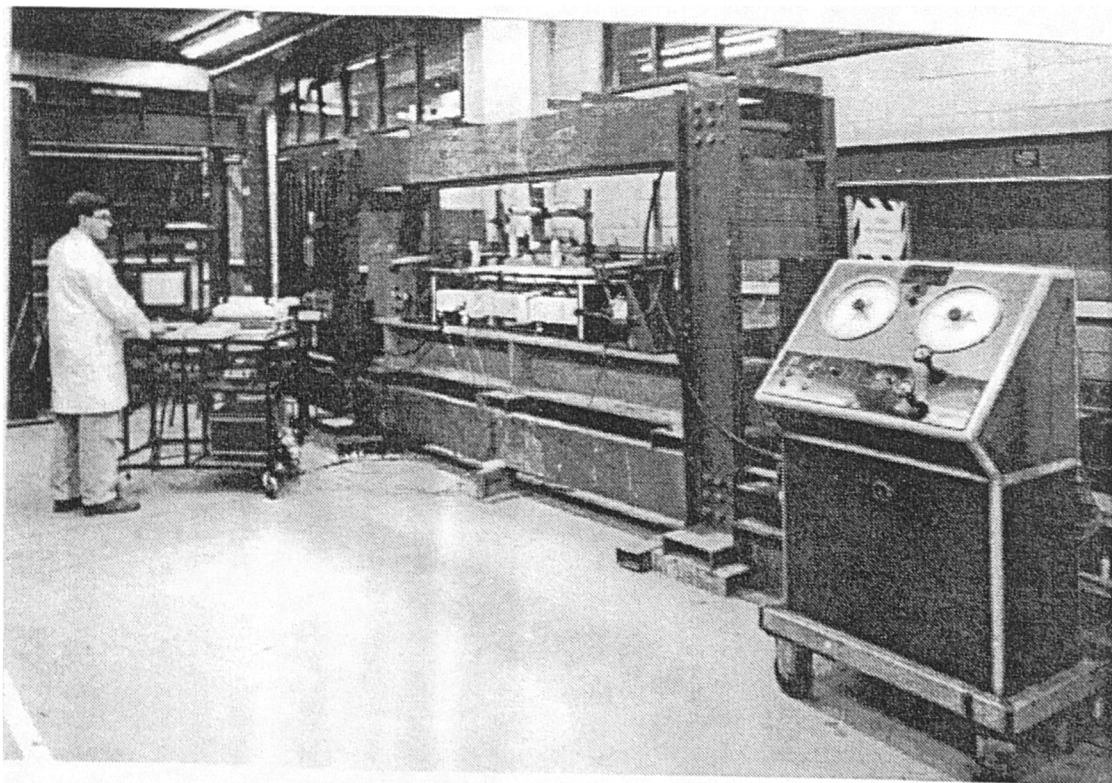


Figure 5.10 General View of the Experimental Rig

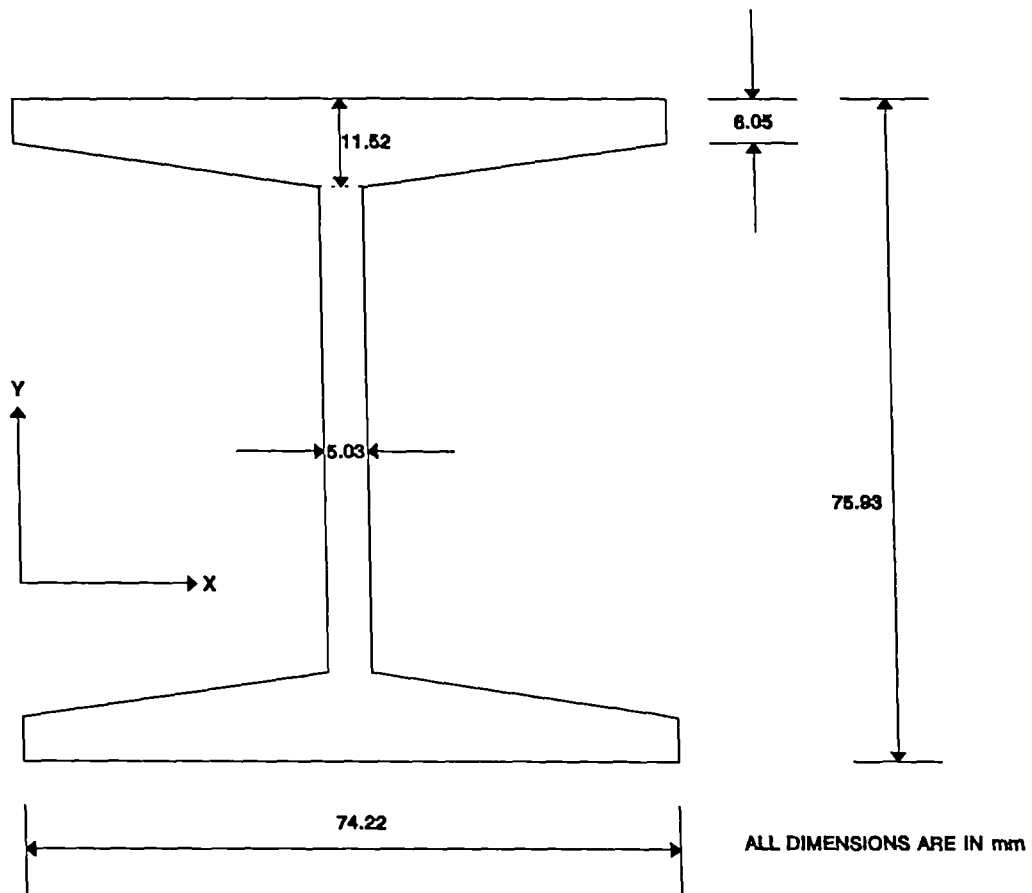


Figure 5.11 Cross Section Dimensions of Test Columns

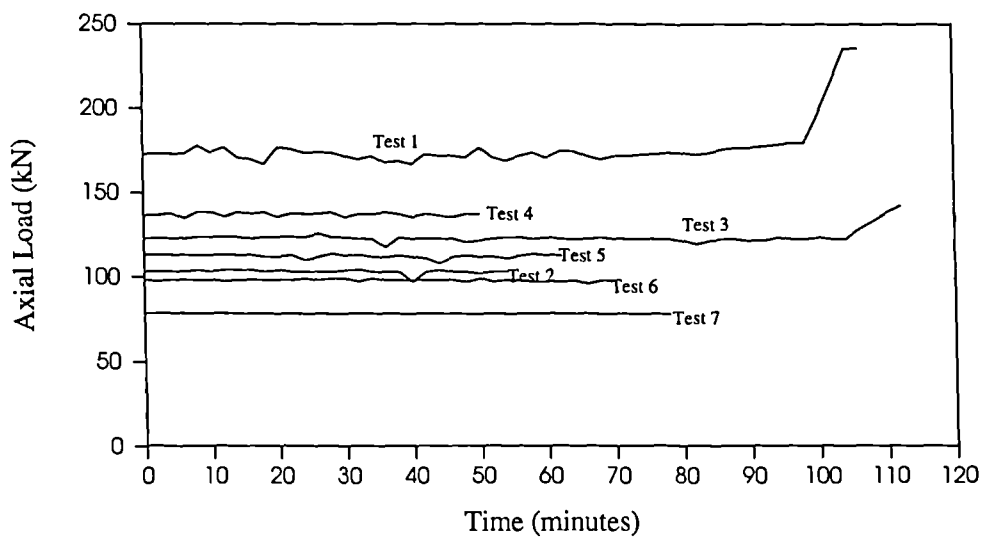


Figure 5.12 Variation of Axial Load With Time For Test 1

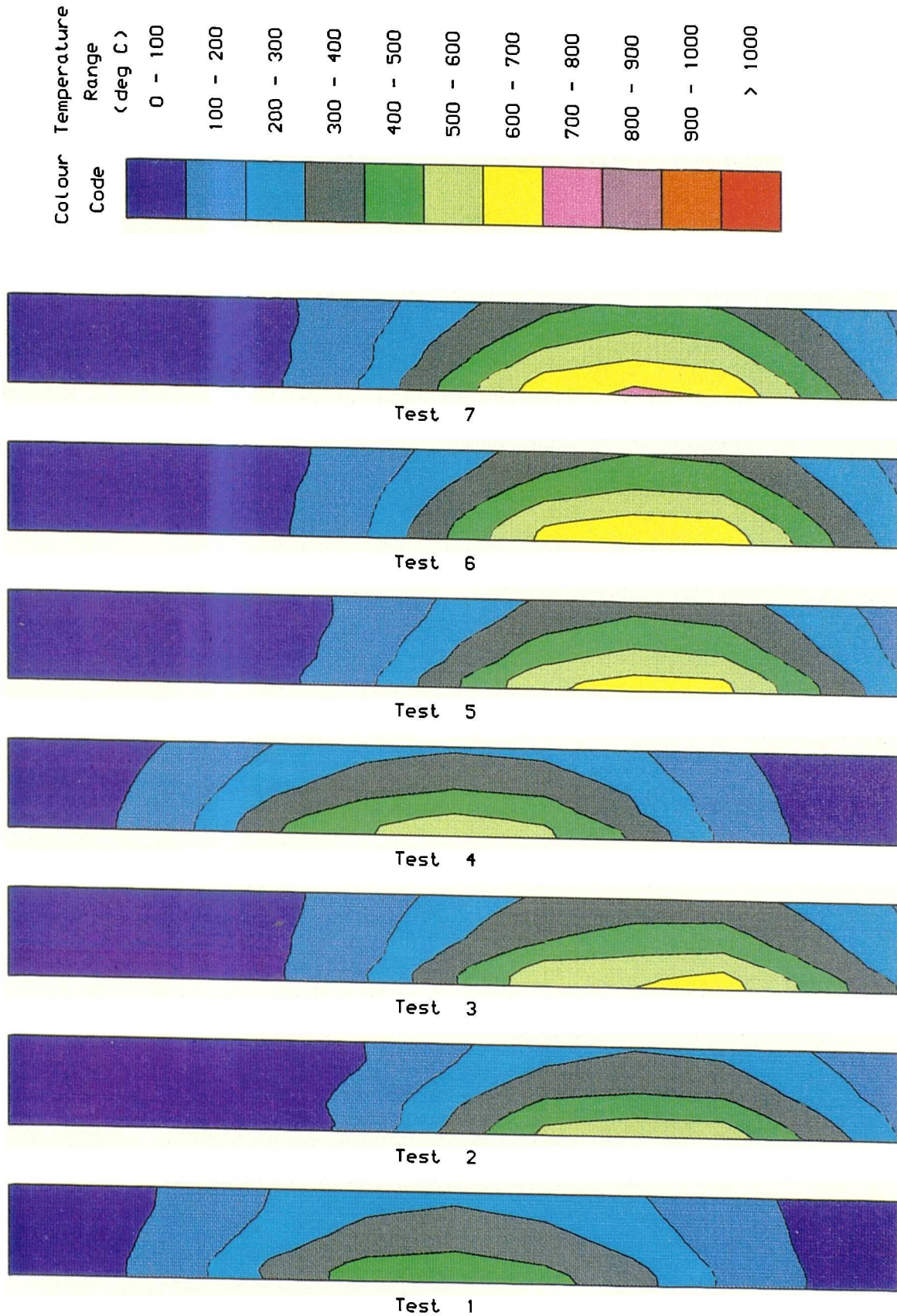


Figure 5.13 Temperature Distribution of Columns at Failure

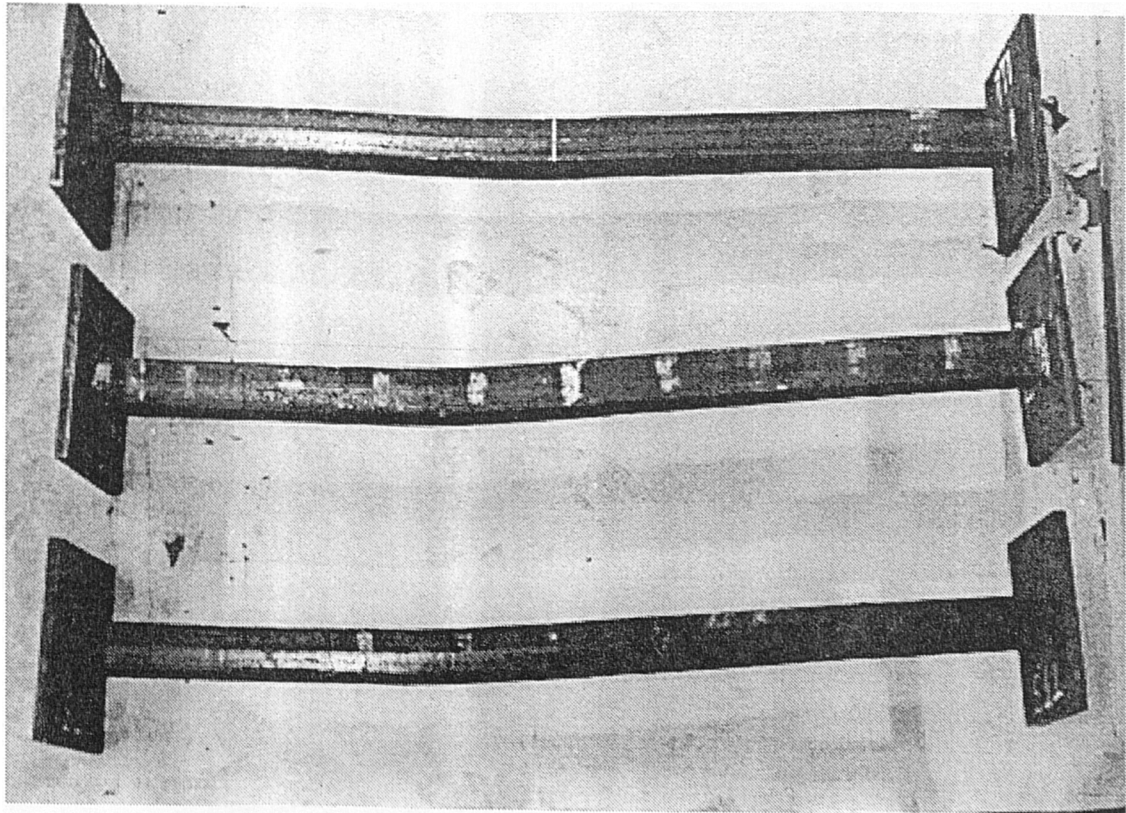
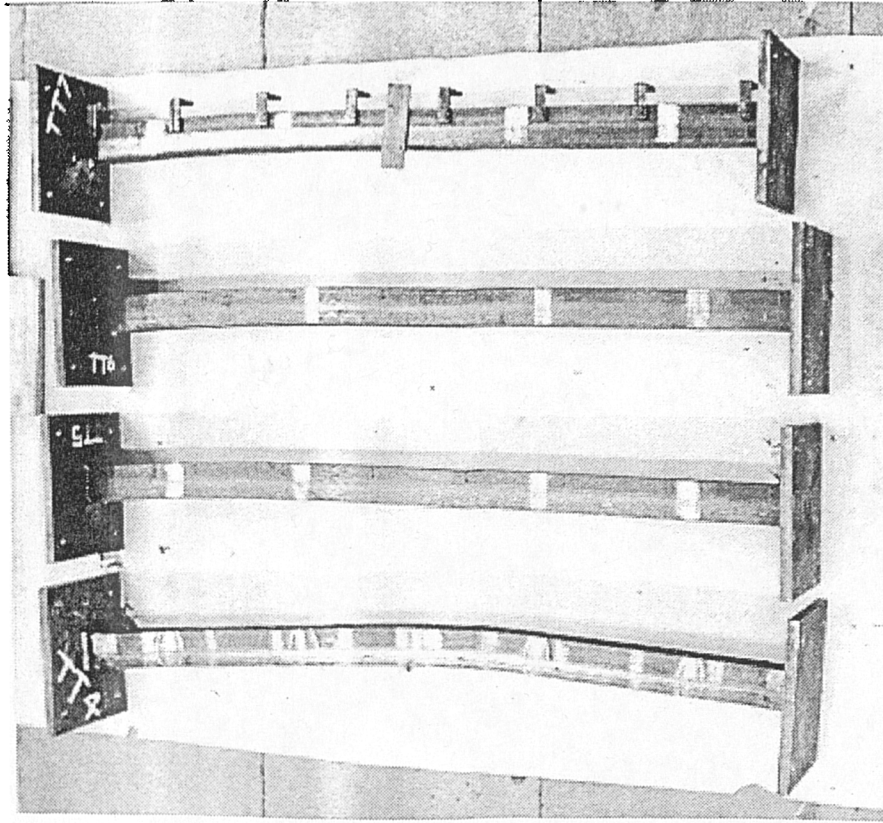


Figure 5.14 Failed Columns - View 1

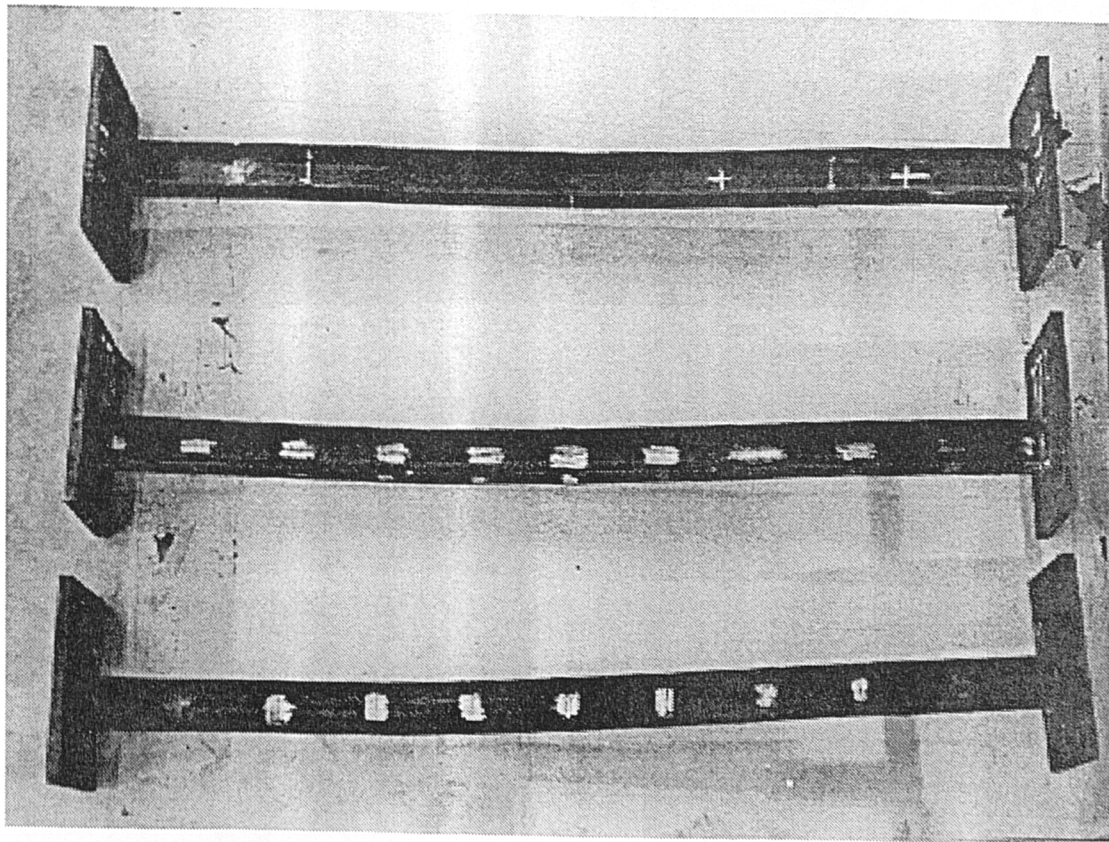
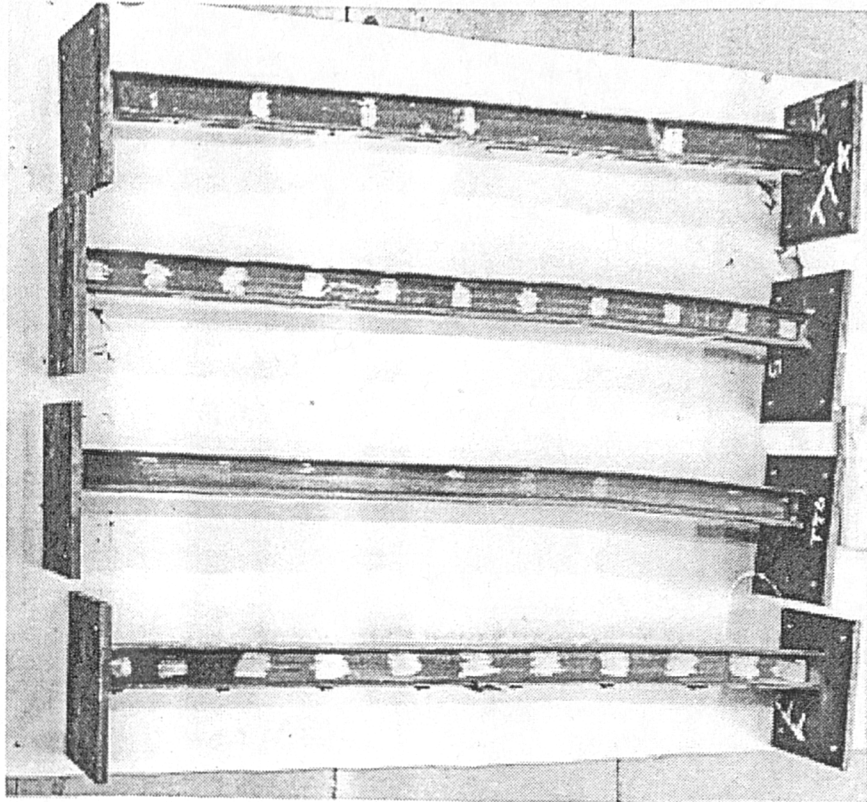


Figure 5.15 Failed Columns - View 2

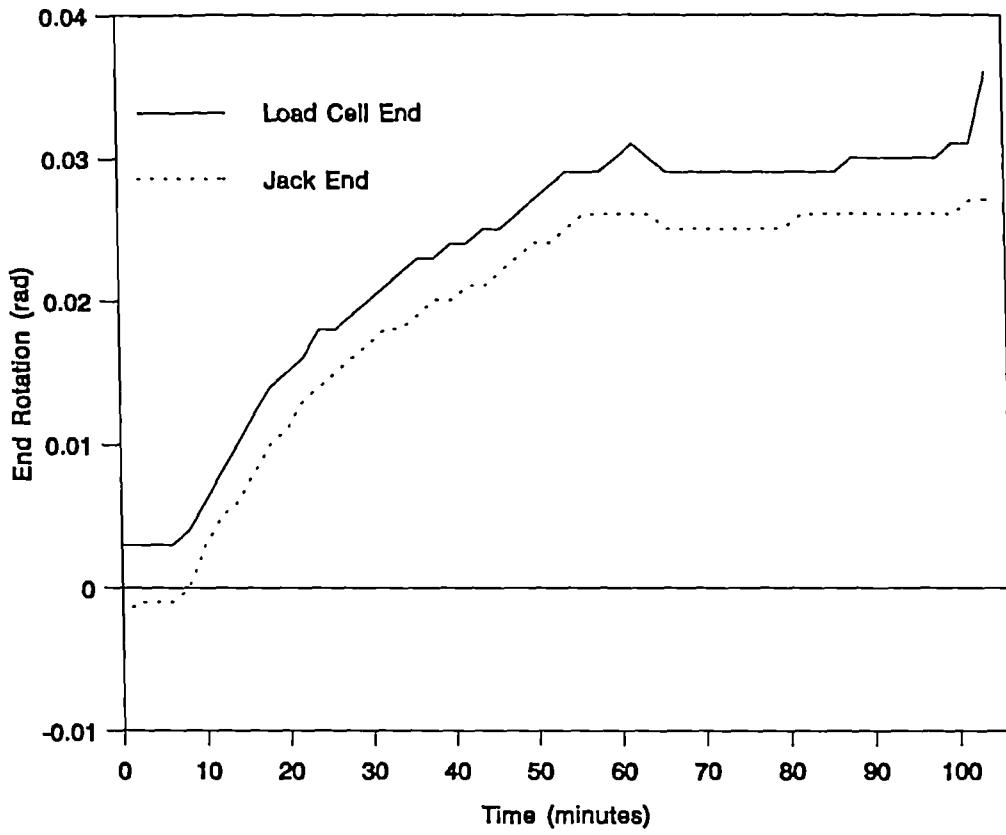


Figure 5.16 Variation of End Rotations With Time For Test 1

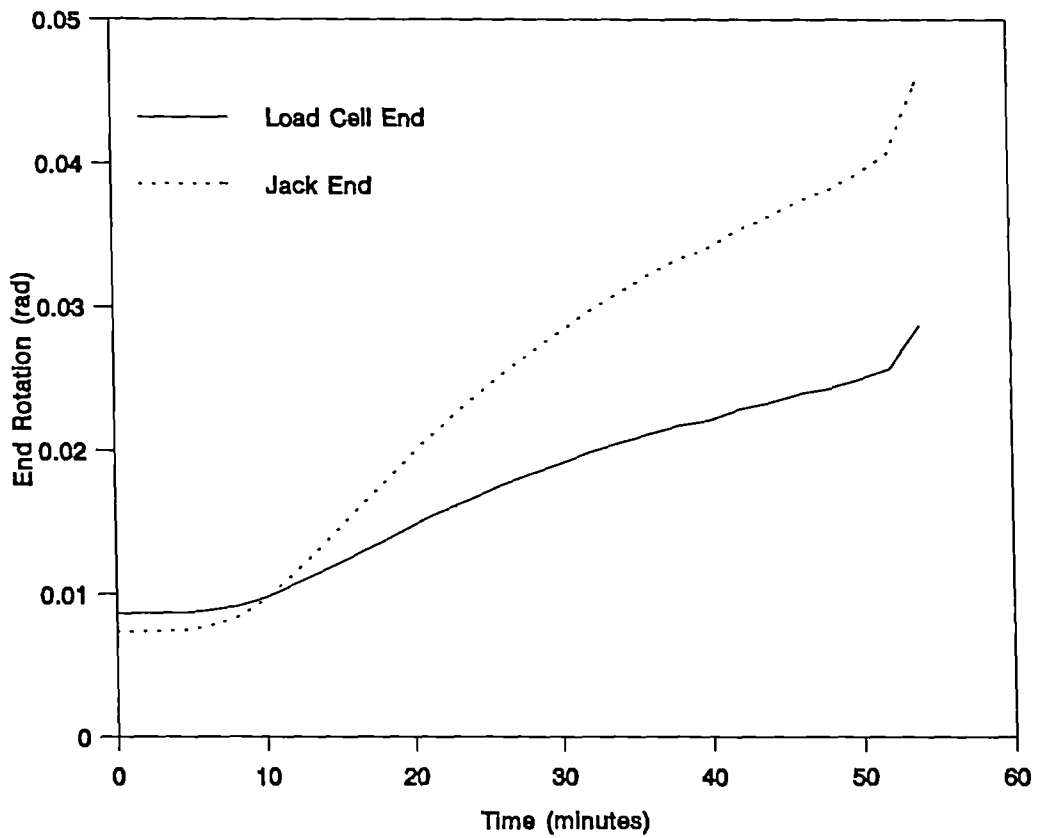


Figure 5.17 Variation of End Rotations With Time For Test 2

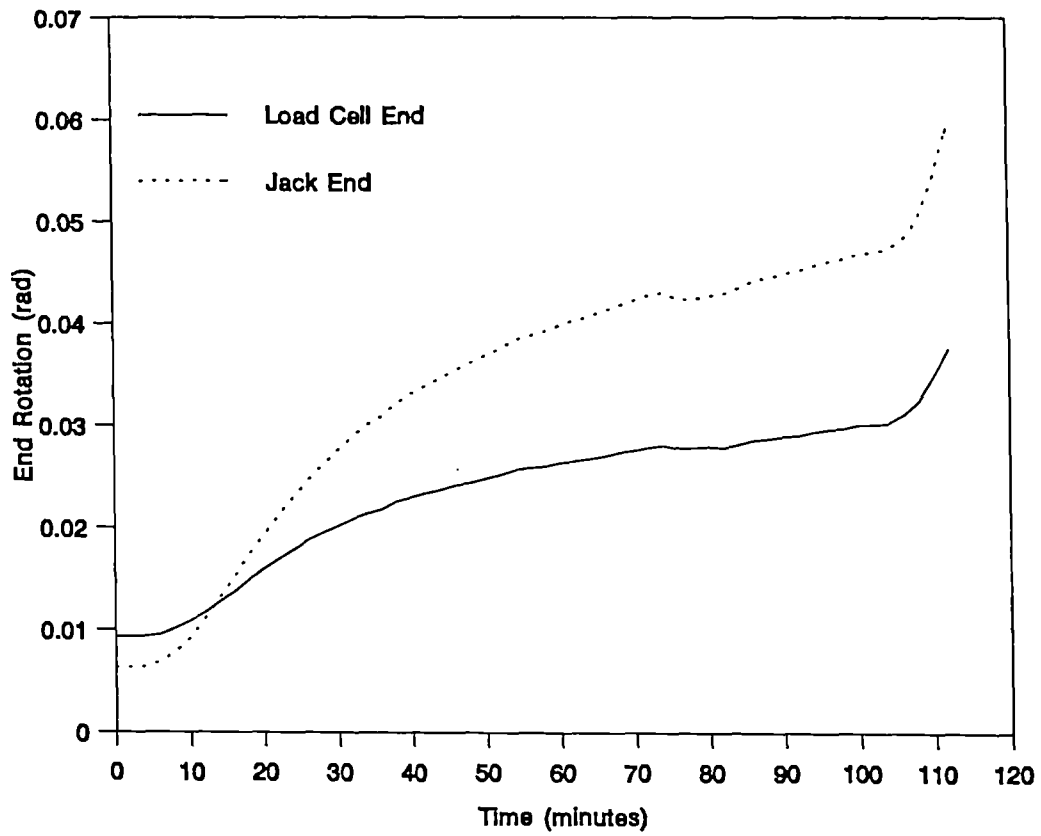


Figure 5.18 Variation of End Rotations With Time For Test 3

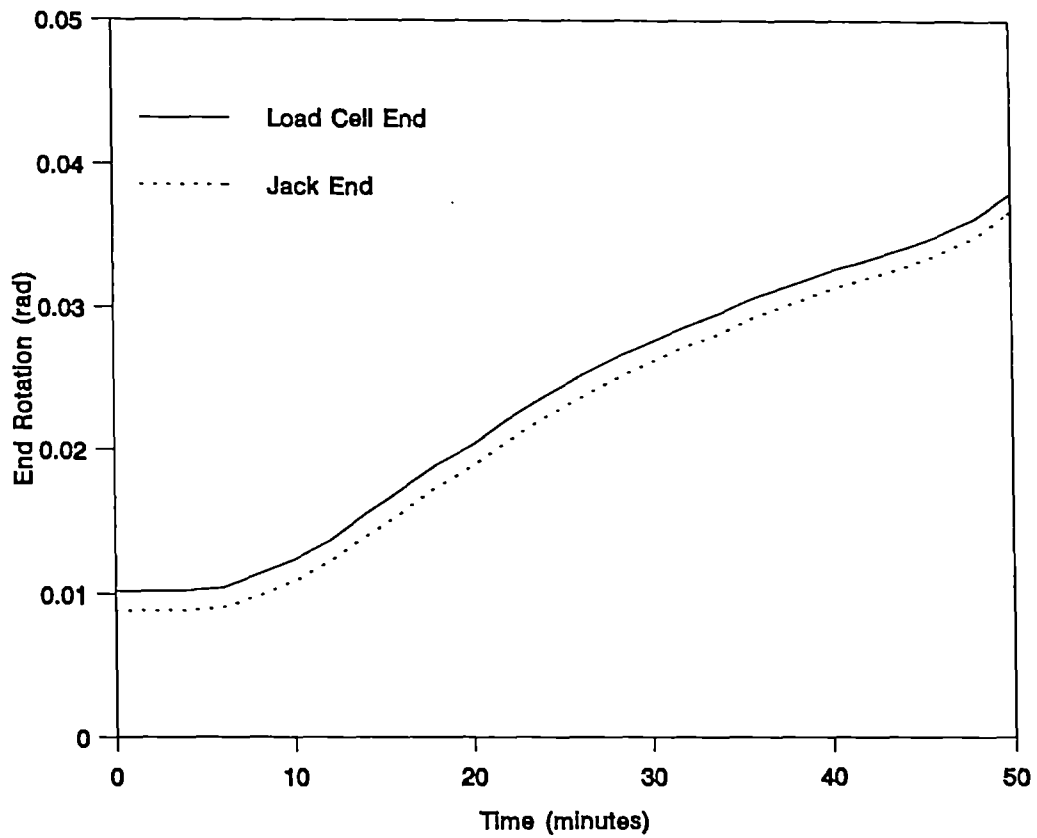


Figure 5.19 Variation of End Rotations With Time For Test 4

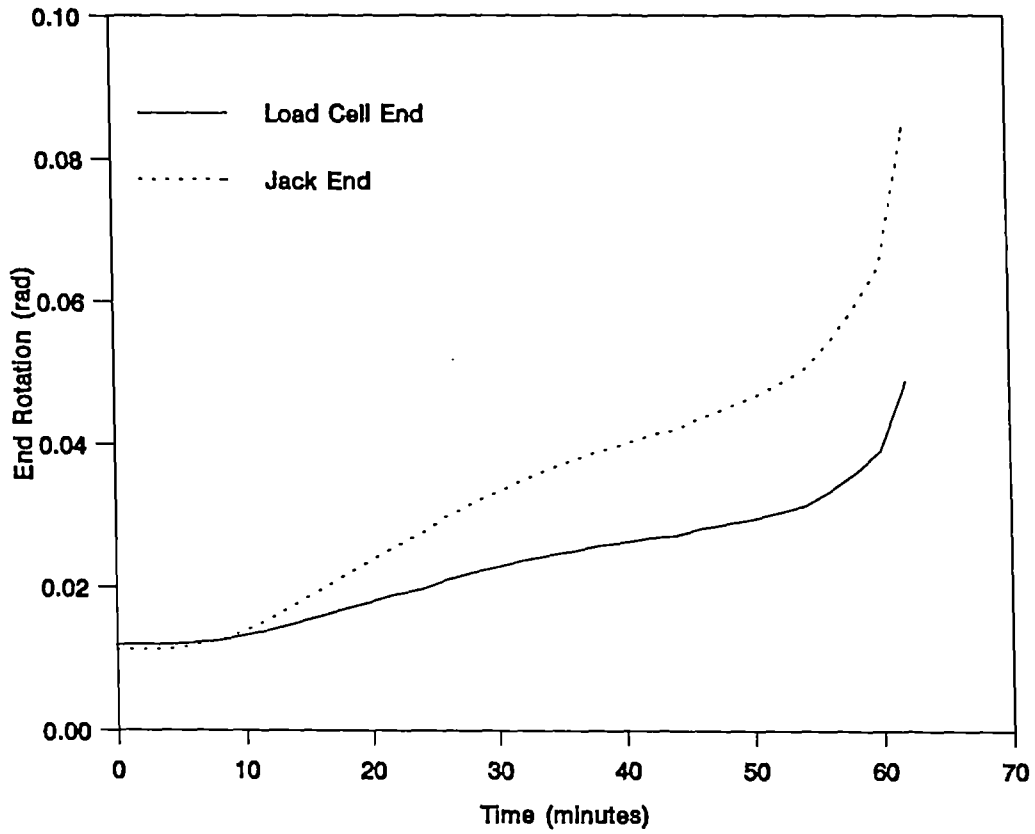


Figure 5.20 Variation of End Rotations With Time For Test 5

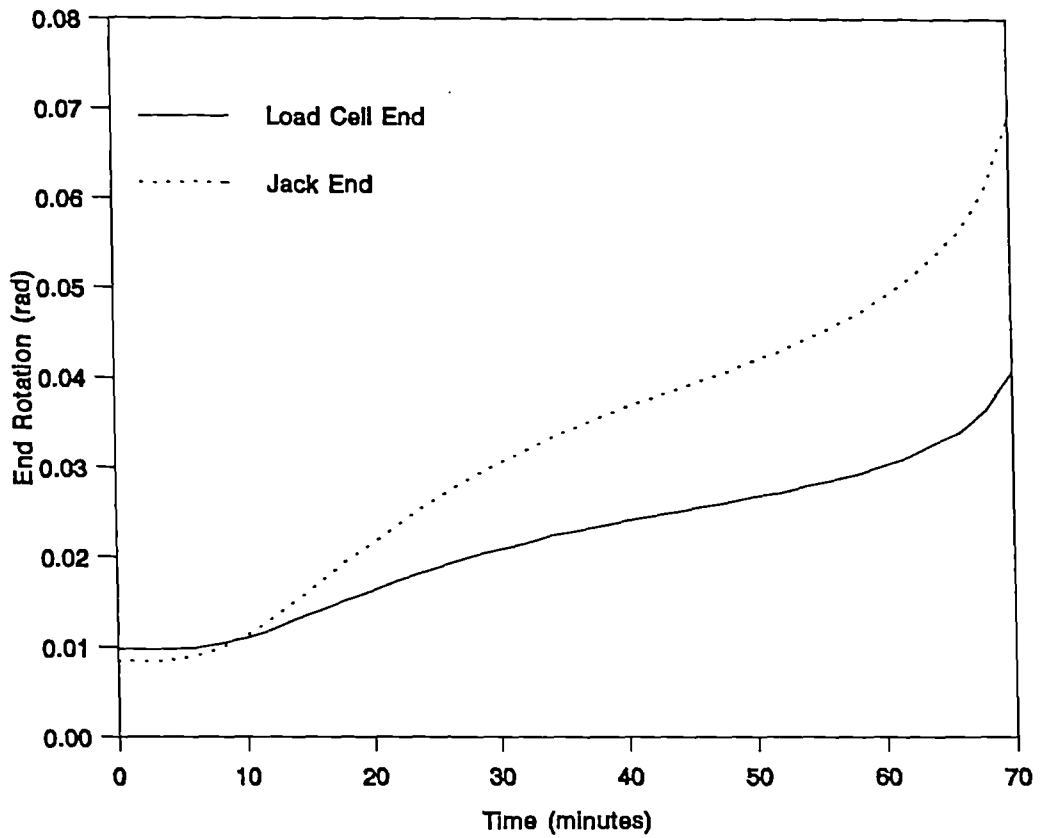


Figure 5.21 Variation of End Rotations With Time For Test 6

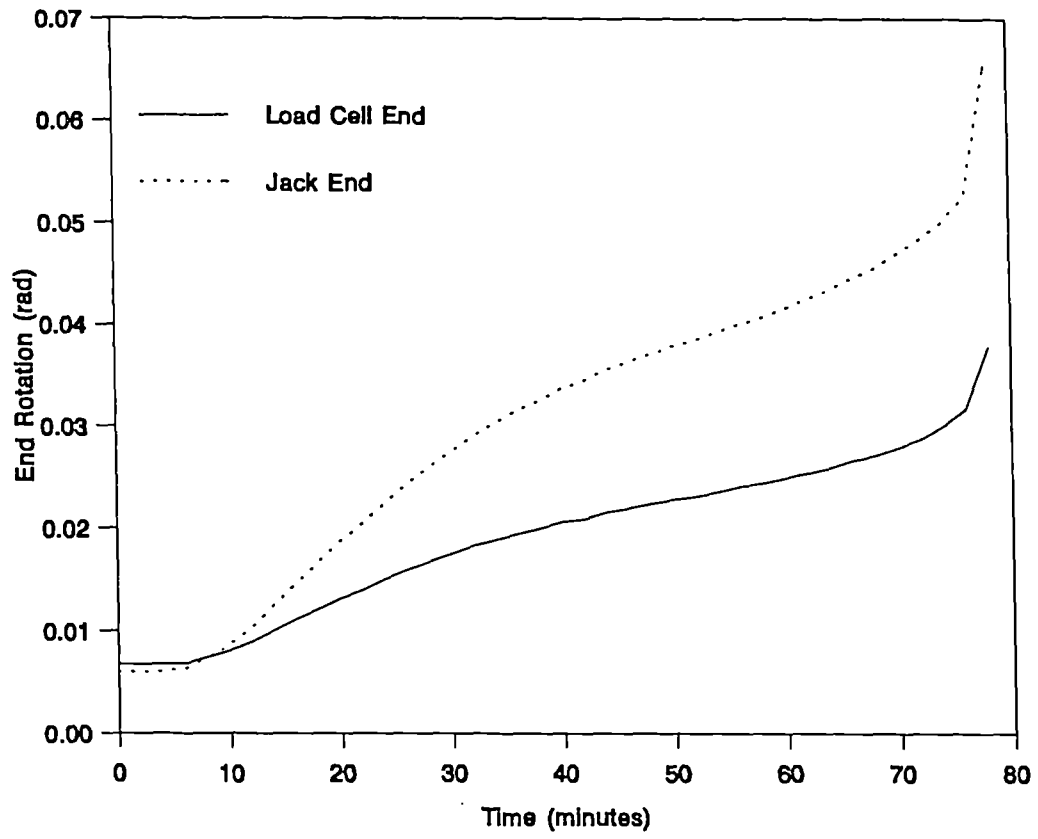
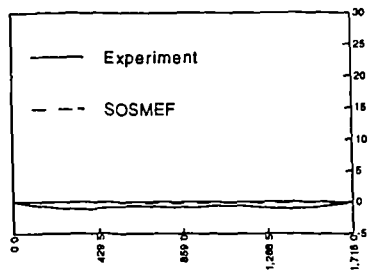
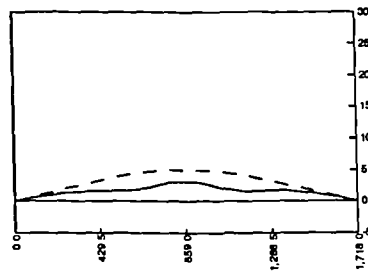


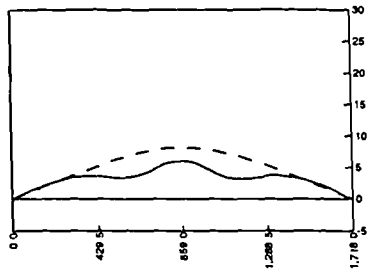
Figure 5.22 Variation of End Rotations With Time For Test 7



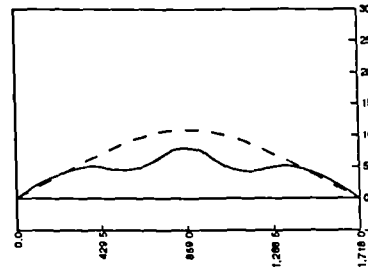
At 0 minutes



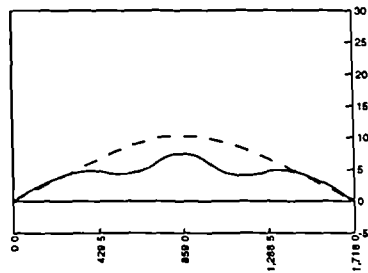
At 20 minutes



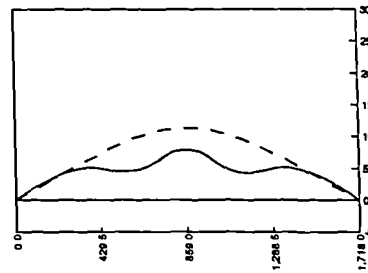
At 40 minutes



At 60 minutes



At 80 minutes



At 102 minutes

Figure 5.23 Comparison of Deflected Shape - Test 1

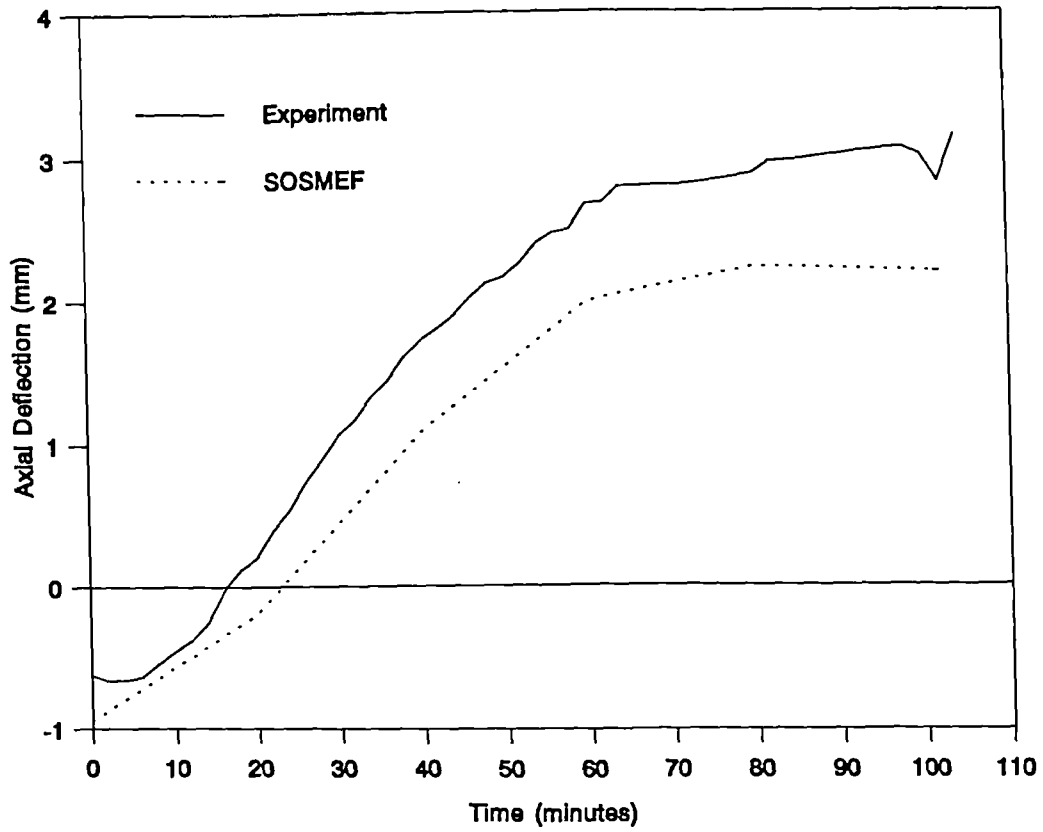


Figure 5.24 Comparison of Axial Deflection - Test 1

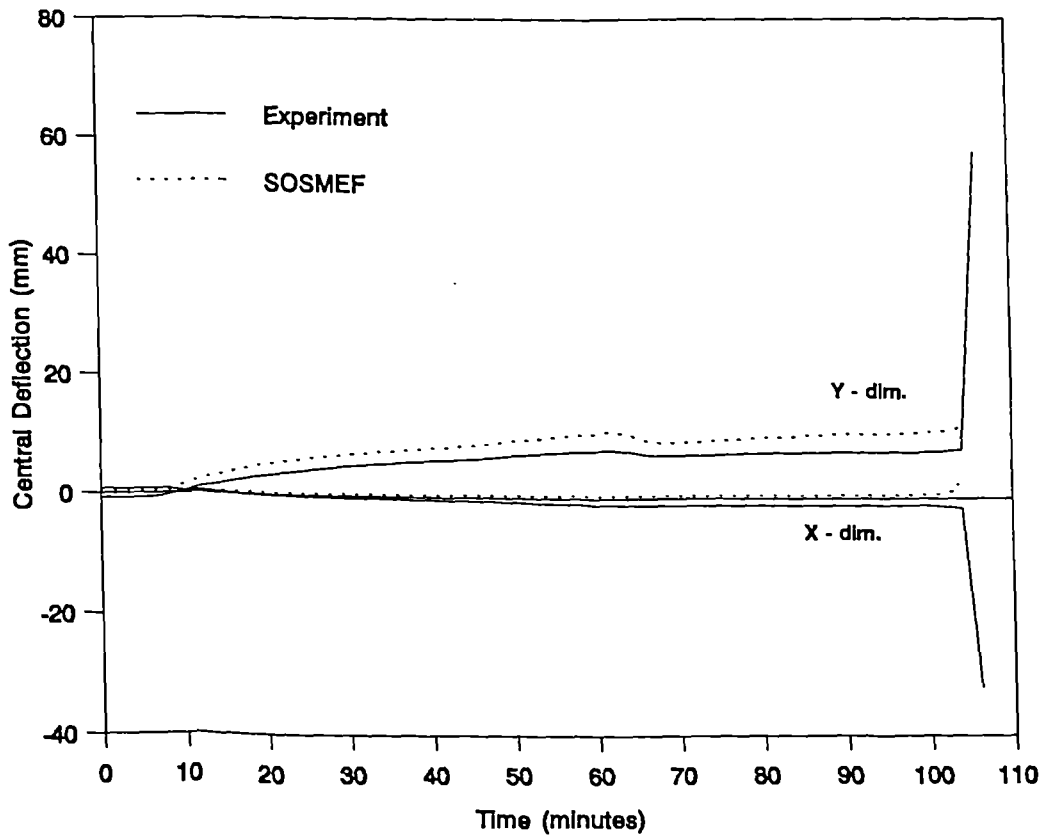
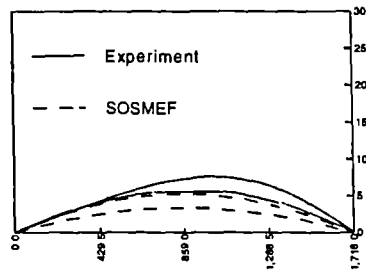
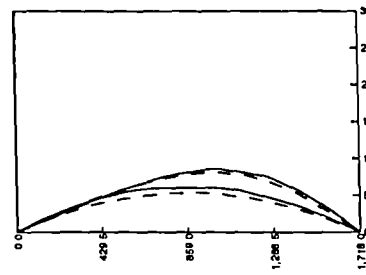


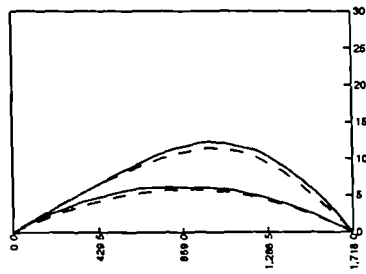
Figure 5.25 Comparison of Central Deflection - Test 1



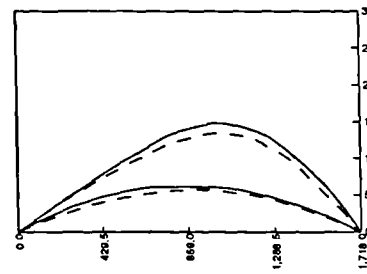
At 0 minutes



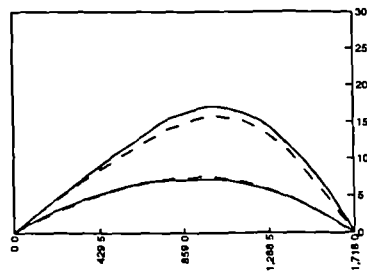
At 20 minutes



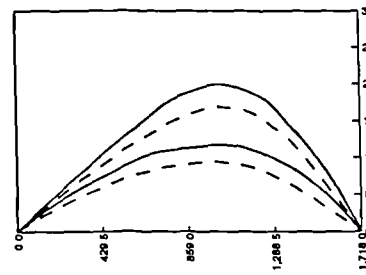
At 30 minutes



At 40 minutes



At 50 minutes



At 54 minutes

Figure 5.26 Comparison of Deflected Shape - Test 2

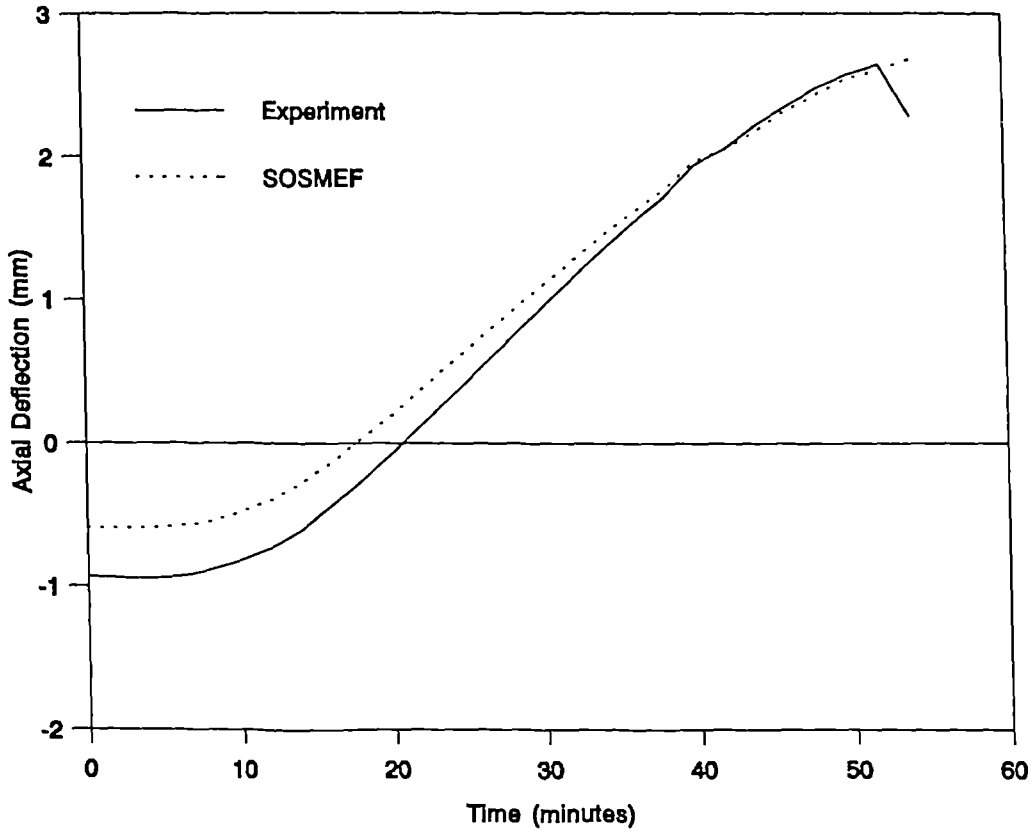


Figure 5.27 Comparison of Axial Deflection - Test 2

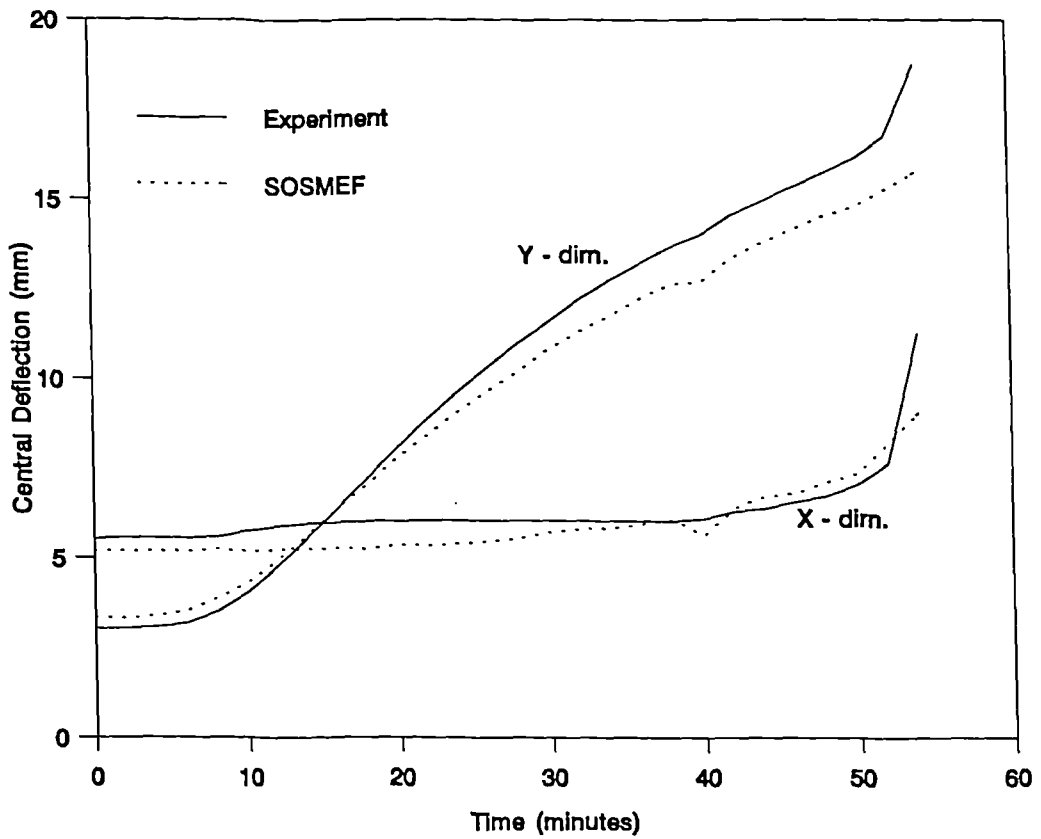
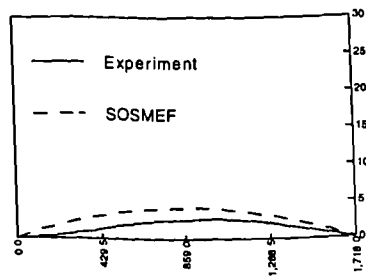
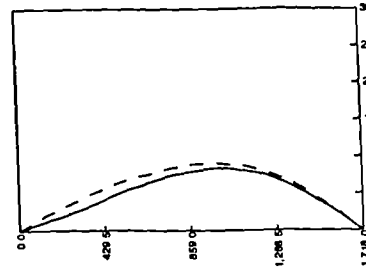


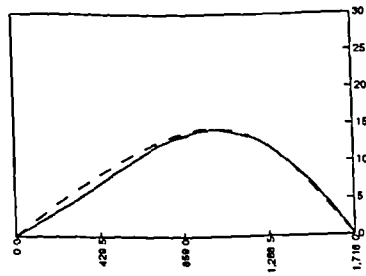
Figure 5.28 Comparison of Central Deflection - Test 2



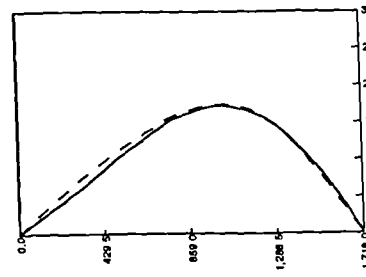
At 0 minutes



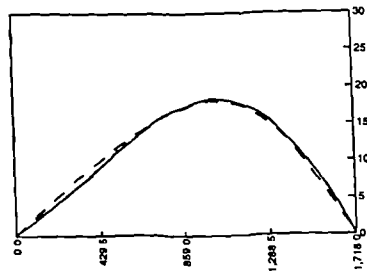
At 20 minutes



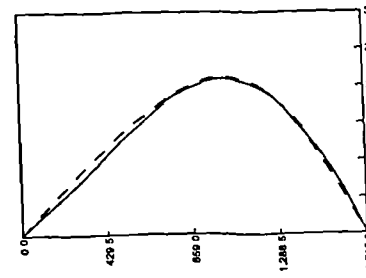
At 40 minutes



At 60 minutes



At 80 minutes



At 106 minutes

Figure 5.29 Comparison of Deflected Shape - Test 3

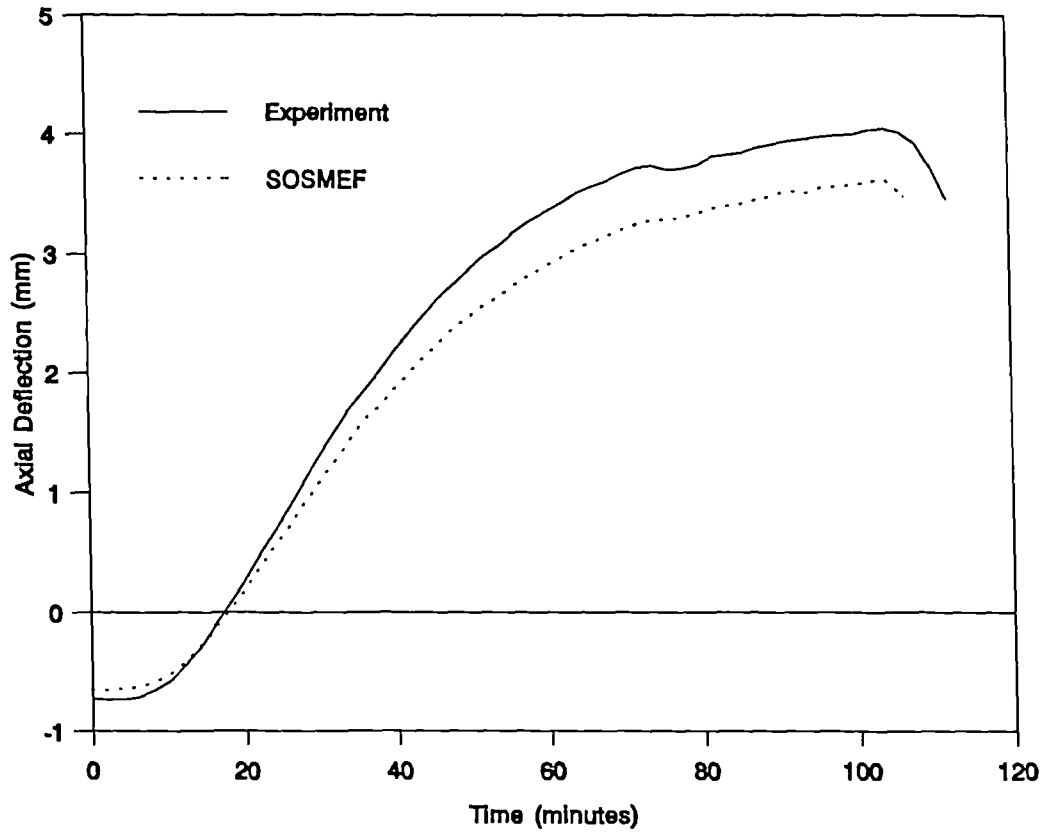


Figure 5.30 Comparison of Axial Deflection - Test 3

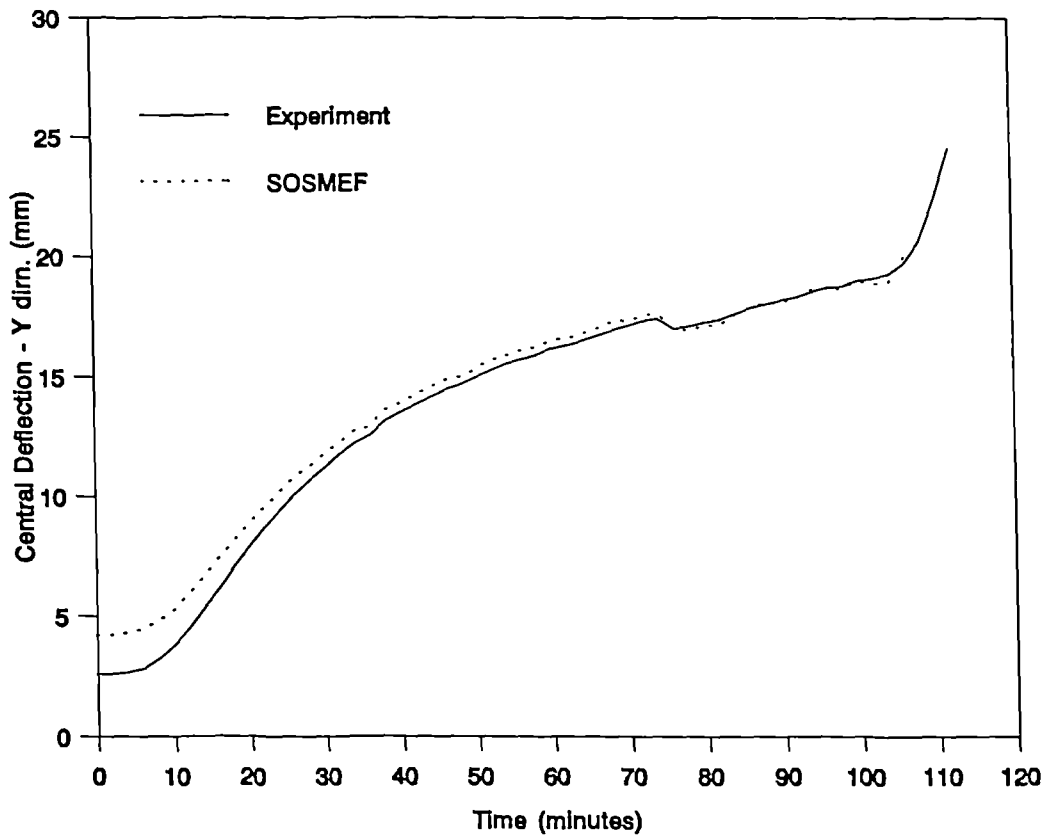
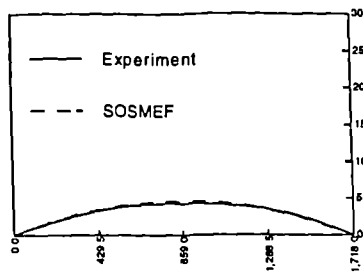
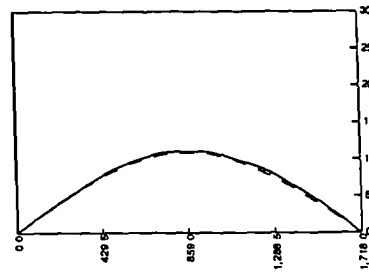


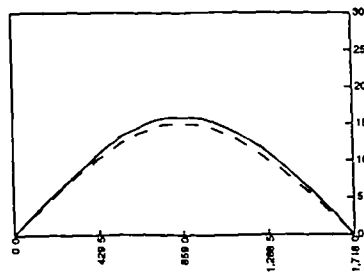
Figure 5.31 Comparison of Central Deflection - Test 3



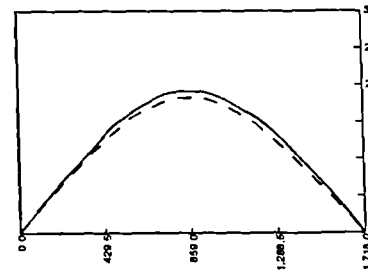
At 0 minutes



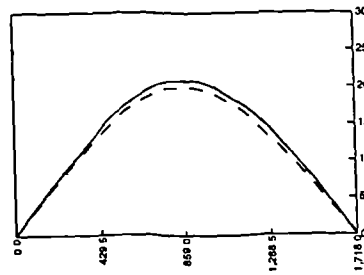
At 20 minutes



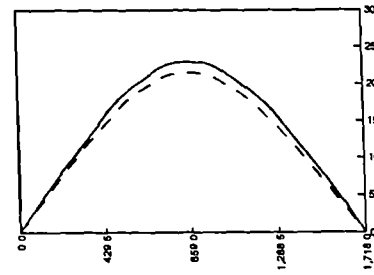
At 30 minutes



At 40 minutes



At 46 minutes



At 50 minutes

Figure 5.32 Comparison of Deflected Shape - Test 4

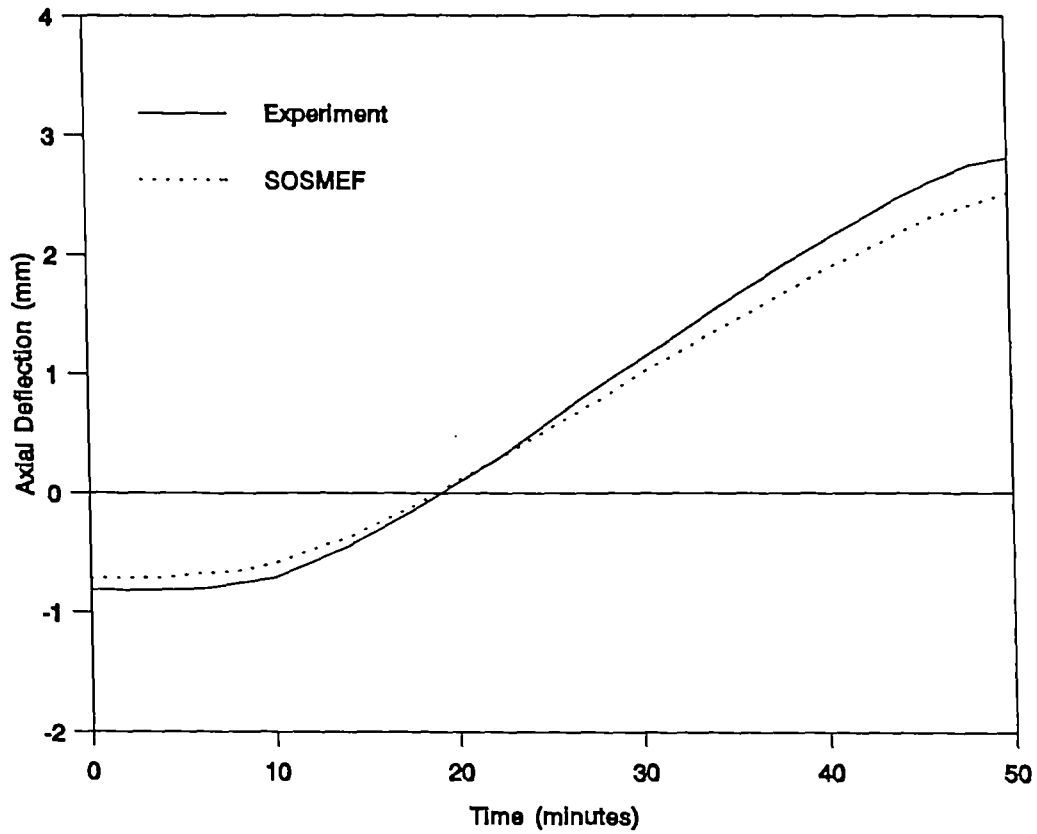


Figure 5.33 Comparison of Axial Deflection - Test 4

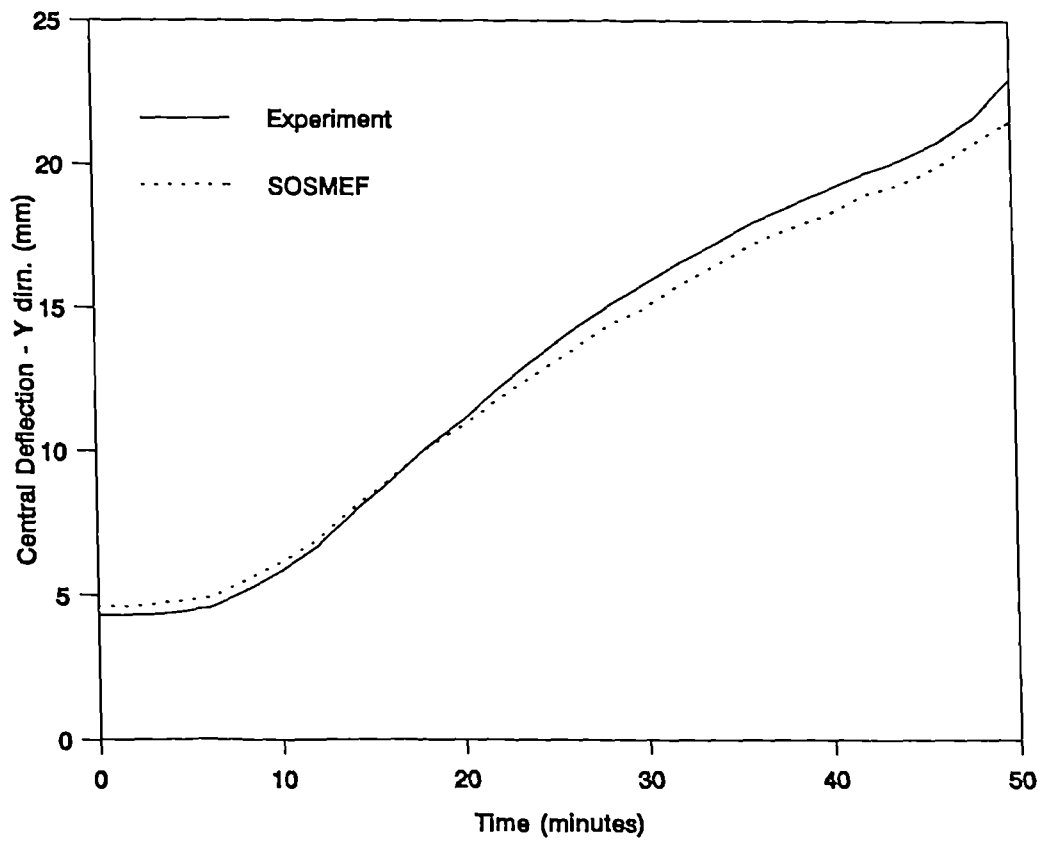
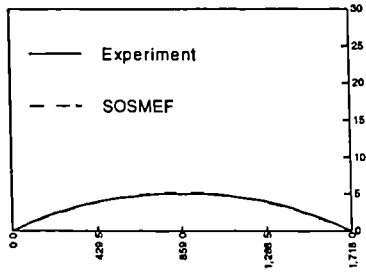
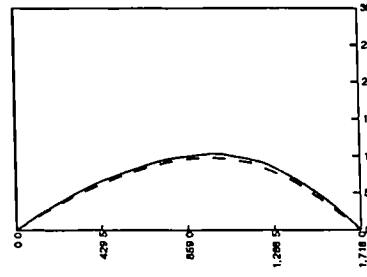


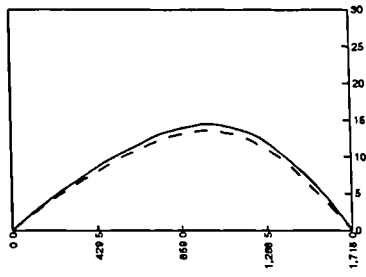
Figure 5.34 Comparison of Central Deflection - Test 4



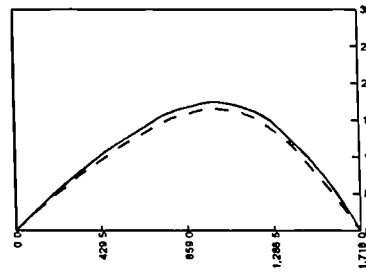
At 0 minutes



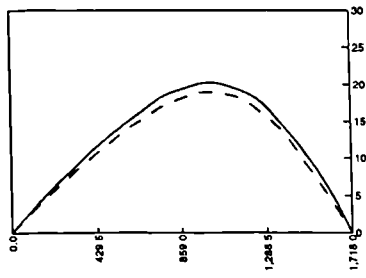
At 20 minutes



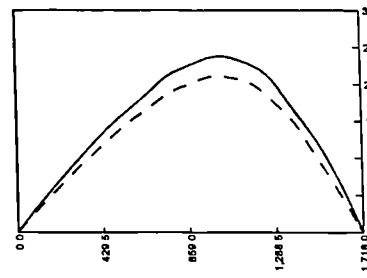
At 30 minutes



At 40 minutes



At 50 minutes



At 56 minutes

Figure 5.35 Comparison of Deflected Shape - Test 5

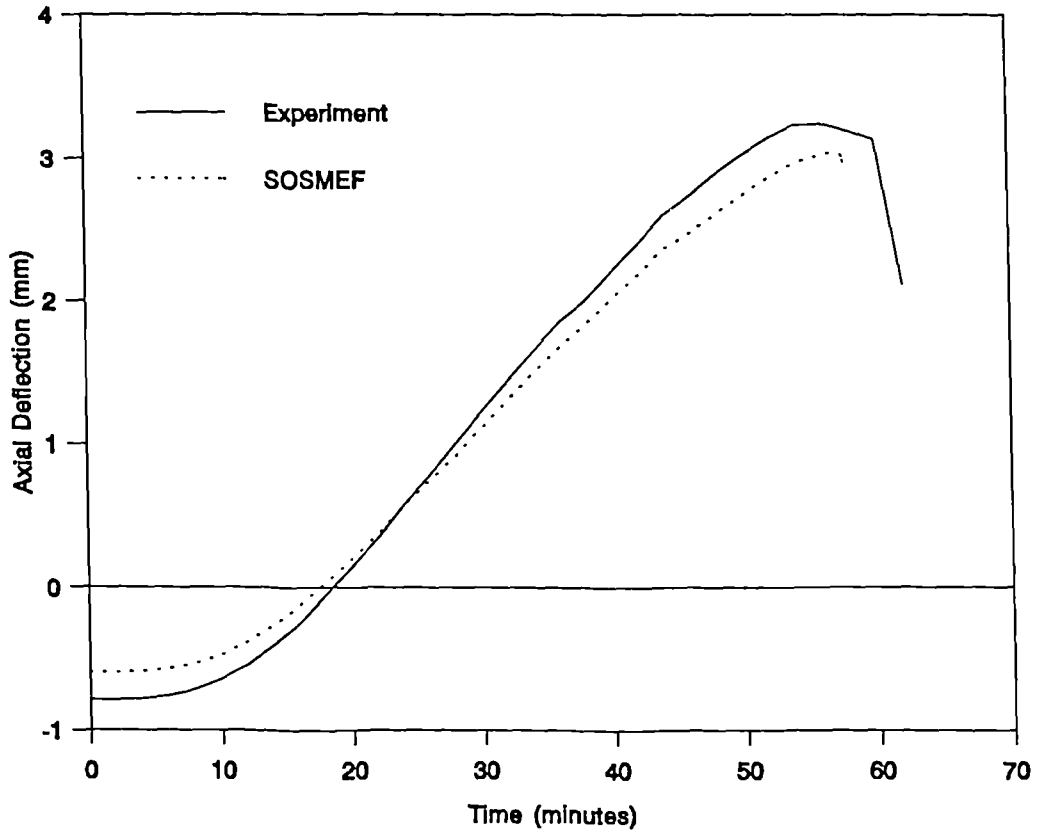


Figure 5.36 Comparison of Axial Deflection - Test 5

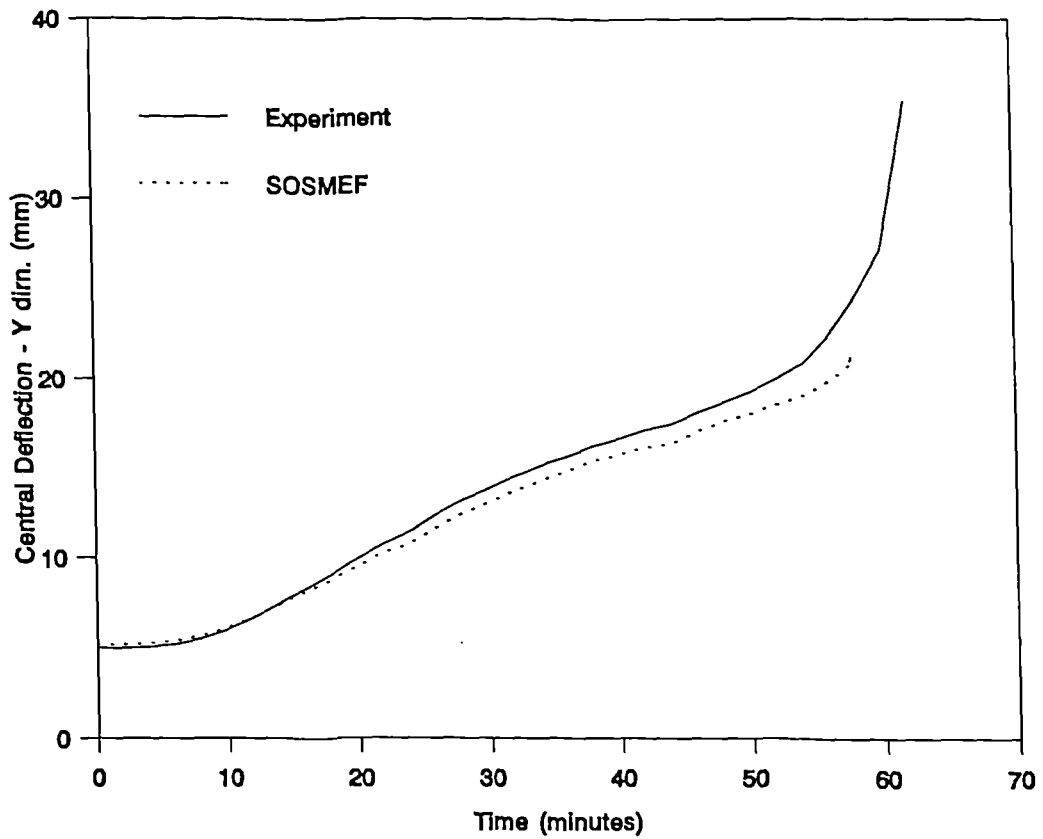
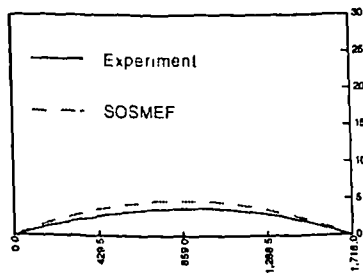
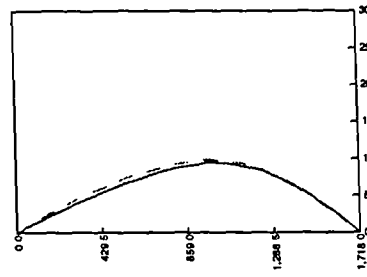


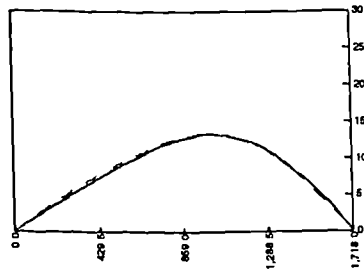
Figure 5.37 Comparison of Central Deflection - Test 5



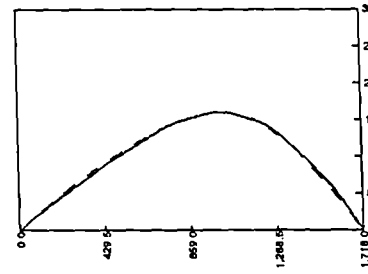
At 0 minutes



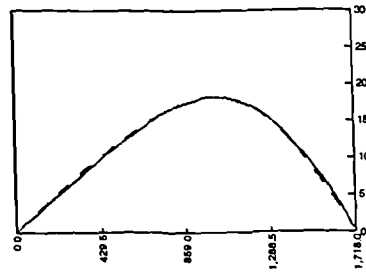
At 20 minutes



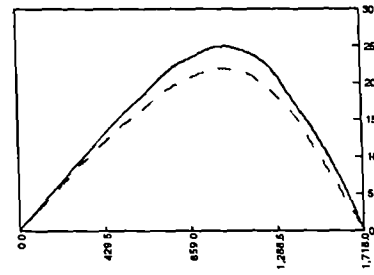
At 30 minutes



At 40 minutes



At 50 minutes



At 66 minutes

Figure 5.38 Comparison of Deflected Shape - Test 6

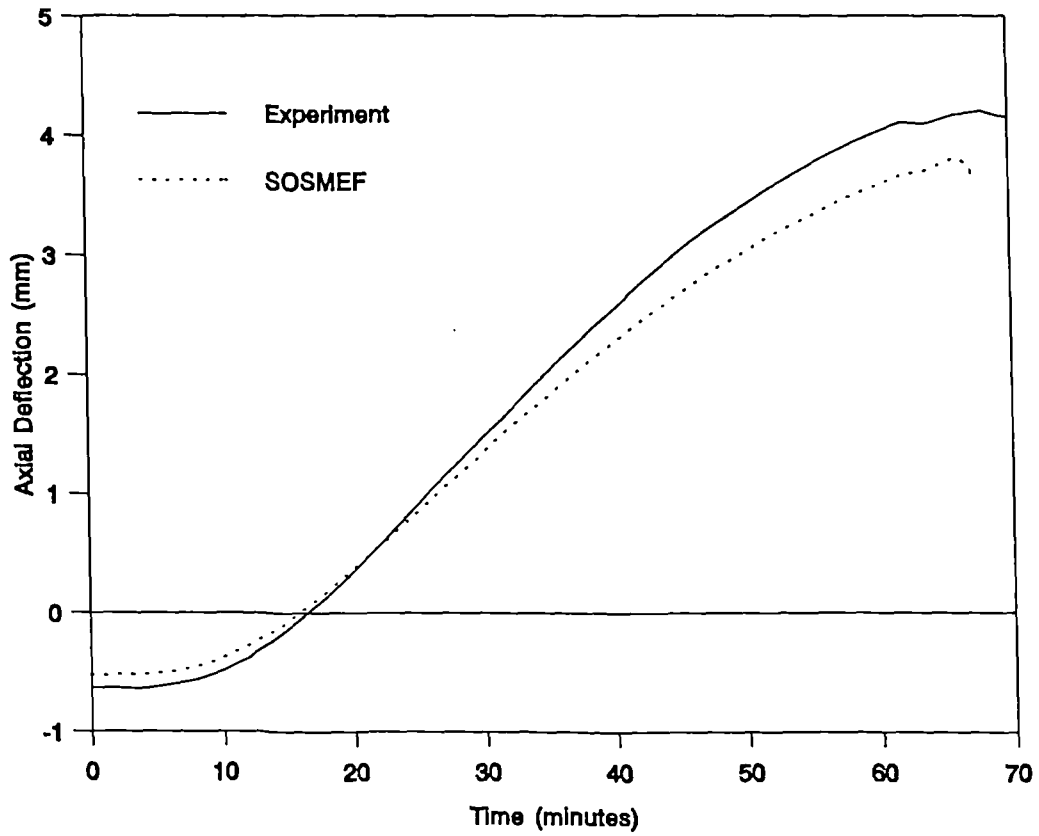


Figure 5.39 Comparison of Axial Deflection - Test 6

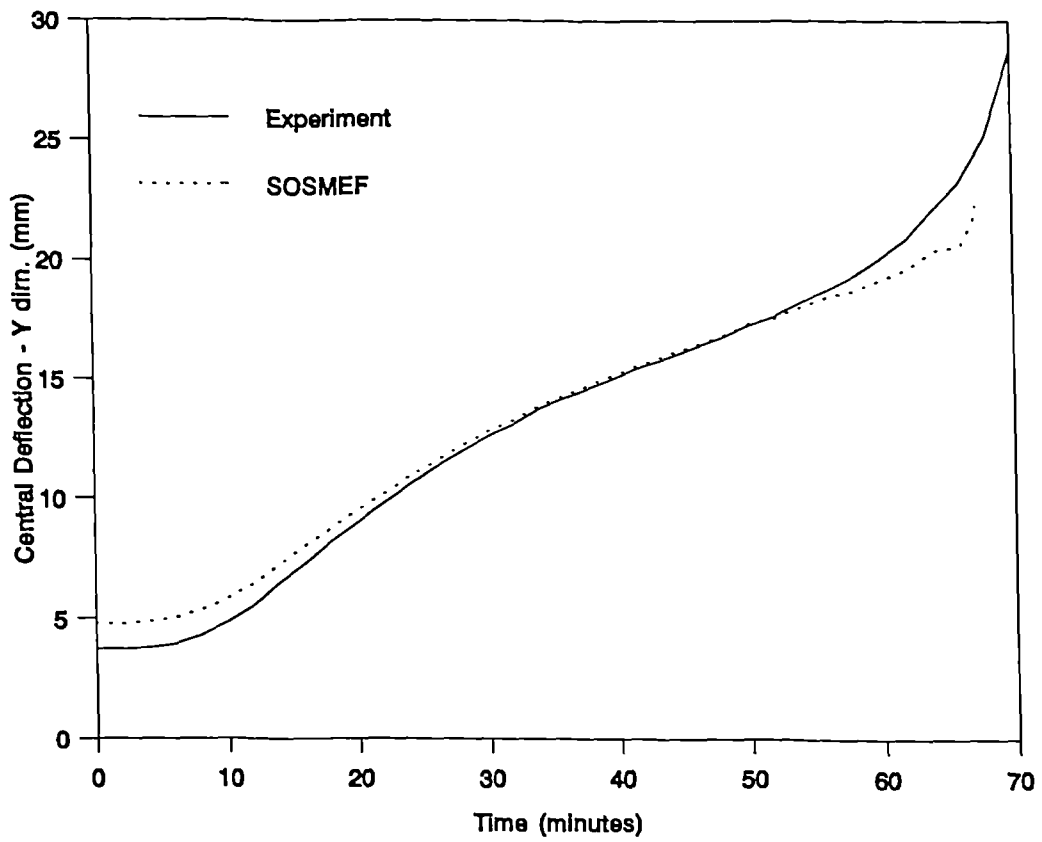
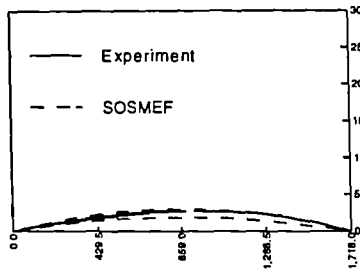
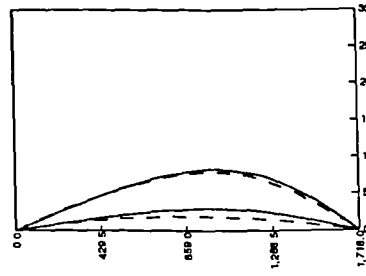


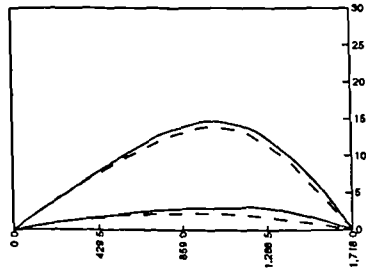
Figure 5.40 Comparison of Central Deflection - Test 6



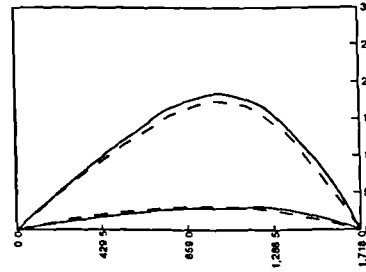
At 0 minutes



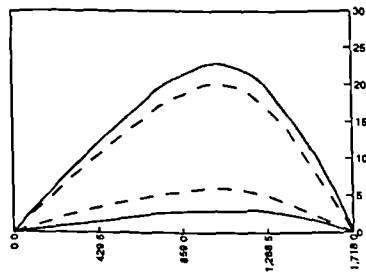
At 20 minutes



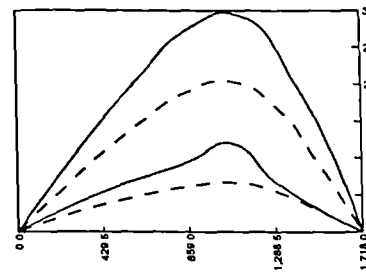
At 40 minutes



At 60 minutes



At 76 minutes



At 78 minutes

Figure 5.41 Comparison of Deflected Shape - Test 7

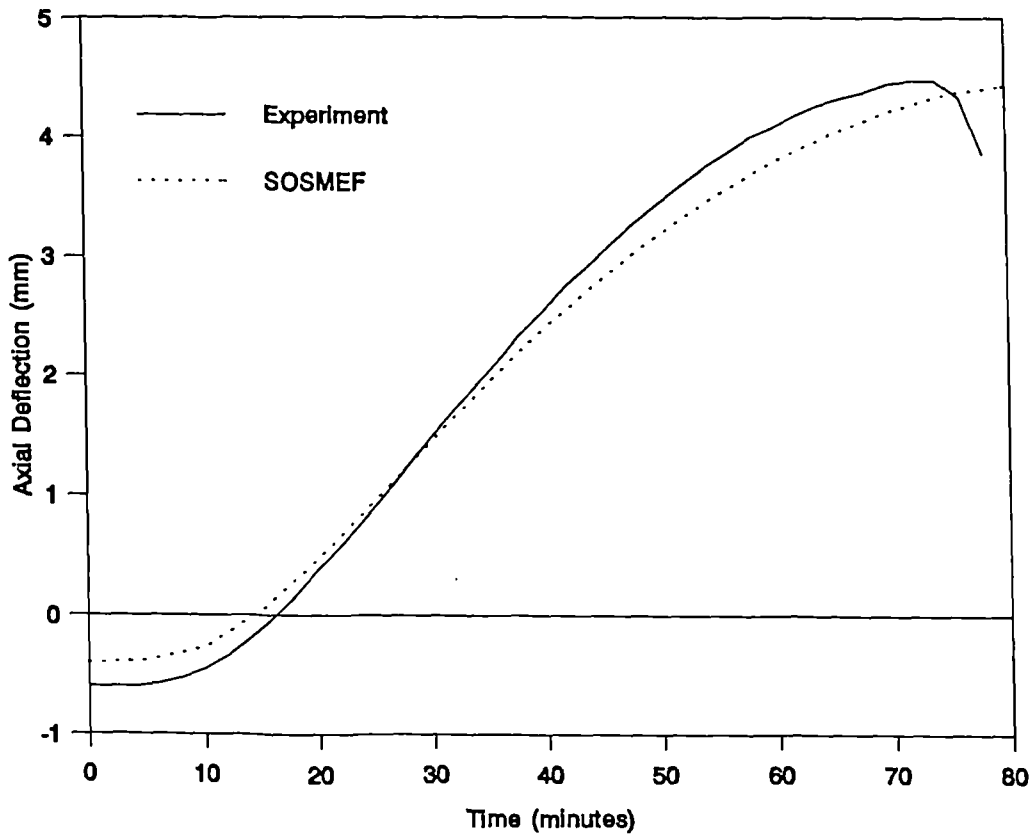


Figure 5.42 Comparison of Axial Deflection - Test 7

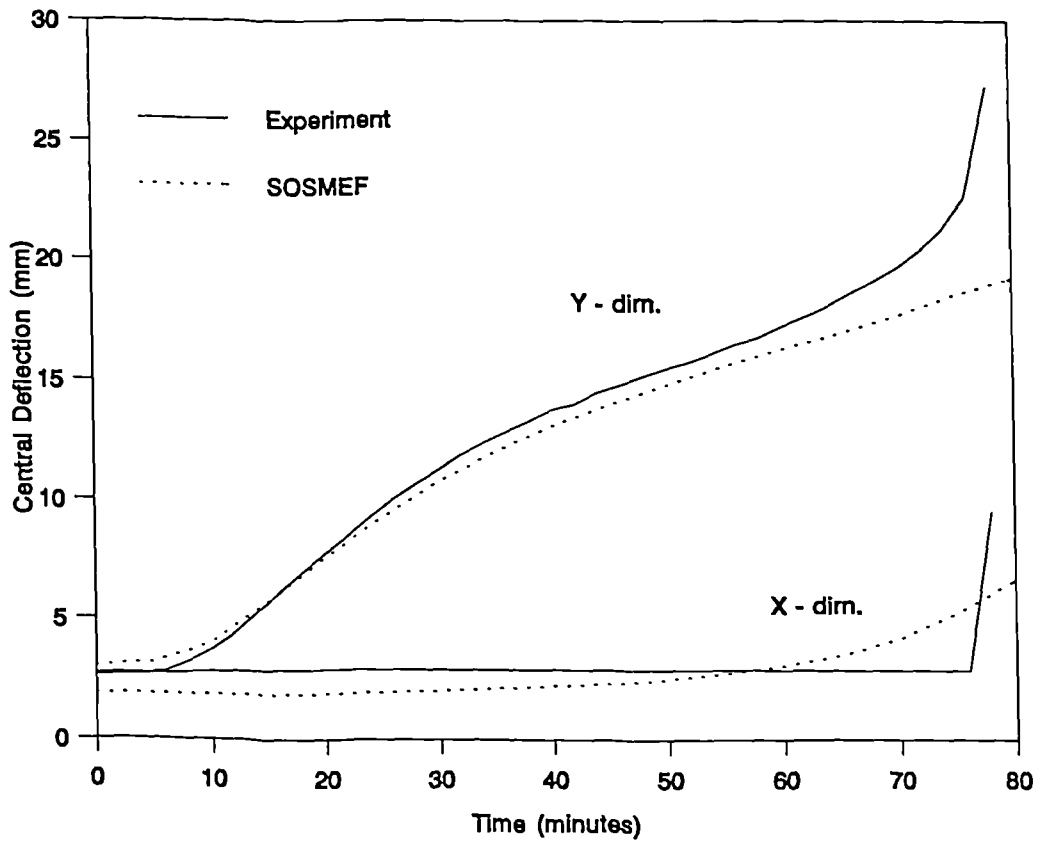


Figure 5.43 Comparison of Central Deflection - Test 7

CHAPTER 6

APPLICATIONS

6.0 Introduction

In this chapter, some applications of the numerical method developed in Chapter 3 are demonstrated. An obvious application of the computer program SOSMEF is for carrying out a rigorous analysis of a particular beam or column as required. Another application is carrying out parametric studies or sensitivity analyses with the aim of developing design aids. The cost and time involved in carrying out these numerical experiments would only be a small fraction of the cost and time of physical experiments. If necessary, a small number of physical experiments may be required to verify and confirm the results of the parametric study.

In this chapter, two parametric studies are described. One is the development of a simple design method for steel columns subjected to a non-uniform temperature distribution across the section. The other is the possibility of enhancing the inherent fire resistance capacity of Slimflor beams by introducing reinforcing bars. In both cases, the computer program TASEF-2 was used for the temperature calculations and the computer program SOSMEF was used for structural response calculations.

6.1 Design of Steel Columns Subjected to a Non-uniform Temperature Distribution Across the Section

6.1.1 Introduction

Due to the fact that the conductivity of steel is very high, it is sometimes assumed that the temperature distribution across the steel member is uniform. This is applicable to bare steel columns and fire protected steel columns exposed to fire on all sides. Some design methods^[9] for steel columns subjected to fire are based on the assumption of a

uniform temperature distribution across the section. These methods have already been reviewed in Chapter 2. In cases of steel columns partially fire protected and/or exposed to fire on only one side, the temperature distribution across the section would be non-uniform. One option for assessing the fire resistance capacity of these columns is to perform a rigorous calculation using a computer program such as SOSMEF. However, as a routine rigorous analysis of individual members is still in the future, a simpler design approach could be usefully employed. In this section, a design method is proposed for computing the response of steel columns subjected to non-uniform temperature distributions across the section. The study reported here is by no means a complete design guide but is only a first step towards the goal of producing a comprehensive design guide.

6.1.2 Design Method at Room Temperature

Before moving on to the elevated temperature design of steel columns, it is appropriate to discuss the current room temperature design methods. The room temperature design method of steel columns subjected to a concentric axial load, as included in BS5950: Part 1^[7], is based on the Perry strut formula.

$$(\sigma_y - \sigma_c)(\sigma_e - \sigma_c) = \eta \sigma_e \sigma_c \quad (6.1)$$

where,

σ_y = Yield strength

σ_c = Compressive strength

σ_e = Euler strength ($\pi^2 E / \lambda^2$)

η = A parameter defining the initial out of straightness of the member

In the derivation of this formula it can be shown that:

$$\eta = c\Delta/r^2 \quad (6.2)$$

where,

Δ = the initial bow or lack of straightness

r = radius of gyration

c = distance from the centroid of the section to the extreme fibre of the section

Equation 6.2 can be rewritten as,

$$\eta = \beta\lambda \quad (6.3)$$

where,

λ = slenderness

$$\beta = \frac{y}{r} \cdot \frac{\Delta}{L}$$

Taking into account that in reality, stocky columns reach their full plastic load carrying capacity, BS5950 defines the Perry factor η as,

$$\eta = \beta(\lambda - \lambda_0) \quad \text{but not less than zero}$$

where,

$$\lambda_0 = \text{limiting slenderness for stocky columns, taken as } 0.2 \left(\frac{\pi^2 E}{\sigma_y} \right)$$

β = a constant (called Robertson constant) ranging from 0.002 to 0.008

The values of β have been selected so as to make the curves included in BS5950 approximate the European column design curves as included in Eurocode 3.

6.1.3 Design Method at Elevated Temperature

The design method, described in the previous section for the design of steel columns at room temperature, may be used for columns subjected to a uniform temperature distribution by changing the material properties to the corresponding properties at

elevated temperature. Such an approach has already been adopted by Vandamme and Janss^[59] using the European column curve c .

When a column is subjected to a non-uniform temperature distribution, material properties at different points of the cross section also vary with the corresponding temperature. In addition to this, if the temperature variation is not symmetrical about any geometrical axis, thermal bowing occurs about that axis. So any design method proposed should take these effects into account in some way or other.

As a first attempt to formulate a design method for fire, only one case is considered in this section. The case considered is of columns made of H sections exposed to fire on only one flange. It is assumed that webs are blocked in by the concrete which does not play any structural part. This represents a situation where a column is built into the wall and exposed to fire only on one side. Figure 6.1 shows a graphical representation of the case considered in this study and a schematic representation of the temperature profile.

In reality, the column is loaded to its working load level and the temperature increases with time in the event of a fire. For design purposes, the load carrying capacity of a column for a given temperature distribution can be calculated and checked to see whether it is greater than the required working load. This is the approach adopted in the design method proposed in this section.

The following sign convention is used in all the calculations in this chapter.

w_t = Web thickness

f_t = Flange thickness

d = Depth of the section

b = Breadth of the section

d_1 = $d - f_t$

d_2 = $d - 2.f_t$

I_x = Second moment of area about minor axis

I_y = Second moment of area about major axis

A	= Area of the section
T_i	= Temperature at point i ($i=1$ to 4)
E_i	= Elastic modulus at temperature T_i
σ_{yi}	= Yield stress at temperature T_i
E	= Elastic modulus at 20°C
σ_y	= Yield stress at 20°C
E_{eff}	= Effective Elastic modulus
σ_{eff}	= Effective yield stress
L	= Length of the column
Δ_T	= Thermal bowing deflection
M_y	= Plastic bending moment capacity about Major axis

Variation of the elastic modulus and yield stress with temperature is assumed to be that given in Eurocode 2: Part 10.

6.1.3.1 Proposed design method for buckling about the minor axis

For symmetrical heating over one flange, the temperature variation is symmetrical about the minor axis, hence there will be no thermal bowing effect about this axis. As the variation of temperature is likely to be small, it is reasonable to ignore such a variation in this direction.

The principle behind the method is to use one of the column design curves even for the fire limit state. The amendments that are needed are for the effective material properties and the effective stiffness of the column.

It is proposed to use the lowest design curve in BS5950:Part 1 (Curve d with the value of Robertson constant as 0.008). The following calculation method is proposed to calculate the effective material properties.

- STEP 1: Divide the section into 4 rectangles as shown in Figure 6.2.
- STEP 2: Find out the temperatures at points 1 to 4. (This may be calculated or obtained from experimental data).
- STEP 3: Calculate the corresponding elastic modulus and yield stress for points 1 to 4 according to EC2: Part 10
- STEP 4: Calculate the effective yield stress using the following formula

$$\sigma_{yeff} = \frac{f_{t,b}(\sigma_{y1} + \sigma_{y4}) + \frac{w_{t,d2}}{2}(\sigma_{y2} + \sigma_{y3})}{2 \cdot [f_{t,b} + w_{t,d2}]} \quad (6.4)$$

- STEP 5: Calculate the effective E using the following formula.

$$E_{eff} = \frac{\frac{1}{12}f_{t,b}^3(E_1 + E_4) + \frac{1}{24}d_2 \cdot w_t^3(E_2 + E_3)}{I_x} \quad (6.5)$$

$$\text{where, } I_x = \frac{1}{12}(2 \cdot f_{t,b}^3 + d_2 \cdot w_t^3)$$

- STEP 7: Once the effective E and σ_y are calculated, use the room temperature design procedure described in BS5950:Part 1 using curve *d*.

6.1.3.2 Proposed design method for buckling about major axis

In this case, the nature of the temperature distribution causes two effects. One is thermal bowing. The other effect is that the section becomes effectively non-symmetric about the geometrical centroidal axis hence creating an eccentricity of the axial load. Figure 6.3 shows the qualitative picture of how the failure load of a column varies with the point of application of the axial load for a given temperature distribution showing the effect of eccentricity created by the temperature distribution.

Due to the complexity of the problem, it is proposed to use the original Perry formula given in Equations 6.1 and 6.2 for the design. To take the thermal bowing into account, it is proposed to calculate the thermal bowing and include it in the Perry formula as the initial lack of straightness. To take the effective eccentricity into account, it is proposed to calculate the effective eccentricity approximately, calculate the plastic bending

moment capacity and then use a linear moment-thrust relationship to calculate the design load. The following calculation method is proposed for the design of columns for buckling about their major axis.

STEP 1: Divide the section into 4 rectangles as shown in Figure 6.2.

STEP 2: Find out the temperatures at points 1 to 4. (These may be calculated or obtained from experimental data).

STEP 3: Calculate the corresponding elastic modulus and yield stress for points 1 to 4 according to EC2: Part 10

STEP 4: Calculate the effective yield stress using Equation 6.4

STEP 5: Calculate the effective E using the following expression

$$E_{eff} = \frac{\frac{(E_1 + E_4)}{12} (b \cdot f_t^3 + \frac{b \cdot f_t \cdot d_1^2}{4}) + \frac{(E_2 + E_3)}{96} (w_t \cdot d_2^3 + w_t \cdot \frac{d_2^3}{4})}{I_y} \quad (6.6)$$

$$\text{where, } I_y = \frac{1}{12} \left(2 \cdot b \cdot f_t^3 + \frac{b \cdot f_t \cdot d_1^2}{4} + w_t \cdot d_2^3 \right)$$

STEP 6: Calculate the plastic bending moment capacity (M_y), using the corresponding yield strengths for each quadrilateral at temperatures T1, T2, T3 and T4.

STEP 7: Calculate the thermal bowing deflection using the following expression

$$\Delta_T = \frac{\alpha L^2 (T_1 - T_4)}{8d}$$

where, α = Coefficient of thermal expansion for steel ($14 \times 10^{-6} / ^\circ\text{C}$)

STEP 8: Calculate the design axial load (P_{cc}) for a concentrically loaded column, using the Perry strut formula given in equations 6.1 and 6.2. It should be noted that the value for Δ in equation 6.2 should be calculated as

$$\Delta = \Delta_T + 0.001L.$$

STEP 9: Calculate the effective eccentricity (e_x) using the following equation

$$e_x = \frac{b \cdot f_t \cdot \sigma_{y1} \frac{f_t}{2} + \frac{w_t \cdot d_2}{2} \left[\sigma_{y2} \cdot \left(f_t + \frac{d_2}{4} \right) + \sigma_{y3} \cdot \left(d_1 - \frac{d_2}{4} \right) \right] + b \cdot f_t \cdot \sigma_{y4} \cdot \left(d - \frac{f_t}{2} \right)}{b \cdot f_t \cdot (\sigma_{y1} + \sigma_{y4}) + \frac{w_t \cdot d_2}{2} \cdot (\sigma_{y2} + \sigma_{y3})}$$

STEP 10: Calculate the final design strength (P_c), using the following expression based on Rankine's formula.

$$P_c = \frac{1}{\left[\frac{1}{P_{cc}} + \frac{e_x}{M_y} \right]}$$

6.1.3.3 Validation of the design methods

To validate the design methods proposed in the previous sections, a number of numerical experiments were performed using the computer programs TASEF and SOSMEF. The cross sectional details and length of the columns analysed are given in Table 6.1. For each cross section, temperature distributions were calculated at 15, 30, 60 and 90 minutes exposure to a standard fire using the computer program TASEF. Table 6.2 shows the temperatures at points 1 to 4, according to Figure 6.2, calculated at different times for each cross section.

For each column, failure loads were calculated, for the two cases of major axis and minor axis buckling, using the computer program SOSMEF for the given temperature distributions at 15, 30, 60 and 90 minutes calculated earlier. In calculating these failure loads, an initial sinusoidal imperfection of Length/1000 was assumed. In the case of major axis buckling, two sets of failure loads were calculated using the initial imperfection in directions towards and away from fire. The lower of the two failure loads obtained was taken as the failure load.

Figure 6.4 and Figure 6.5 show the non-dimensional failure loads obtained using both the calculation methods. The failure loads have been non-dimensionalised in terms of the fully plastic load (P_y).

$$\text{where, } P_y = b.f_t \left[\sigma_{y1} + \sigma_{y4} \right] + w_t \frac{d_2}{2} \left[\sigma_{y2} + \sigma_{y3} \right]$$

The correlation between the proposed design method and the results from program SOSMEF is reasonably good.

Table 6.1 Cross sectional and buckling length details of columns analysed

Cross Section	Buckling Lengths (m)
152x152x23 UC	2, 4, 6 and 8
203x203x71 UC	1, 3, 5 and 7
305x305x240 UC	2, 4, 6 and 8
356x406x551 UC	3, 6, 9 and 12

Table 6.2 Calculated Temperatures at Points 1 to 4

Cross Section	Time (min)	Temperature (°C)			
		T1	T2	T2	T4
152x152x23 UC	15	340	148	37	23
	30	577	299	84	44
	60	800	478	180	104
	90	917	587	258	165
203x203x71 UC	15	232	85	22	20
	30	446	201	38	23
	60	719	381	86	42
	90	872	488	138	70
305x305x240 UC	15	165	64	21	20
	30	340	157	30	21
	60	616	326	64	32
	90	772	446	102	51
356x406x551 UC	15	117	49	20	20
	30	248	112	24	20
	60	482	268	46	20
	90	665	394	74	38

6.1.4 Conclusions

From the comparison made in Figures 6.4 and 6.5, one can conclude that the design methods proposed in the previous section may be used to calculate the load carrying capacity of a steel column subjected to a non-uniform temperature distribution across the section. Before the above design procedure can be adopted in a code of practice, considerably more extensive studies need to be made.

6.2 Enhancement of Inherent Fire Resistance capacity of Slimflor Beams

6.2.1 Introduction

The slim floor beams were mainly developed for use with prefabricated precast concrete floor elements. To reduce the depth of the floor, hence the total height of the building, the beams are integrated into the concrete floor, leaving only the bottom flange exposed. As most of the steel is encased in concrete the inherent fire resistance capacity of the slim floor beam is greater than that of a similar downstand beam which is exposed to fire on three sides. There are different types of slim floor beams currently used in Scandinavia and the UK. Some of these beams are shown in Figure 6.6. This chapter is limited to the system called Slimflor beam, shown in Figure 6.6(d), recently introduced into the UK by the Steel Construction Institute and British Steel Plc.

A Slimflor beam is constructed by welding a plate (typically 12mm or 15mm thick) to the bottom flange of a Universal Column section. The minimum outstand of the plate is 100mm. These Slimflor beams are divided into three categories^[126] as shown in Figure 6.7. The applications and fire resistance details of these three types are given in Table 6.3. A design guide for the room temperature design of slimflor beams was recently published by the SCI^[103]. In addition to this design guide a computer program was also developed by the SCI to do design calculations at room temperature and moment capacity calculations at 60 minutes of standard fire exposure.

Table 6.3 Different Types of Slimflor Beams

Type	Application	Construction	Maximum Fire Resistance
1	Domestic - light loads/shorter spans	Non-Composite	30 minutes
2	Light Commercial - medium loads/spans	Semi-Composite	60 minutes
3	Speculative/Retail - heavy loads/long spans	Composite	60 minutes

6.2.2 Proposed Method to Enhance Inherent Fire Resistance

It is proposed that by adding few reinforcing bars in appropriate places the fire resistance capacity of a Slimflor beam can be significantly increased. To verify this method, a number of standard fire tests were numerically simulated using two computer programs. The temperature analysis was carried out using TASEF-2, a public domain code developed in Sweden. The structural analysis was carried out using SOSMEF.

6.2.3 Parametric Study

For the parametric study, only the beams with an inherent fire resistance of 60 minutes (Type 2 and Type 3) were considered. The sections and loads were selected according to the initial guide beam selector table given in reference [126].

Failure Criterion-Deflection

BS476:Part20^[5] defines the failure of a beam in a fire test by the following criterion:

The failure of a horizontal load bearing element shall be taken as either of the following, whichever is exceeded first:

(a) Deflection of $L/20$

Where L is the clear span of the element

OR

(b) where the rate of deflection R (in mm/min) calculated over 1 minute intervals starting at 1 minute from the commencement of the heating period, exceeds the limit set by the following equation

$$R = L^2 / (9000d)$$

where L = Span in mm

d is the distance from the top of the structural section to the bottom of the design tension zone (in mm). However, this rate of deflection limit shall not apply before a deflection of $L/30$ is exceeded.

Failure Criterion-Ultimate

BS5950: Part 8^[7] adopts the ultimate limit state approach as the failure criterion. It is sufficient to check that the beam can support the load at the fire limit state, and no restrictions are given about any specific deflection or deflection rate.

The failure times according to both the deflection and ultimate failure criterion are given in the results of the parametric study.

6.2.4 Calculations

The stress-strain-temperature properties and thermal expansion properties of steel and concrete used in the calculations are as recommended in Eurocode 3:Part 10^[9] for steel and Eurocode 2: Part 10^[8] for concrete.

Type 2 - Semi - Composite Slimflor Beams

Seven beams with different spans and loadings were analysed. The concrete surrounding the Universal Column section and the precast concrete floor elements was taken into account in the thermal response calculations. In the structural response calculations no concrete was taken into account. The reasons for ignoring concrete in structural response calculations are:

- ⌘ There are no shear connectors provided to enable the concrete and steel to act compositely.

- ⌘ In fire conditions the neutral axis of the section will be very close to the top flange hence the concrete will have no contribution in structural capacity as it is assumed to have no tensile capacity.

The load applied was calculated according to the information given in the beam selector tables given in reference 3. For each beam three cases were analysed.

CASE 1: Slimflor beam with no modification

CASE 2: Slimflor beam with 2 reinforcing bars placed symmetrically either side of the web.

CASE 3: Slimflor beam with 4 reinforcing bars placed symmetrically either side of the web

Figure 6.5 illustrates the cross section details of the above three cases. The results of the simulated fire tests with all the other necessary details are given in Table 6.4

Type 3 - Composite Slimflor Beams

Five beams with different spans and loadings were analysed. As in the case of Type 2 beams, insitu concrete and precast elements were taken into account in the thermal response calculations. In the structural response calculations, the concrete surrounding the Universal section and the topping of the precast unit up to span/4 width was taken into account. It was also assumed that the depth of the insitu concrete topping above the top of the universal column was 90 mm.

The load applied was calculated according to the information given in the beam selector tables given in reference 1. For each beam three cases were analysed.

CASE 1: Slimflor beam with no modification

CASE 2: Slimflor beam with 2 reinforcing bars placed symmetrically either side of the web.

CASE 3: Slimflor beam with 4 reinforcing bars placed symmetrically either side of the web

Figure 6.6 illustrates the cross section details of the above three cases. The results of the simulated fire tests with all the other necessary details are given in Table 6.5.

Table 6.4 Results of Type 2 Slimflor Beams

UC Size	Plate Width (mm)	Length (m)	Load (kN/m)	Diameter of reinforcement (mm)	Number of reinforcements	Failure Time (minutes)	
						Deflection	Ultimate
203 UC 52	404	5	41.0	20	0	52.5	59.9
					2	57.3	74.4
					4	60.0	95.5
203 UC 86	410	6	41.0	20	0	59.5	65.8
					2	65.8	71.3
					4	76.1	95.3
254 UC 107	460	7	48.6	25	0	57.7	63.0
					2	65.7	76.6
					4	80.9	101.0
254 UC 167	466	8	56.0	25	0	62.2	69.5
					2	68.0	78.5
					4	75.1	95.1
305 UC 137	510	7	74.4	32	0	*57.2	61.8
					2	70.2	76.9
					4	92.2	109.7
305 UC 198	514	8	83.7	32	0	64.1	67.4
					2	73.5	80.8
					4	90.1	104.1
305 UC 283	522	9	82.8	32	0	72.6	78.0
					2	81.2	90.6
					4	94.9	113.3

* Rate of deflection of $L^2 / (9000d)$ reached before $L/20$ is achieved

Table 6.5 Results of Type 3 Slimflor Beams

UC Size	Plate Width (mm)	Length (m)	Load (kN/m)	Diameter of reinforcement (mm)	Number of reinforcements	Failure Time (minutes)	
						Failure Criterion	
						Deflection	Ultimate
254 UC 107	460	6	90.3	25	0	*63.5	63.7
					2	*79.0	80.1
					4	*107.0	107.3
254 UC 167	466	7	118.8	25	0	*57.3	61.1
					2	*68.7	71.4
					4	90.5	93.9
305 UC 198	514	8	114.4	32	0	*61.6	64.8
					2	*74.0	76.0
					4	95.7	98.9
305 UC 240	518	9	116.8	32	0	*61.8	65.3
					2	*70.5	73.6
					4	82.1	87.1

* Rate of deflection of $L^2 / (9000d)$ reached before $L/20$ is achieved

6.2.5 Conclusions

From the results given in Tables 6.4 and 6.5, it can be seen that the inherent fire resistance capacity of the Slimflor beam can be significantly increased by adding reinforcements. It is shown that by using the correct amount of reinforcement and placing it appropriately so that the temperature of reinforcement does not reach higher values, one can design a slimflor beam with a higher value of inherent fire resistance than the currently rated 60 minutes. Economical aspects of the individual cases should be considered in deciding whether to provide fire protection to the bottom plate or to use a few reinforcing bars to achieve the required fire resistance.

In an instance like this, where a rigorous analysis is used to improve a design procedure, it may be necessary to validate the new design with a limited number of experiments.

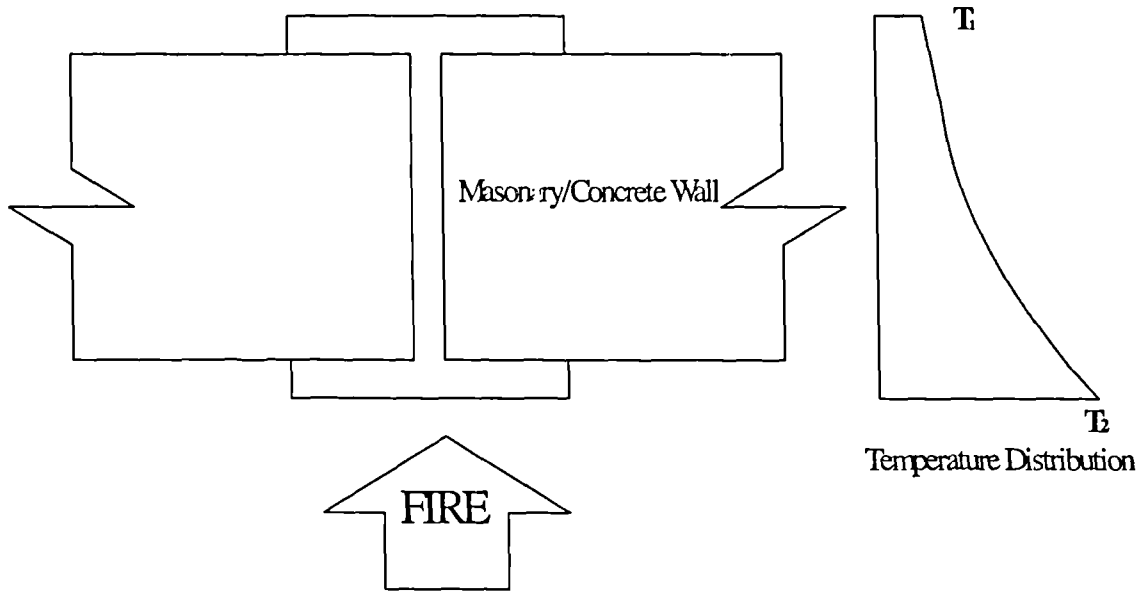


Figure 6.1 Column Exposed to Fire on One Flange

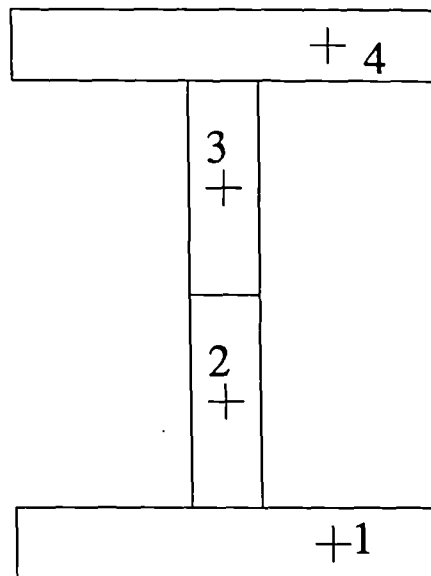


Figure 6.2 Idealisation of Section

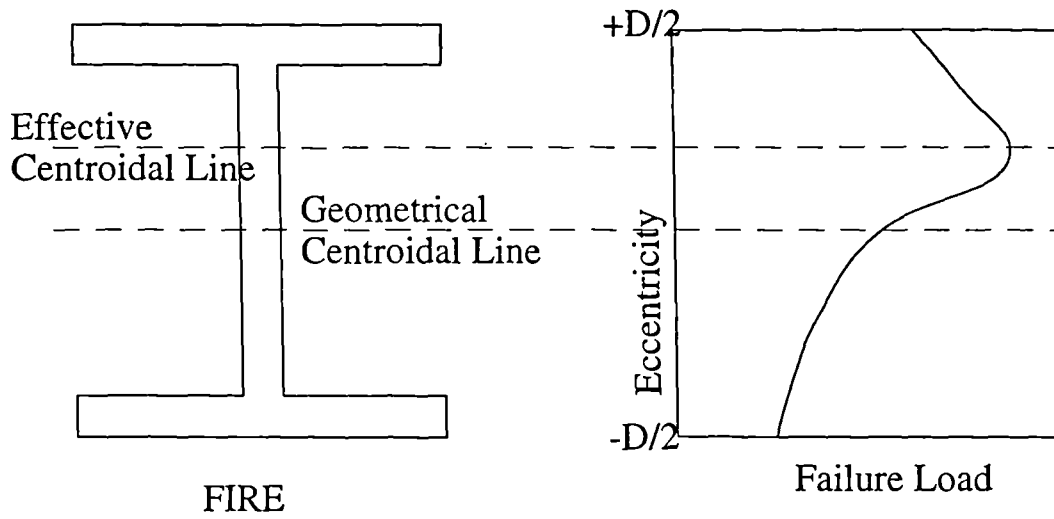


Figure 6.3 Variation of Failure Load With Eccentricity

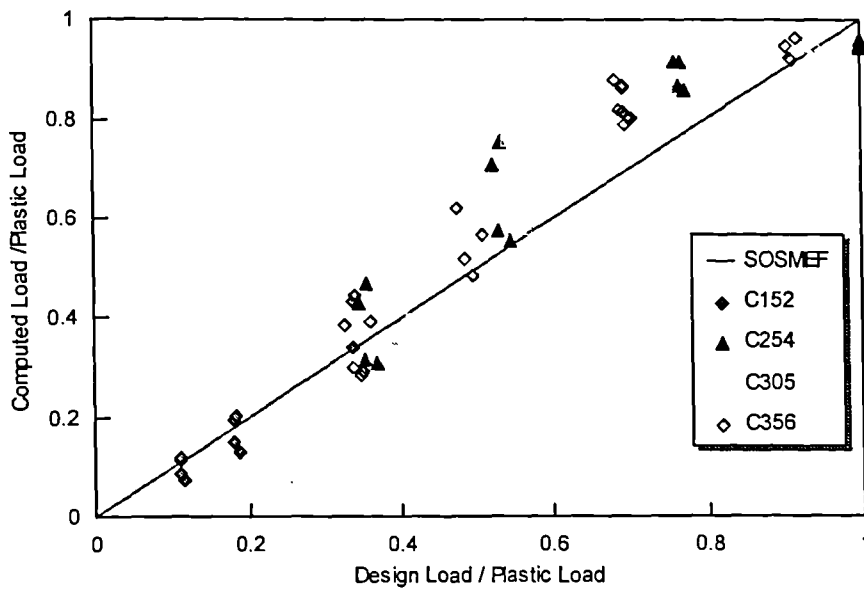


Figure 6.4 Comparison of Results - Minor Axis Buckling

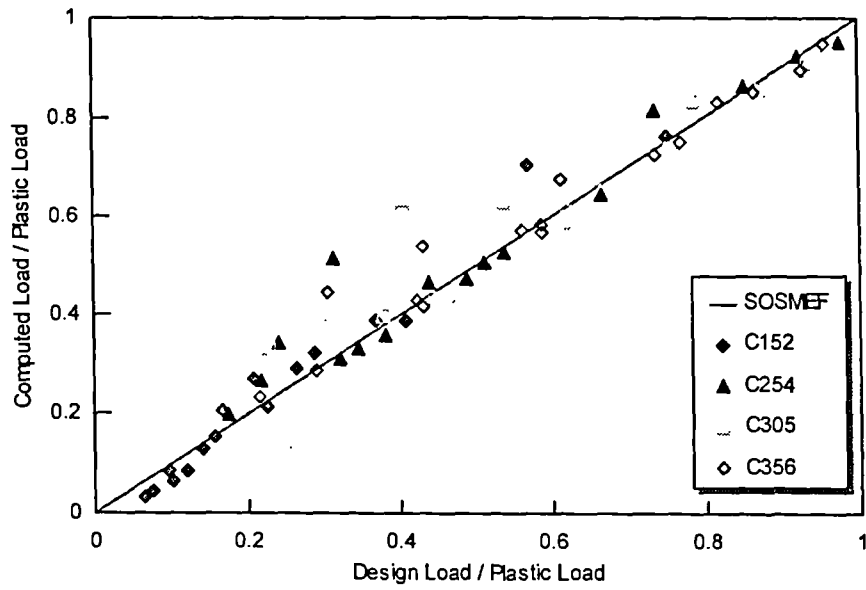


Figure 6.5 Comparison of Results - Major Axis Buckling

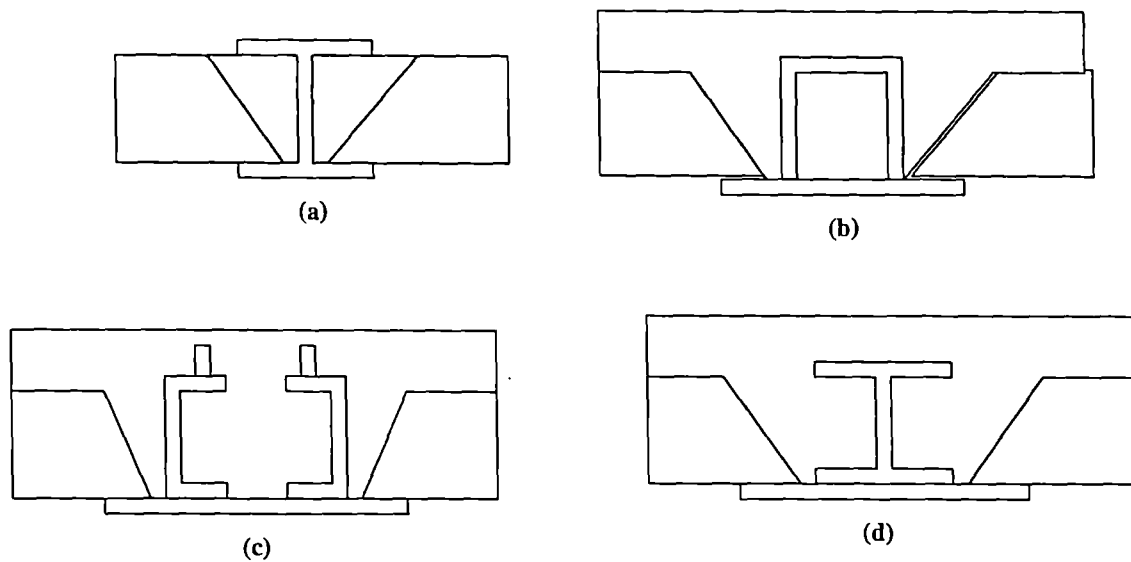
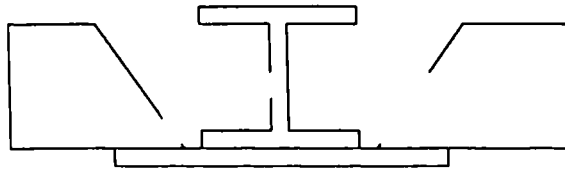
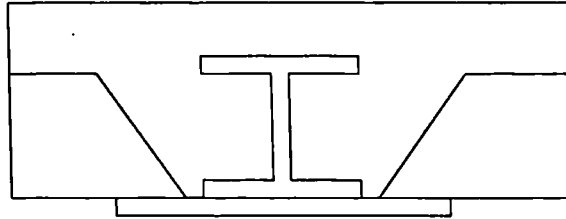


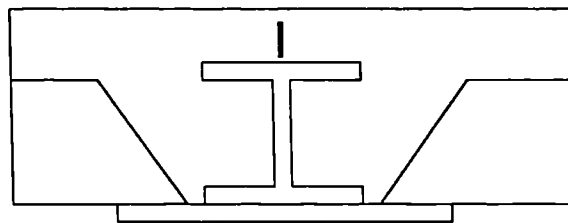
Figure 6.6 Different Types of Slim Floor Construction



Type 1 - Non-Composite

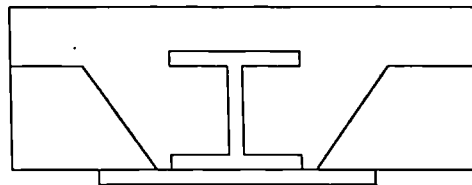


Type 2 - Semi-Composite

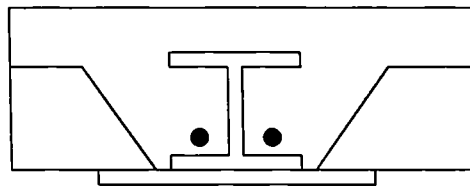


Type 3 - Composite

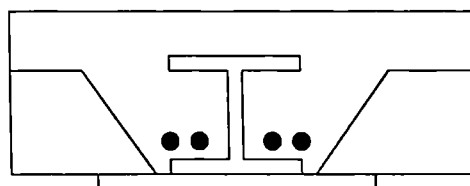
Figure 6.7 Types of Slimflor Beam



CASE 1



CASE 2



CASE 3

Figure 6.8 Cases Analysed

CHAPTER 7

CONCLUSIONS

7.0 Introduction

In this thesis, a new numerical method and an associated computer program were developed for the structural analysis of beams and columns exposed to fire. Experimental work was carried out on seven steel columns subjected to non-uniform heating and axial load with varying biaxial eccentricities. The test specimens were heated using electrical heating elements. The computer programs developed in this thesis were used to carry out two parametric studies. One study led to the proposal of a simple design method for steel columns subjected to a non-uniform temperature distribution. Another study looks at a possible way of enhancing the inherent fire resistance capacity of Slimflor beams.

7.1 Review of Previous Work

7.1.1 Material Properties

A review of previous work indicates that the material properties of steel at elevated temperatures are reasonably well defined. British code BS5950: Part 8 and European code EC3: Part 10 provide effectively the same material data in slightly different formats.

Properties of concrete at elevated temperatures are not so well defined when compared to steel. Data presented in European code EC2: Part 10 only provides the stress-strain relationship and free thermal expansion data. It contains no information on transient strain which is an important part of the total strain of concrete at elevated temperatures. This indicates the need for further research into this area.

7.1.2. Structural Analysis - Simple Calculation Models

The most common assumption made in simple calculation models for steel beams and columns is that the member is subjected to a uniform temperature distribution. This assumption limits the applicability range of these simple models to bare steel members or fully fire protected steel members. The moment capacity method for beams allows for the non-uniform temperature distribution across the section. No design or simple calculation method is available for the analysis of steel columns subjected to a non-uniform temperature distribution across the section.

For reinforced concrete members, the only simple calculation method available, in addition to the moment capacity method for beams, is in the form of tabulated data. These tabulated data, established on the basis of experiments, prescribe the cover and minimum cross sectional dimensions required for different fire resistance requirements. The moment capacity method is also applicable to steel/concrete composite beams.

7.1.3. Structural Analysis - Rigorous Calculation Models

Most of the numerical methods are very recent. This indicates that analytical work has been receiving attention in the recent past. Most of the numerical methods are based on finite element modelling. None of the methods reviewed was capable of analysing all types of steel, reinforced concrete and steel/concrete beams and columns subjected to a non-linear variation of temperature in all three dimensions and with axial and lateral loading. This demonstrated the need for the numerical method with all the above mentioned capabilities developed in this thesis.

7.1.4 Experimental Work

A considerable amount of experimental work has been carried out on all types of beam and column in many countries. In the case of steel columns the majority of experimental work has the test specimen exposed to fire on all sides resulting in a uniform temperature

distribution throughout the specimen. Little experimental data is available on the behaviour of steel columns subjected to a non-uniform temperature distribution both across the section and along the length of the member. The experimental work in this thesis was specifically designed to provide such data.

7.2 Numerical Method

A new numerical method for the structural analysis of beams and columns subjected to a non-linear variation of temperatures in all three directions has been developed. The method is based on the finite difference approach, which ensures equilibrium at a number of points along the length of the member. Internal forces at these points are calculated using the Gaussian integration procedure, which is an established and efficient method of numerical integration. The related computer program SOSMEF is a user friendly program with data editing, and pre and post processing facilities. The program is coded in FORTRAN 77 and uses the GINO-F graphical libraries to produce graphical output.

7.2.1 Idealisation of Geometry

The cross section of the members is idealised using a number of quadrilaterals, enabling the analysis of a wide variety of cross sections. A cross section can consist of quadrilaterals of different materials. Reinforcement can be represented as concentrated areas. The variation of temperature is allowed in all three directions. The variation of cross section along the length, such as in the case of tapered members, is also allowed. The bending of the member can be bi-axial as in reality. However, it is also possible to analyse a member with uniaxial bending option. The member can be subjected to any combination of axial loading, lateral loading and end moments. Four types of analyses can be carried out. For a given temperature distribution data, either the ultimate axial load capacity or ultimate lateral load factor can be calculated. For a given loading, either the failure temperature (assuming uniform temperature distribution through the member) or the failure time (time-temperature distribution data should be given) can be calculated.

7.2.2 Material properties

The numerical model can incorporate any material model which is given in the form of stress-strain-temperature relationship either in mathematical formulae or in tabulated form. The material properties, stress-strain-temperature and thermal strain- temperature properties, for steel and concrete according to Eurocodes 3 and 2 have been included in the computer code. An option of prescribing the material properties in tabulated form is also included for the user to specify a different model other than the standard ones for steel or concrete, or to use it for a different material altogether.

7.2.3 End Conditions

All three types of end conditions anticipated in an isolated member, simply supported, rotationally restrained and rotationally flexible, have been included. For rotationally flexible support condition, the moment-rotation relationship data should be provided.

7.3 Validation and Experimental Work

The numerical method has been validated by comparing results with a number of experimental results from literature and with the experiments carried out under this research programme. Correlation between experimental and numerical results are very good for steel beams and columns. Good correlation for steel/concrete composite beams and columns and for reinforced concrete beams and columns has also been demonstrated.

Seven experiments have been carried out on columns with non-uniform temperature distribution along the length and across the depth. The test rig, with an axial loading capacity of 600 kN, was designed and manufactured at City University.

To ensure the tests are full scale, the smallest rolled section available was used for the test specimens. The end conditions at both ends were designed to represent pinned supports. Two columns were tested with varying biaxial eccentricities and five columns were tested with varying uniaxial eccentricities in the major axis direction.

7.3.1 Heating Arrangements

Electrical heating elements were used to heat the specimens. To achieve a nonuniform temperature distribution along the length and across the section, heating elements were placed either at the centre or at the one end of the specimen.

7.3.2 Instrumentation and Data Recording

To obtain a comprehensive temperature profile of the test columns several thermocouples were used. Deflection measurements were made at different positions. An electronically operated hydraulic jack was used to apply the axial load. A load cell was used to monitor the axial load applied. Data was recorded at 2 minute intervals.

7.3.3 Results

The main objective of the experiments was to provide data on the behaviour of steel columns subjected to a non-uniform temperature distribution along the length and across the section and axial load. This objective was successfully achieved. The data obtained can be used to validate the numerical methods such as the one developed in this research programme.

Although only two columns were subjected to biaxial eccentricities, all seven columns failed in a biaxial mode. It was also noted that all the failures were due to buckling about the minor axis. The maximum deflection was always observed to be at the approximate location where the column was experiencing the maximum temperature.

The agreement obtained between the numerical and experimental results is excellent. This shows that the numerical method developed can accurately model the behaviour of steel columns exposed to fire.

7.4 Parametric Studies

7.4.1 Design Method for Steel Columns

A parametric study has been carried out to develop a simple design method for steel column H sections subjected to a non-uniform temperature distribution across the depth of the section. A number of numerical experiments were performed using the computer programs TASEF and SOSMEF for this study. A simple method, based on the Perry strut formula, is proposed for the design of steel columns subjected to a non-uniform temperature distribution across the depth. The agreement between the design method and numerical results is good. This study is only a step forward towards the goal of providing design guidance for steel columns subjected to non-uniform temperature distributions across the section. It is necessary to conduct further extensive studies covering all the possibilities and all the other different sectional shapes before producing a general design guide.

7.4.2 Parametric Study on Slimflor Beams

A parametric study has been carried out on the possibility of increasing the inherent fire resistance capacity of Slimflor beams. Again the computer programs TASEF and SOSMEF were used to perform a number of numerical experiments. From this study, it has been concluded that the current fire rating of 60 minutes for Type 2 and Type 3 composite beams can be improved significantly by using appropriate levels of reinforcement. It is necessary to perform further parametric studies and a few controlled experiments on Slimflor beams with reinforcement bars before any recommendation can be made as to design guidance.

These parametric studies clearly demonstrate the application of the numerical method developed under this research programme to the development of improved design methods for steel or composite beams and columns.

7.5 Summary

The original objectives of the thesis have been fulfilled as follows:

- ⌘ A numerical method and an associated computer software has been developed and validated.
- ⌘ Experimental data has been obtained from seven tests on steel columns subjected to a non-linear variation of temperature along the length and across the depth.
- ⌘ A design method for steel columns subjected to a non-uniform temperature distribution across the depth is proposed. This is only the first step towards the goal of producing a comprehensive design guide.
- ⌘ A possible way of increasing the inherent fire resistance capacity of Slimflor beams is proposed.

7.6 Further Research

The numerical method presented in this thesis is only applicable for isolated beams and columns. The next step was to develop this method for the analysis of frames. This has recently been completed at City University under another project. The analysis of panel structures such as walls and slabs is another area of research which needs attention. It is necessary to do more work on obtaining data for a better understanding of the material properties of concrete at elevated temperatures as the current specifications are inadequate.

REFERENCES

1. MALHOTRA,H.L. (1982). *Design of fire resisting structures*. Surrey University Press, London.
2. BSI. (1932). *BS476, British standards definitions for fire resistance, incombustibility and non-flammability of building materials and structures*. British Standards Institution, London.
3. BSI. (1953). *BS476, Fire tests on building material and structures*. British Standards Institution, London.
4. BSI. (1972). *BS476: Part 8, Fire tests on building material and structures, Test methods and criteria for the fire resistance of elements of building construction*. British Standards Institution, London.
5. BSI. (1987). *BS476: Part 20, Fire tests on building material and structures, Test methods and criteria for the fire resistance of elements of building construction*. British Standards Institution, London.
6. ISO. (1975). Fire resistance tests - Elements of building construction. *International Standard ISO834*, International Organization for Standardization.
7. BSI. (1990). *BS5950: Part8, Code of practice for fire resistant design*. British Standard Institution, London.
8. CEC. (1990a). *Eurocode No.2. Design of concrete structures, Part 10. Structural fire design. (Draft 1990)*. Commission of European Communities.
9. CEC. (1990b). *Eurocode No.3. Design of steel structures, Part 10. Structural fire design. (Draft 1990)*. Commission of European Communities.
10. CEC. (1990c). *Eurocode No.4. Design of composite structures, Part 10. Structural fire design. (Draft 1990)*. Commission of European Communities.
11. LAWSON,R.M. (1987). Fire engineering in theUK and Europe. *Steel Construction Today* 1: 159-165.
12. KIRBY,B.R. (1986). Recent developments and applications in structural fire engineering design - A review. *Fire Safety Journal* 11(3): 141-179.

13. LIE,T.T. (1972). *Fire and buildings*. Applied Science Publishers, London.
14. LAW,M. and O'BRIEN,T. (1989). *Fire safety of bare external structural steel*. SCI Publication 009, The Steel Construction Institute, Ascot, Berkshire, Uk.
15. PETTERSSON,O., MAGNUSSON,S. and THOR,J. (1976). Fire engineering design of steel structures. *Publication 50*, Swedish Institute of Steel Construction, Stockholm, Sweden.
16. CULVER,C.G. (1976) Survey results for fire loads and live loads in office buildings. *NBS Building Science Series 85*, National Bureau of Standards, Washington.
17. WICKSTROM,U. (1983). *TASEF-2 a computer program for temperature analysis of structures exposed to fire*. Lund Institute of Technology, Sweden.
18. IDING,R.J., BRESLER,B. and NIZAMUDDIN,Z. (1977). FIRES-T3 a computer program for the fire response of structures - Thermal. *Report No. UCB FRG 77-15.*, University of California, Berkeley.
19. TERRO,M.J., SULLIVAN,P.J.E. and KHOURY,G.A. (1992). Computer modelling of structures under fire. IN: *Structural design for Hazardous Loads - The Role of Physical Testing*, Edited by J.L.Clarke, F.K.Garas and G.S.T.Armer, E&FN Spon, London.
20. FRANSSEN,J.M. (1986). Comportmentde colonnes massives en acier soumises a l'incendie. (Behaviour of heavy steel columns under fire conditions). *Construction Metallique* 23(1): 37-45.
21. HERTZ,K. (1981). *Simple temperature calculation of fire exposed concrete constructions*. Report No. 159, Institute of Building Design, Technical University of Denmark, Lyngby, Denmark.
22. STANZAK,W.W. and LIE,T.T. (1973). Fire resistance of unprotected steel columns. *Journal of the structural division, ASCE*, 99(ST5): 837-852.
23. MACKAY,D.C. and THOMPSON,D.B. (1992). Simulation of fire tests by finite element analysis. IN: *Structural design for Hazardous Loads - The Role of Physical Testing*, Edited by J.L.Clarke, F.K.Garas and G.S.T.Armer, E&FN Spon, London.

24. BARTHELEMY,B. (1976). Heating calculation of structural steel members. *Journal of the Structural division, ASCE*, **102**(ST8): 1549-1558.
25. BENNETTS,I.D., PROE,D.J. and THOMAS,I.R. (1985). Simulation of the fire testing of structural elements by calculation - Thermal response. *Steel Construction, Journal of Australian Institute of Steel Construction* **19**(3).
26. ECCS. (1983). *European recommendations for the fire safety of steel structures*. Elsevier Scientific Publishing Company, Amsterdam.
27. COOKE,G.M.E. (1987). The structural response of steel I-section members subjected to elevated temperature gradient across the section. *PhD Thesis*: Department of Civil Engineering, City University, London EC1V 0HB, UK.
28. COOKE,G.M.E. (1988a). An introduction to the mechanical properties of structural steel at elevated temperatures. *Fire Safety Journal* **13**: 45-54.
29. ANDERBERG,Y. (1988). Modelling steel behaviour. *Fire Safety Journal* **13**(1): 17-26.
30. RAMBERG,W. and OSGOOD,W.R. (1943). *Description of stress-strain curves by three parameters*. NACA Technical note No. 902.
31. OLAWALE,A.O. and PLANK,R.J. (1988). The collapse analysis of steel columns in fire using a finite strip method. *International Journal for Numerical Methods in Engineering* **26**(12): 2755-2764.
32. HARMATHY,T.Z. (1967). A comprehensive creep model. *Journal of Basic Engineering, Transactions of the ASME*: 496-502.
33. KIRBY,B.R. and PRESTON,R.R. (1988). High temperature properties of hot rolled, structural steels for use in fire engineering design studies. *Fire Safety Journal* **13**:27-37.
34. ANDERBERG, Y. and THELANDERSON, S. (1973). Stress and deformation characteristics of concrete at high temperatures - 1. General discussion and critical review of literature. *Bulletin No. 34*, Division of Structural Mechanics and Concrete Construction, Lund Institute of Technology, Lund, sweden.

35. ANDERBERG, Y. and THELANDERSON, S. (1976). Stress and deformation characteristics of concrete at high temperatures - 2. Experimental investigation and material behaviour model. *Bulletin No. 54*, Division of Structural Mechanics and Concrete Construction, Lund Institute of Technology, Lund, sweden
36. HERTZ,K. (1985). *Analysis of prestressed concrete structures exposed to fire*. Report No. 174, Institute of Building Design, Technical University of Denmark, Lyngby, Denmark.
37. LIE,T.T., LIN,T.D., ALLEN,D.E. and ABRAMS,M.S. (1984). *Fire resistance of reinforced concrete columns*. DBR Paper No. 1167, Division of Building Research, National Research Council of Canada.
38. BALDWIN,R. and NORTH,M.A. (1973). A stress-strain relationship for concrete at high temperatures. *Magazine of Concrete Research* **25**(85): 208-212.
39. TERRO,M.J. (1991), Numerical modelling of thermal and structural response of reinforced concrete structures in fire. PhD Thesis, Department of Civil Engineering, Imperial College of Science and Technology, University of London, London, UK.
40. ASFPCM (1988). *Fire protection for structural steel in buildings.*, Association of Structural Fire Protection Contractors and Manufacturers Limited, PO Box 111, Aldershot, Hampshire, GU11 1YW, UK.
41. KRUPPA,J. (1979). Collapse temperature of steel structures. *Journal of the structural division, ASCE*, **105**(ST9): 1769-1788.
42. RUBERT,A. and SCHAUMANN,P. (1988). Critical temperatures of steel columns exposed to fire. *Fire Safety Journal* **13**: 39-44.
43. BENNETTS, I.D., PROE, D.J. and THOMAS, I.R. (1987). Guidelines for assessment of fire resistance of structural steel members, Australian Institution of Steel Construction, Australia.
44. BENNETTS, I.D., GOH, C.C., O'MEAGHER, A.J. and THOMAS, I.R. (1989). Restraint of compression members in fire, Report No. MRL/PS65/89/002, BHP Research - Melbourne Laboratories, Australia.

45. NEWMAN, G.M. (1989). The fire resistance of composite floors with steel decking. *SCI Publication 110*, Steel Construction Institute, Ascot, Berkshire, UK.
46. COOKE and MORGAN (1988). Thermal bowing in fire and how it affects building design. BRE Information Paper IP21/88. Building Research Establishment, Borehamwood, Herts., England.
47. GATEWOOD, B.E. (1957). *Thermal stresses*. McGraw-Hill Book Company inc.
48. HARMATHY, T.Z. (1976). Creep deflection of metal beams in transient heating process, with particular reference to fire. *Canadian Journal of Civil Engineering* 13(2): 219-228.
49. CHENG, W.C. (1983). Theory and application on the behaviour of steel structures at elevated temperatures. *Computers and Structures* 16(1-4): 27-35.
50. PLANK, R.J. (1987). The collapse behaviour of steel beams in fire - An analytical treatment. IN: Proceedings of the International Conference on Steel and Aluminium Structures, Cardiff, UK, 8-10 July 1987. - Steel Structures. edited by R. Narayanan.
51. CONTRO, R., POGGI, C. and CAZZANI, A. (1988). Numerical analysis of fire effects on beam structures. *Engineering Computing* 5(1): 53- 58.
52. THOR, J. (1973). Deformation and critical loads of steel beams under fire exposure conditions. *Document D16*, Swedish Institute of Steel Construction.
53. SKOWRONSKI, W. (1988). A study of the steel beam deformation during fire. *Building and Environment* 23(2): 159-167.
54. BURGESS, I.W., EL-RIMAWI, J.A. and PLANK, R.J.A. (1988). A secant stiffness approach to the fire analysis of steel beams. *Journal of Constructional Steel Research* 11(2): 105-120.
55. BURGESS, I.W., EL-RIMAWI, J.A. and PLANK, R.J.A. (1990). Analysis of Beams with non-uniform temperature profile due to fire exposure. *Journal of Constructional Steel Research* 16: 169-192.
56. CULVER, C.G. (1972). Steel column buckling under thermal gradients. *Journal of the Structural Division, ASCE*, 98(ST8): 1853-1865.

57. CULVER,C.G., AGGARWAL,V. and OSSENBRUGGEN,P. (1973) Buckling of steel columns at elevated temperatures. *Journal of the Structural Division, ASCE*, **99**(ST4): 175-726.
58. OSSENBRUGGEN,P.J., AGGARWAL,V. and CULVER,C.G. (1973) Steel column failure under thermal gradients. *Journal of the Structural Division, ASCE*, **99**(ST4): 727-739.
59. VANDAMME,M. and JANSS,J. (1981). Buckling of axially loaded steel columns in fire conditions. *IABSE Periodica 3/1981, Proceedings P-43/81*: 81-95.
60. PROE,D.J., BENNETTS,I.D. and THOMAS,I.R. (1986). Simulation of the fire testing of structural elements by calculation - Mechanical response. *Steel Construction, Journal of Australian institute of Steel Construction* **19**(4): 2-18.
61. PROE,D.J., BENNETTS,I.D. and THOMAS,I.R. (1986). Simulation of the fire testing of structural elements by calculation - Overall behaviour. *Steel Construction, Journal of Australian institute of Steel Construction* **19**(4): 19-31.
62. BOCK,H.M. (1987). Uber das tragverhalten von stahlstutzen wahrend eines normbrand versuches. (Structural behaviour of steel columns during a standard fire test). *Stahlbau* **56**(6): 161-168.
63. ARIBERT,J.M. and ABDEL AZIZ,M. (1987). Simulation du comportement a l'incendie de poteaux comprimes et flechis en presence de gradients quelconques de temperature. *Construction Metallique* **24**(2): 3-40.
64. SHARPLES,J.R. (1987). The strength of partially exposed steel columns in fire. *MPhil Thesis*: University of Sheffield, Department of Civil and Structural Engineering.
65. POH, K.W. and BENNETTS, I.D. (1990a). Nonlinear analysis of steel cross sections with two-dimensional temperature distribution. Report No. BHP RML/PS69/90/001, BHP Research - Melbourne Laboratories, Australia.
66. POH, K.W. and BENNETTS, I.D. (1990b). Nonlinear analysis of steel beam-columns in fire conditions. Report No. BHP RML/PS69/90/001, BHP Research - Melbourne Laboratories, Australia.

67. WAINMAN and KIRBY (1987). Compendium of UK standard fire test data - Unprotected structural steel - 1, Report No. RS/RSC/S10328/1/87/B, British Steel Technical, Swindon Laboratories, Rotherham, UK.
68. WAINMAN and KIRBY (1989). Compendium of UK standard fire test data - Unprotected structural steel - 2, Report No. RS/R/S1199/8/88/B, British Steel Technical, Swindon Laboratories, Rotherham, UK.
69. OLESSEN (1980). Fire test on steel columns, Report No. 8003, Institute of Building Technology and Structural Engineering, Aalborg, Denmark. (In Danish)
70. KRUPPA, J. (1981/2). Some results on the fire behaviour of external steel columns. *Fire Safety Journal* 4(4): 247-257.
71. AASEN, B. and LARSEN, P.K. (1987). Fire simulated tests of high strength steel columns. IN: Proceedings of the International Conference on Steel and Aluminium Structures, Cardiff, UK, 8-10 July 1987. - Steel Structures. edited by R. Narayanan.
72. SAITO, H., UESUGI, H. and MIYAMOTO, K. (1987). Load bearing and deformation capacity of H shaped steel members at elevated temperature. *Fire Science and Technology* 17(2): 43-52.
73. WITTEVEEN, J. and TWILT, L. (1981/2). A critical view on the results of standard fire resistance tests on steel columns. *Fire Safety journal* 4(4): 259-270.
74. POH, K.W. and BENNETTS, I.D. (1991). Fire tests on steel sections. Report No. BHP RML/PS69/91/003, BHP Research - Melbourne Laboratories, Australia.
75. ELLINGWOOD, B. and SHAVER, J.R. (1976). Analysis of reinforced concrete beams subjected to fire. *NBS Building Science Series 76*, National Bureau of Standards, Washington, USA.
76. ELLINGWOOD, B. and SHAVER, J.R. (1977). Reliability of reinforced concrete beams subjected to fire. *Journal of the Structural Division*, ASCE, 103(ST5) 1047-1059.
77. SALSE, E.A and Lin, T.D. (1976). Structural fire resistance of concrete. *Journal of the Structural Division*, ASCE 102(ST1): 51-63.
78. TASSIOS, T.P. and CHRONOPOULOS, M.P. (1991). Structural response of RC elements under fire. *The Structural Engineer* 69: 277-281.

79. WADE, C (1991). Method for fire engineering design of structural concrete beams and floor systems. Technical Recommendation 8, C1/SfB/HQ4 (K), BRANZ, New Zealand.
80. Lie, T.T. (1992). Structural fire protection: Manual of practice. *ASCE Manuals and reports of engineering practice; No: 78*, American Society of Civil Engineers, USA.
81. BSI. (1985). *BS8110, Structural use concrete: Part1 Code of practice for design and construction* . British Standards Institution, London.
82. FIP (1978). FIP/CEB report on methods of assesment of the fire resistance of concrete structural members., Cement and Concrete Association, UK.
83. UDDIN, T. and CULVER, C.G. (1975). Effects of elevated temperature on structural members. *Journal of the Structural Division ASCE* **101**(ST7): 1531-1549.
84. COOKE, G.M.E. (1992). The deflections of unrestrained precast reinforced concrete floor slabs exposed to standard fires and natural fire. *Report No. CR65/92*, Fire Research Station, BRE, Borehamwood, Herts., England.
85. Warrington Fire Research Centre. (1987). Report No. WARRES 40728.
86. Warrington Fire Research Centre. (1987). Report No. WARRES 40764.
87. Warrington Fire Research Centre. (1987). Report No. WARRES 40766.
88. Warrington Fire Research Centre. (1987). Report No. WARRES 40811.
89. Warrington Fire Research Centre. (1987). Report No. WARRES 40812.
90. Warrington Fire Research Centre. (1987). Report No. WARRES 40813.
91. Warrington Fire Research Centre. (1987). Report No. WARRES 40859.
92. Warrington Fire Research Centre. (1989). Report No. WARRES 46086.
93. Warrington Fire Research Centre. (1989). Report No. WARRES 46087.
94. Warrington Fire Research Centre. (1989). Report No. WARRES 46088.
95. Warrington Fire Research Centre. (1989). Report No. WARRES 46089.
96. Warrington Fire Research Centre. (1989). Report No. WARRES 46090.
97. Warrington Fire Research Centre. (1989). Report No. WARRES 47855.

98. JEYARUPALINGAM, N. and VIRDI, K.S. (1993). Processing of results of fire tests on reinforced concrete slabs. Report No. SRC/FIRE/04. Structures Research centre, Department of Civil Engineering, City University, London.
99. LIN, T.D, LIE, T.T., BURG, R.G. and CORLEY, W.G. (1992). Fire loading of modern reinforced concrete columns. IN: *Structural design for Hazardous Loads - The Role of Physical Testing*, Edited by J.L.Clarke, F.K.Garas and G.S.T.Armer, E&FN Spon, London.
100. NG, A.B., MIRZA, M.S., and LIE, T.T. (1990). Response of direct models of reinforced concrete columns subjected to fire., *ACI Structural Journal*, **87**(3), 113-325.
101. HAKSEVER, A. and ANDERBERG, Y. (1981-2). Comparison between measured and computed structural response of some reinforced concrete columns in fire., *Fire Safety Journal*, **4**, 293-297
102. THOR, J. (1990). A new fire-safe composite steel beam., *Steel Construction Today*, **4**, 137-140.
103. MULLETT, D.L. (1992). Slimfloor design and construction., *SCI Publication 110*, Steel Construction Institute, Ascot, Berkshire, UK.
104. ARBED Recherches. (1988). Practical design tools for composite steel-concrete construction elements submitted to ISO fire considering the interaction between axial load N and bending moment M: REFAO - II., CEC Agreement No. 7210-SA/504, Luxembourg.
105. Fire Insurers Research and Testing Organisation. (1990). Fire Test on ConstrucThor Column., Report No. TE80426.
106. O'MEAGHER, A.J., BENNETTS, I.D., STEVENS, L.K. and HUTCHINSON, G.L. (1993). Behaviour of composite columns in fire. Report No. BHPR/PPA/R/93/001/SG3C, BHP Research - Melbourne Laboratories, Australia.
107. SCHLEICH, J.B. (1987). Computer assisted analysis of the fire resistance of steel and composite concrete-steel structures (REFAO-CAFIR). *Report No. EUR10828EN.*, Commission of the European Communities.

108. COOKE, G.M.E. (1988). An assesment of the fire resistance of Arbed AF composite concrete/steel columns incorporating steel I-sections and reinforcing bars for use in the United Kingdom *Client Report No. CR 47/88*, Building Research Establishment, Watford, UK.
109. BECKER, J. and BRESLER, B. (1974). - FIRES-RC, A computer program for the fire response of structures - Reinorced concrete frames., *Report No. UCB FRG 74-3*, University of California, Berkeley, California, USA.
110. IDING, R., BRESLER, B. and NIZAMUDDIN, Z. (1977). FIRES-RC II, A computer program for the fire response of structures - Reinforced concrete frames., *Report No. UCB FRG 77-8*, University of California, Berkeley, California, USA.
111. JEANES, D.C. (1985). Application of the computer in modelling fire endurance of structural steel floor systems., *Fire Safety Journal*, **9**, 119-135
112. FORSEN, N.E. (1982). A theoretical study on the fire resistance of concrete structures., *Report No. STF65 A82062*, Cement and Concrete Research Institute, The Norwegian Institute of Technology, Norway.
113. FORSEN, N.E. (1983). *STEELFIRE - Finite element program for nonlinear analysis of steel frames exposed to fire.*, Multiconsult AS Consulting Engineers, Norway.
114. RUDOLPH, K., RICHTER, E., HASS, R. and QUAST, U. (1985). Principles for calculation of load bearing and deformation behaviour of composite structural elements under fire action., *Fire safety science, Proceedings of 1st International Symposium*.
115. FRANSSEN, J.M. (1987). A study of the behaviour of composite steel-concrete structures in fire., *PhD Thesis*, Universite de Liege, Belgium.
116. WEEKS, N.J. (1985). Lateral instability of slender reinforced concrete columns in a fire environment., *PhD Thesis*, Aston University, UK.
117. CHUNG, K.F. (1990). Fire engineering software - BFIRE, Information paper circulated by Steel Construction Institute to Fire modelling group members.

118. TERRO, M.J., SULLIVAN, P.J.E. and KHOURY, G.A. (1992). Computer modelling of structures under fire., IN: *Structural design for Hazardous Loads - The Role of Physical Testing*, Edited by J.L.Clarke, F.K.Garas and G.S.T.Armer, E&FN Spon, London.
119. Minutes of the fire modelling group meeting held on 24-09-1992.
120. WANG, Y.C. and MOORE, D.B. (1992). Fire resistance of steel frames.,IN: *Structural design for Hazardous Loads - The Role of Physical Testing*, Edited by J.L.Clarke, F.K.Garas and G.S.T.Armer, E&FN Spon, London.
121. VIRDI K.S. and DOWLING P.J. (1973). The ultimate strength of composite columns in biaxial bending., *Proceedings, The Institution of Civil Engineers*, 58(2),251-272.
122. VIRDI K.S. and DOWLING P.J. (1976). The ultimate strength of biaxially restrained columns., *Proceedings, The Institution of Civil Engineers*, 61(2),41-58.
123. VIRDI K.S. (1981). Design of circular and rectangular hollow section columns. *Journal of Constructional Steel Research*, 1(4), 33-45
124. ZIENKIEWICZ, O.C. and TAYLOR, R.L. (1989). *The finite element method Volume 1: Basic formulation and linear problems.*, 4th edition, McGraw-Hill Book Company, London
125. DOWLING, J. (1990). Fire test on shelf angle floor beam, *Personal correspondance*
126. BRITISH STEEL. Design in Steel 2 Slim Floor Construction., Information booklet issued by British Steel sections Strutral Advisory service.
127. JEYARUPALINGAM, N. and VIRDI, K.S. (1996). Experiments on steel columns with temperature gradients., Report No: SRC/FIRE/STEEL/1/96, Structures Research Centre, Department of Civil Engineering, City University, London.

APPENDIX 1

Example Output from Programs VIEW DATA and POST PROCESSOR

- Fig A1 Cross section details of an ARBED composite column, showing the steel section , enclosed concrete, as well as the longitudinal reinforcing bars.
- Fig A2 Temperature contours for the section shown in Fig A1. Calculations done using TASEF-2, contours plotted by VIEW DATA.
- Fig A3 Graphical representation of axial and lateral loading on a column.
- Fig A4 Typical deflection versus time graph plotted by the POSTPROCESSOR program. Calculations performed by the program SOSMEF.
- Fig A5 Typical biaxial deflected shapes plotted by the POSTPROCESSOR program. Calculations performed by the program SOSMEF.

DATE://////
TIME://////

SOSMEF

Version 3.0

CITY
UNIVERSITY

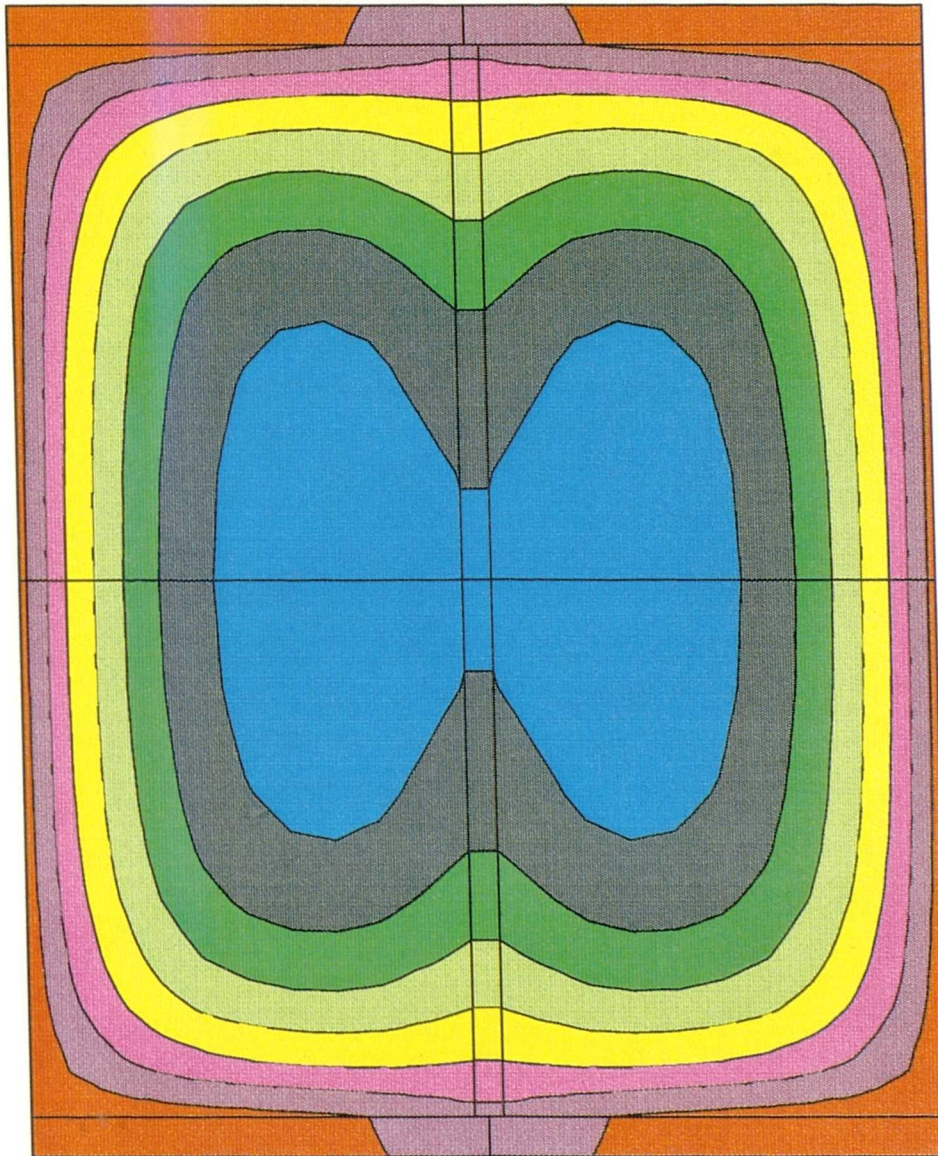
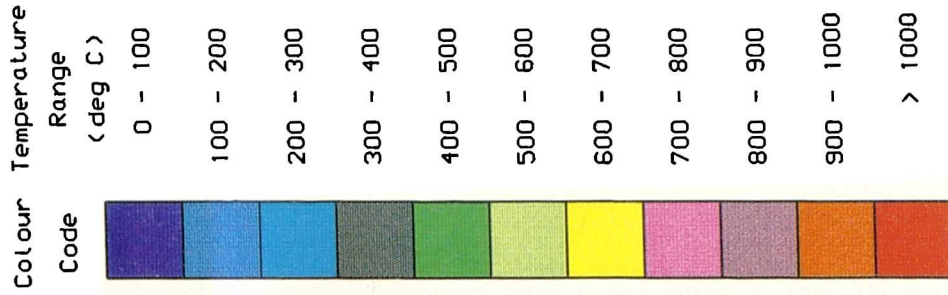
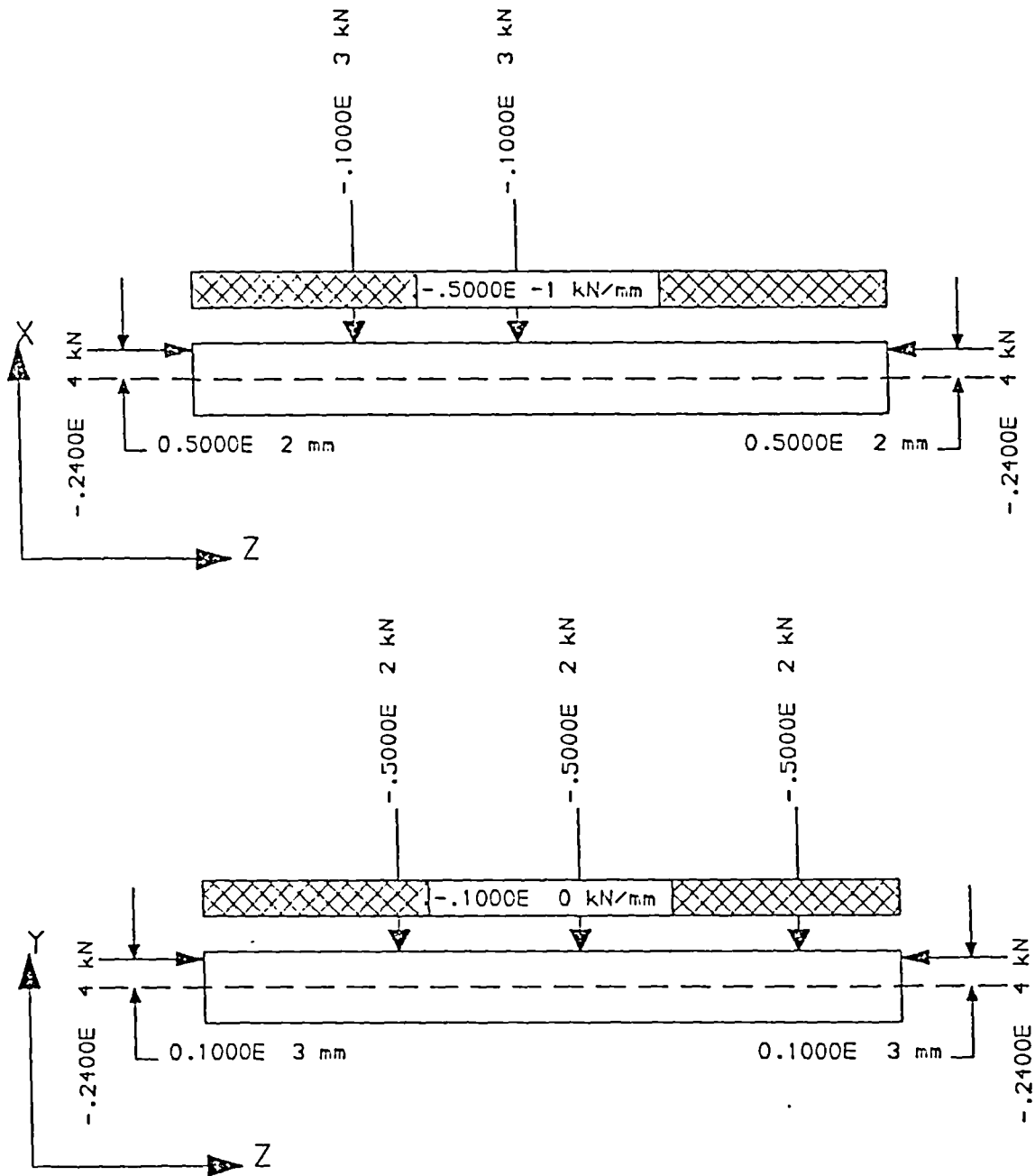


FIG. A2 VIEW DATA EXAMPLE 2

DATE:
TIME:10:51:12

SOSMEF
Version 3.0

CITY
UNIVERSITY



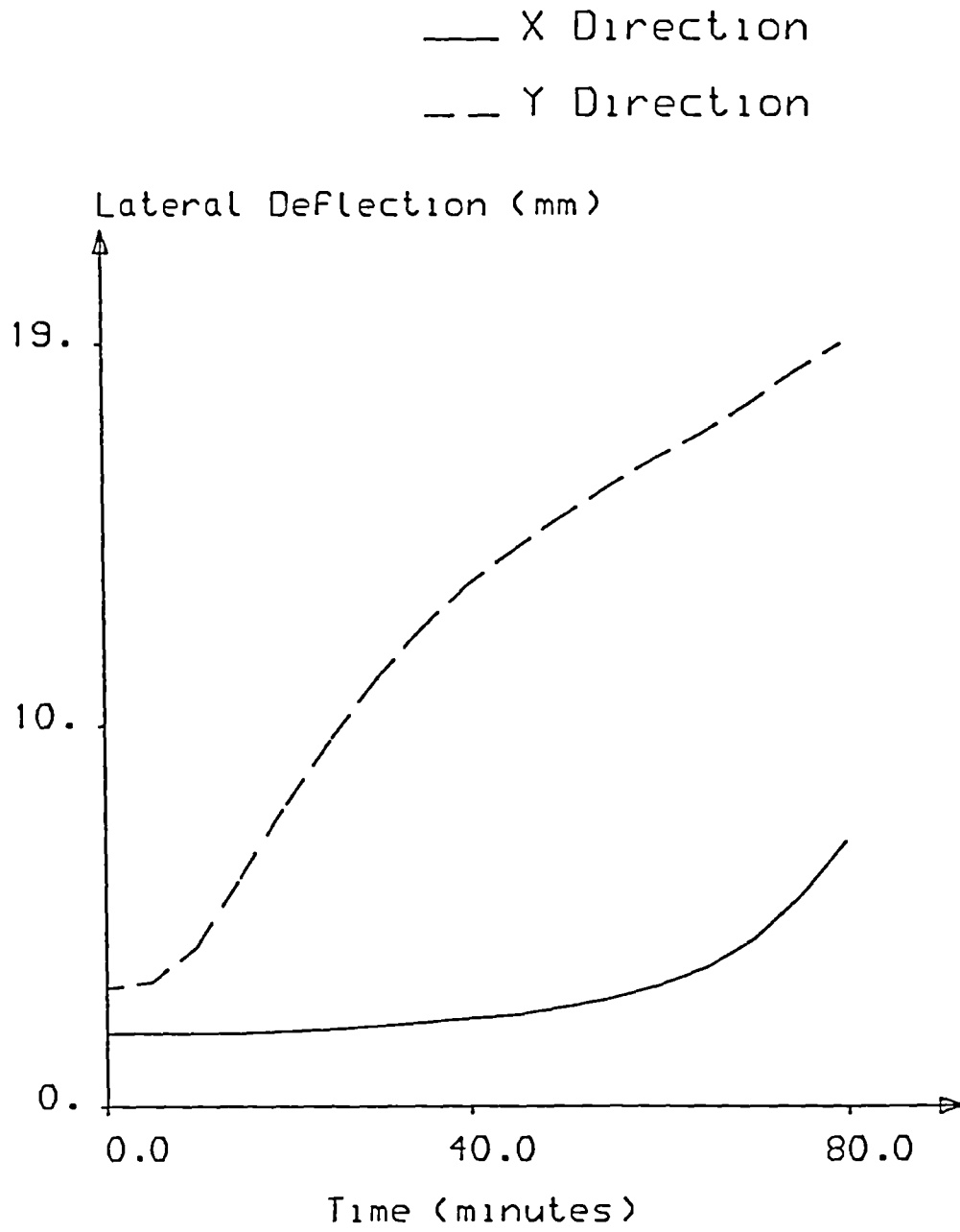
LOADING DETAILS

FIG.A3 VIEW DATA - EXAMPLE 3

DATE:
TIME:10:38:40

SOSMEF
Version 3.0

CITY
UNIVERSITY



Time - Lateral deflection

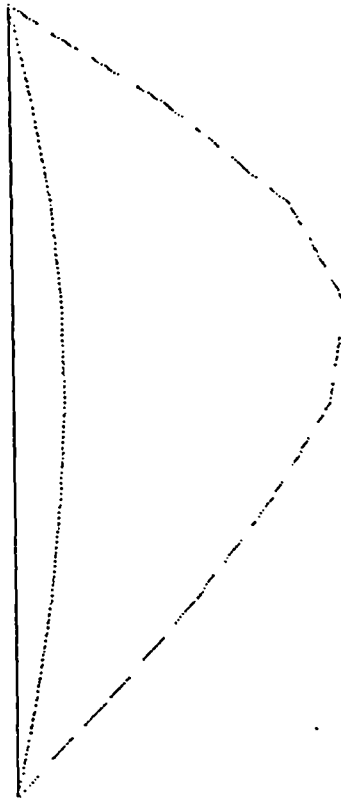
FIG.A4 POSTPROCESSOR - EXAMPLE 1

DATE: -
TIME:10:40:21

SOSMEF
Version 3.0

CITY
UNIVERSITY

— X Direction
- - - Y Direction



Deflected Shape

FIG.A5 POSTPROCESSOR - EXAMPLE 2

APPENDIX 2

Sample Raw Experimental Data

Tables A2.1- A2.2
Tables A2.3- A2.8

Deflection transducer readings for Test 7(mm)
Thermocouple readings for Test 7(°C)

Table A2.1. Test 7 - Displacement Transducer Readings (DT1-DT7)

Time (min)	DT1	DT2	DT3	DT4	DT5	DT6	DT7
0.000	1.707	2.709	2.415	-1.450	-2.416	-2.825	-2.553
2.000	1.707	2.709	2.415	-1.450	-2.416	-2.831	-2.553
4.000	1.707	2.709	2.415	-1.457	-2.443	-2.875	-2.610
6.000	1.707	2.709	2.415	-1.494	-2.530	-2.992	-2.760
8.000	1.707	2.771	2.418	-1.674	-2.846	-3.426	-3.193
10.000	1.704	2.802	2.424	-1.862	-3.220	-3.935	-3.725
12.000	1.704	2.827	2.424	-2.117	-3.725	-4.635	-4.459
14.000	1.707	2.864	2.427	-2.425	-4.370	-5.534	-5.371
16.000	1.707	2.877	2.433	-2.756	-5.010	-6.421	-6.283
18.000	1.711	2.883	2.433	-3.070	-5.629	-7.276	-7.165
20.000	1.714	2.895	2.433	-3.364	-6.227	-8.076	-8.002
22.000	1.714	2.889	2.510	-3.626	-6.747	-8.801	-8.763
24.000	1.714	2.889	2.510	-3.937	-7.342	-9.601	-9.599
26.000	1.714	2.889	2.981	-4.212	-7.887	-10.339	-10.372
28.000	1.717	2.889	2.981	-4.450	-8.362	-10.996	-11.053
30.000	1.717	2.889	2.981	-4.655	-8.787	-11.585	-11.662
32.000	1.717	2.883	2.978	-4.897	-9.253	-12.224	-12.324
34.000	1.714	2.883	2.990	-5.105	-9.639	-12.734	-12.882
36.000	1.717	2.883	2.990	-5.277	-9.978	-13.195	-13.363
38.000	1.717	2.883	2.990	-5.452	-10.319	-13.656	-13.832
40.000	1.717	2.883	2.987	-5.641	-10.666	-14.098	-14.312
42.000	1.714	2.883	2.987	-5.711	-10.840	-14.356	-14.585
44.000	1.717	2.877	2.984	-5.929	-11.214	-14.854	-15.076
46.000	1.717	2.877	2.981	-6.065	-11.472	-15.191	-15.424
48.000	1.717	2.877	2.981	-6.207	-11.729	-15.529	-15.775
50.000	1.714	2.877	2.978	-6.339	-11.966	-15.843	-16.104
52.000	1.714	2.870	2.975	-6.442	-12.166	-16.113	-16.395
54.000	1.714	2.870	2.972	-6.584	-12.427	-16.457	-16.755
56.000	1.714	2.870	2.972	-6.750	-12.717	-16.844	-17.157
58.000	1.714	2.870	2.969	-6.859	-12.924	-17.102	-17.462
60.000	1.714	2.870	2.966	-7.050	-13.259	-17.550	-17.924
62.000	1.714	2.870	2.966	-7.234	-13.565	-17.943	-18.413
64.000	1.839	2.864	2.963	-7.415	-13.867	-18.367	-18.904
66.000	1.836	2.864	2.959	-7.659	-14.283	-18.883	-19.504
68.000	1.836	2.864	2.956	-7.856	-14.631	-19.350	-20.053
70.000	1.872	2.864	2.953	-8.116	-15.068	-19.915	-20.717
72.000	1.866	2.864	2.947	-8.419	-15.629	-20.609	-21.508
74.000	1.714	2.864	2.947	-8.814	-16.315	-21.494	-22.516
76.000	1.467	2.864	2.944	-9.420	-17.362	-22.789	-24.070
78.000	5.436	9.540	6.867	-11.066	-20.648	-27.251	-29.390
80.000	8.081	17.340	16.165	-10.236	-20.368	-27.307	-32.078

Table A2.2. Test 7 - Displacement Transducer Readings (DT8-DT14)

Time (min)	DT8	DT9	DT10	DT11	DT12	DT13	DT14
0.000	-1.746	-2.475	-0.449	2.111	-2.953	-0.670	2.618
2.000	-1.746	-2.475	-0.449	2.111	-2.953	-0.673	2.618
4.000	-1.791	-2.508	-0.455	2.114	-2.966	-0.667	2.618
6.000	-1.896	-2.647	-0.478	2.131	-3.013	-0.586	2.636
8.000	-2.186	-3.076	-0.574	2.260	-3.222	-0.408	2.681
10.000	-2.545	-3.571	-0.694	2.377	-3.432	-0.156	2.708
12.000	-3.039	-4.257	-0.864	2.530	-3.720	0.219	2.753
14.000	-3.653	-5.142	-1.071	2.746	-4.084	0.667	2.807
16.000	-4.264	-5.992	-1.277	2.948	-4.404	1.138	2.834
18.000	-4.863	-6.813	-1.471	3.138	-4.705	1.631	2.851
20.000	-5.438	-7.608	-1.663	3.331	-4.971	2.153	2.878
22.000	-5.961	-8.318	-1.827	3.480	-5.173	2.607	2.878
24.000	-6.526	-9.113	-2.025	3.700	-5.433	3.093	2.887
26.000	-7.058	-9.842	-2.192	3.866	-5.648	3.589	2.896
28.000	-7.523	-10.481	-2.344	4.022	-5.794	4.063	2.896
30.000	-7.949	-11.061	-2.485	4.165	-5.924	4.518	2.896
32.000	-8.399	-11.693	-2.641	4.325	-6.064	4.954	2.896
34.000	-8.782	-12.201	-2.751	4.438	-6.148	5.357	2.896
36.000	-9.119	-12.644	-2.856	4.548	-6.230	5.742	2.887
38.000	-9.447	-13.093	-2.958	4.657	-6.249	6.107	2.887
40.000	-9.770	-13.549	-3.062	4.784	-6.334	6.462	2.887
42.000	-9.967	-13.797	-3.119	4.840	-6.301	6.779	2.887
44.000	-10.311	-14.279	-3.227	4.976	-6.408	7.086	2.878
46.000	-10.554	-14.611	-3.301	5.056	-6.408	7.379	2.878
48.000	-10.785	-14.950	-3.376	5.153	-6.431	7.645	2.878
50.000	-11.012	-15.269	-3.441	5.229	-6.451	7.902	2.878
52.000	-11.210	-15.517	-3.495	5.302	-6.467	8.141	2.878
54.000	-11.452	-15.855	-3.566	5.389	-6.499	8.386	2.878
56.000	-11.713	-16.239	-3.649	5.505	-6.594	8.610	2.869
58.000	-11.932	-16.510	-3.717	5.581	-6.626	8.831	2.869
60.000	-12.235	-16.963	-3.797	5.684	-6.756	9.031	2.869
62.000	-12.545	-17.368	-3.880	5.781	-6.873	9.255	2.869
64.000	-12.869	-17.808	-3.966	5.887	-7.013	9.466	2.869
66.000	-13.291	-18.382	-4.084	6.050	-7.247	9.666	2.869
68.000	-13.670	-18.856	-4.179	6.157	-7.436	9.853	2.860
70.000	-14.110	-19.444	-4.307	6.293	-7.699	10.119	2.860
72.000	-14.644	-20.161	-4.452	6.482	-8.031	10.315	2.860
74.000	-15.336	-21.060	-4.639	6.765	-8.496	10.515	2.869
76.000	-16.373	-22.466	-4.923	7.126	-9.260	10.676	2.869
78.000	-19.440	-27.272	-6.153	8.207	-12.698	12.166	12.026
80.000	-20.566	-28.850	-6.817	6.273	-12.561	12.830	-18.527

Table A2.3. Test 7 - Thermocouple Readings (TC1-TC8)

Time (min)	TC1	TC2	TC3	TC4	TC5	TC6	TC7	TC8
0.0	20.6	20.3	20.5	20.3	20.6	20.4	20.8	20.6
2.0	20.5	20.3	20.5	20.2	20.6	20.4	20.8	20.6
4.0	20.5	20.3	20.5	20.3	20.6	20.4	20.8	20.6
6.0	20.5	20.2	20.5	20.2	20.6	20.4	20.8	20.6
8.0	20.5	20.2	20.5	20.2	20.6	20.4	20.8	20.6
10.0	20.5	20.2	20.5	20.2	20.6	20.4	20.8	20.6
12.0	20.5	20.2	20.5	20.2	20.6	20.4	20.8	20.6
14.0	20.5	20.2	20.5	20.2	20.6	20.4	20.8	20.6
16.0	20.5	20.2	20.5	20.2	20.6	20.4	20.9	20.6
18.0	20.5	20.2	20.5	20.2	20.6	20.4	20.9	20.8
20.0	20.5	20.2	20.5	20.2	20.6	20.4	21.0	20.9
22.0	20.5	20.2	20.5	20.2	20.6	20.4	21.2	21.1
24.0	20.5	20.3	20.6	20.3	20.7	20.5	21.4	21.4
26.0	20.6	20.4	20.7	20.4	20.8	20.5	21.7	21.8
28.0	20.7	20.4	20.8	20.5	20.9	20.6	22.0	22.2
30.0	20.8	20.5	20.9	20.6	20.9	20.7	22.4	22.6
32.0	20.9	20.7	21.0	20.7	21.1	20.9	22.8	23.2
34.0	21.0	20.9	21.2	20.9	21.3	21.0	23.4	23.9
36.0	21.2	21.1	21.4	21.1	21.5	21.3	24.0	24.6
38.0	21.4	21.4	21.7	21.4	21.7	21.5	24.6	25.4
40.0	21.6	21.5	21.9	21.6	21.9	21.7	25.5	26.2
42.0	21.8	21.8	22.1	21.8	22.2	21.9	26.3	27.1
44.0	22.1	22.1	22.5	22.1	22.5	22.2	27.1	28.0
46.0	22.3	22.3	22.7	22.4	22.7	22.5	28.0	28.9
48.0	22.5	22.6	23.0	22.7	23.0	22.8	28.9	30.0
50.0	22.8	22.9	23.3	23.0	23.4	23.1	29.9	31.0
52.0	23.1	23.2	23.6	23.4	23.7	23.5	30.9	32.0
54.0	23.5	23.5	23.9	23.7	24.0	23.8	31.8	32.9
56.0	23.8	23.8	24.2	24.0	24.3	24.1	32.8	34.0
58.0	24.1	24.1	24.5	24.3	24.6	24.4	33.8	35.0
60.0	24.4	24.5	24.8	24.6	24.9	24.7	34.7	35.9
62.0	24.6	24.7	25.2	25.0	25.3	25.0	35.7	36.9
64.0	24.9	25.0	25.5	25.3	25.6	25.5	36.6	37.9
66.0	25.3	25.5	25.9	25.7	26.1	25.8	37.7	39.0
68.0	25.7	25.8	26.3	26.1	26.4	26.2	38.7	40.0
70.0	26.1	26.1	26.5	26.4	26.8	26.6	39.7	40.8
72.0	26.3	26.4	26.9	26.7	27.1	26.9	40.5	41.8
74.0	26.6	26.6	27.1	27.0	27.4	27.2	41.4	42.5
76.0	26.8	26.8	27.3	27.2	27.6	27.4	42.2	43.2
78.0	27.1	27.1	27.7	27.6	27.9	27.8	43.1	44.0
80.0	27.2	27.1	27.5	27.5	27.9	27.8	43.5	44.3

Table A2.4. Test 7 - Thermocouple Readings (TC9-TC16)

Time (min)	TC9	TC10	TC11	TC12	TC13	TC14	TC15	TC16
0.0	20.7	20.6	20.7	20.7	21.0	20.9	21.3	21.6
2.0	20.7	20.6	20.7	20.6	21.0	20.9	21.3	21.6
4.0	20.7	20.6	20.7	20.7	21.0	20.9	21.3	21.6
6.0	20.7	20.6	20.7	20.6	21.0	21.0	21.3	21.6
8.0	20.7	20.6	20.7	20.6	21.0	21.0	21.4	21.7
10.0	20.7	20.6	20.7	20.6	21.1	21.2	21.5	21.9
12.0	20.7	20.6	20.7	20.7	21.4	21.5	21.7	22.2
14.0	20.7	20.6	20.7	20.7	21.7	21.8	22.1	22.6
16.0	20.8	20.7	20.8	20.7	22.2	22.3	22.7	23.3
18.0	20.9	20.8	20.9	20.8	22.9	22.8	23.5	24.1
20.0	21.1	20.9	21.1	21.0	23.9	23.8	24.6	25.1
22.0	21.3	21.2	21.3	21.2	24.9	24.8	25.8	26.4
24.0	21.6	21.5	21.6	21.4	26.2	25.9	27.2	27.8
26.0	22.0	21.8	21.9	21.8	27.8	27.4	28.8	29.4
28.0	22.4	22.3	22.4	22.3	29.5	28.8	30.6	31.0
30.0	22.9	22.7	22.9	22.7	31.3	30.5	32.5	32.8
32.0	23.5	23.4	23.5	23.4	33.3	32.2	34.6	35.0
34.0	24.2	24.1	24.2	24.0	35.5	34.3	36.8	36.7
36.0	24.9	24.8	25.0	24.7	37.8	36.5	39.2	38.9
38.0	25.8	25.7	25.9	25.6	40.2	38.4	41.6	41.4
40.0	26.6	26.5	26.7	26.5	42.5	41.0	43.9	43.5
42.0	27.6	27.4	27.7	27.4	45.0	42.7	46.5	46.1
44.0	28.5	28.4	28.6	28.4	47.4	45.0	48.9	48.1
46.0	29.5	29.4	29.7	29.4	49.8	47.0	51.2	51.0
48.0	30.5	30.4	30.7	30.4	52.2	49.2	53.7	53.1
50.0	31.6	31.6	31.9	31.5	54.7	51.2	56.3	55.1
52.0	32.6	32.5	32.9	32.6	57.0	53.7	58.5	57.6
54.0	33.7	33.6	34.0	33.7	59.4	55.4	60.8	59.7
56.0	34.8	34.7	35.2	34.8	61.6	57.8	63.1	62.0
58.0	35.8	35.8	36.2	35.9	63.9	60.2	65.2	63.9
60.0	36.7	36.7	37.2	36.8	66.0	61.3	67.6	65.9
62.0	37.9	37.9	38.3	38.0	68.2	63.4	69.7	68.6
64.0	38.9	38.9	39.4	39.0	70.3	65.4	71.5	70.4
66.0	40.0	40.1	40.5	40.1	72.4	67.0	73.7	72.5
68.0	41.0	41.0	41.5	41.2	74.4	68.9	75.6	73.6
70.0	41.9	42.0	42.6	42.2	76.3	70.2	77.5	75.7
72.0	42.8	42.9	43.5	43.2	78.1	72.1	79.1	77.4
74.0	43.8	43.9	44.4	44.0	79.8	74.0	80.9	79.0
76.0	44.3	44.7	45.2	44.9	81.4	75.3	82.3	81.0
78.0	45.2	45.4	46.0	45.6	82.9	76.8	83.9	82.3
80.0	45.7	45.8	46.6	46.3	84.3	79.1	84.9	82.5

Table A2.5. Test 7 - Thermocouple Readings (TC17-TC24)

Time (min)	TC17	TC18	TC19	TC20	TC21	TC22	TC23	TC24
0.0	21.6	21.6	21.6	21.5	21.6	21.5	21.6	21.6
2.0	21.6	21.6	21.5	21.5	21.6	21.6	21.6	21.6
4.0	21.6	21.6	21.6	21.6	21.7	21.8	21.9	21.8
6.0	21.7	21.7	21.6	21.7	22.1	22.4	22.6	22.6
8.0	21.8	21.9	21.8	22.3	23.0	23.7	24.2	24.4
10.0	21.9	22.3	22.4	23.3	24.7	26.1	27.0	27.5
12.0	22.3	22.7	23.5	25.0	27.6	29.6	31.3	31.8
14.0	22.8	23.4	25.0	27.7	31.5	34.4	37.0	38.0
16.0	23.6	24.3	27.6	31.2	36.3	40.0	43.8	44.9
18.0	24.6	25.5	30.8	35.4	42.1	46.5	51.6	52.7
20.0	25.8	26.7	34.8	40.5	48.3	53.5	59.8	61.1
22.0	27.2	28.2	39.4	46.2	54.9	60.8	68.6	69.8
24.0	28.6	29.9	44.4	52.3	62.4	68.7	77.6	78.7
26.0	30.5	31.8	50.1	58.9	69.8	76.3	86.7	87.8
28.0	32.4	33.8	56.0	65.7	77.1	84.2	95.7	96.8
30.0	34.5	36.0	62.2	73.4	84.3	91.2	104.4	105.3
32.0	36.7	38.3	68.6	79.7	92.5	99.8	113.6	114.6
34.0	39.1	40.8	74.9	87.3	99.7	106.8	122.1	123.0
36.0	41.6	43.3	81.5	94.4	107.6	112.5	130.4	131.2
38.0	44.1	45.9	88.0	101.9	114.9	120.6	138.8	139.6
40.0	46.8	48.7	94.3	107.8	124.2	125.8	146.3	146.8
42.0	49.4	51.1	100.4	114.4	128.9	133.5	154.0	154.5
44.0	51.8	53.7	106.4	120.2	137.5	138.6	161.0	161.4
46.0	54.8	56.5	112.2	126.7	143.5	145.3	168.1	168.8
48.0	57.3	59.1	117.9	132.5	147.9	151.9	174.9	175.5
50.0	59.5	61.6	123.4	137.4	156.7	156.9	181.5	181.7
52.0	62.3	64.2	128.6	142.7	162.0	162.9	188.1	188.1
54.0	64.8	66.8	133.6	147.5	168.4	167.8	194.0	193.6
56.0	67.1	69.2	138.4	152.4	172.3	175.8	200.3	198.9
58.0	69.5	71.8	143.1	157.7	178.3	178.8	205.5	205.0
60.0	71.8	74.1	147.5	161.5	182.3	184.3	210.8	210.1
62.0	74.4	76.3	151.7	166.2	187.3	187.4	215.8	215.8
64.0	76.4	78.4	155.6	169.9	191.8	190.9	220.1	219.9
66.0	78.6	80.7	159.4	173.8	194.3	198.3	225.5	224.1
68.0	80.3	83.0	163.0	178.1	200.3	198.9	229.2	229.5
70.0	82.5	85.1	166.6	181.4	202.4	204.2	233.4	233.1
72.0	84.4	87.0	169.6	184.5	206.0	207.7	237.4	236.7
74.0	85.9	88.7	172.7	187.2	208.7	214.1	241.7	239.9
76.0	87.8	90.3	175.6	190.9	212.9	212.2	244.0	244.6
78.0	89.4	92.2	178.7	194.0	217.0	214.6	247.4	247.8
80.0	90.4	93.5	181.4	195.9	218.6	219.9	250.6	249.3

Table A2.6. Test 7 - Thermocouple Readings (TC25-TC32)

Time (min)	TC25	TC26	TC27	TC28	TC29	TC30	TC31	TC32
0.0	21.6	21.6	21.6	21.6	21.6	21.6	21.7	21.7
2.0	21.6	21.6	21.7	21.8	21.9	21.9	21.6	21.7
4.0	21.6	21.9	22.6	23.5	24.2	24.5	21.7	21.9
6.0	22.0	22.9	25.0	27.8	29.2	30.2	22.1	22.9
8.0	22.9	25.5	30.2	36.2	39.2	40.9	23.1	25.5
10.0	24.9	30.0	38.6	48.8	54.2	57.0	25.4	30.3
12.0	28.6	37.2	50.8	66.8	75.2	78.8	29.5	37.8
14.0	34.5	47.4	66.8	88.5	100.8	105.9	36.1	48.9
16.0	42.5	60.5	85.9	112.0	128.3	135.1	45.1	62.5
18.0	52.5	74.5	104.6	136.4	156.1	164.2	56.6	78.6
20.0	64.1	88.8	123.7	161.9	184.2	193.8	70.1	96.3
22.0	76.7	103.9	144.2	185.2	211.1	221.8	85.0	115.0
24.0	90.3	118.0	165.2	210.8	238.2	249.9	101.1	134.5
26.0	104.6	134.0	186.6	235.3	264.8	277.6	118.2	155.0
28.0	119.0	149.4	207.5	258.6	289.7	304.2	135.7	175.5
30.0	133.4	164.3	225.2	282.2	315.2	330.2	153.4	197.1
32.0	147.9	179.4	244.5	304.6	338.9	354.9	171.1	218.9
34.0	162.0	193.6	261.4	325.0	360.1	377.6	189.0	239.0
36.0	176.0	209.0	277.8	344.6	381.4	398.8	206.7	259.3
38.0	189.5	225.3	295.0	363.6	402.4	419.2	224.1	279.4
40.0	202.7	237.4	309.6	382.7	422.5	438.4	240.8	297.6
42.0	215.4	250.4	324.8	399.7	441.1	457.3	256.7	314.9
44.0	227.4	262.8	337.7	415.2	457.7	471.8	271.6	331.0
46.0	239.1	275.4	350.4	430.6	474.7	489.6	285.7	346.7
48.0	250.1	284.9	364.2	444.2	489.8	505.5	299.3	360.8
50.0	260.5	297.0	376.8	458.1	504.0	517.9	311.7	374.7
52.0	270.6	306.9	387.6	471.0	517.6	531.3	323.7	387.7
54.0	279.8	317.6	398.1	481.5	528.8	542.2	334.9	398.9
56.0	288.4	325.3	409.4	493.3	540.5	554.7	345.0	409.9
58.0	296.5	333.9	417.2	503.6	551.8	565.6	354.7	420.5
60.0	304.2	341.9	426.1	512.8	560.9	575.3	363.6	430.7
62.0	311.4	349.7	433.2	522.3	570.7	585.8	372.0	439.2
64.0	318.2	356.5	439.8	529.4	576.8	593.0	379.7	447.5
66.0	324.5	363.7	448.8	538.1	579.2	602.2	386.8	457.2
68.0	330.4	369.3	452.0	542.5	586.9	610.9	393.3	463.0
70.0	335.8	375.4	458.8	550.6	595.1	617.5	399.5	469.5
72.0	340.9	380.9	466.5	556.9	601.3	623.2	405.2	477.2
74.0	345.6	386.5	472.0	561.7	606.6	629.7	410.5	481.6
76.0	350.3	390.9	473.5	562.9	612.3	636.7	415.9	488.1
78.0	354.4	397.8	476.5	563.1	615.4	642.7	420.4	491.2
80.0	359.2	401.2	486.7	559.5	616.6	647.5	425.8	499.4

Table A2.7. Test 7 - Thermocouple Readings (TC33-TC40)

Time (min)	TC33	TC34	TC35	TC36	TC37	TC38	TC39	TC40
0.0	21.7	21.8	21.7	21.7	21.7	21.7	21.7	21.7
2.0	21.7	21.9	21.8	21.9	21.6	21.7	21.8	21.8
4.0	22.5	23.3	23.6	23.9	21.7	21.9	22.5	23.1
6.0	24.6	26.8	27.9	28.7	22.0	22.9	24.6	26.5
8.0	29.4	34.6	37.0	39.0	22.9	25.3	29.2	33.9
10.0	37.7	46.9	51.2	54.5	24.9	29.7	37.5	44.8
12.0	50.2	64.8	71.7	76.8	28.6	36.7	49.5	61.9
14.0	66.8	88.2	97.8	104.8	34.5	46.9	65.7	82.5
16.0	86.1	113.2	125.3	133.6	42.7	59.6	83.5	106.8
18.0	107.4	141.2	155.3	165.5	53.3	74.5	104.2	132.9
20.0	130.0	167.8	184.6	196.4	65.7	90.6	125.4	158.8
22.0	153.5	194.2	214.1	227.8	79.4	107.4	146.6	183.1
24.0	177.0	224.1	245.8	260.8	94.3	125.2	169.8	210.0
26.0	201.7	254.8	277.7	293.1	109.9	143.7	192.4	235.0
28.0	225.8	282.2	306.9	323.1	125.8	161.5	213.2	259.3
30.0	250.0	311.0	337.2	354.4	141.7	179.2	236.5	283.8
32.0	275.1	336.4	364.2	381.5	157.6	197.3	256.7	304.8
34.0	297.0	362.9	392.3	411.4	173.3	214.2	276.3	328.1
36.0	318.8	385.9	416.9	436.6	188.9	231.8	295.6	352.1
38.0	341.3	410.6	441.2	460.0	204.3	248.8	314.6	370.3
40.0	360.7	431.8	464.4	483.8	219.1	264.9	331.5	393.8
42.0	379.2	452.8	486.3	505.7	233.4	281.1	347.8	408.0
44.0	396.6	471.4	506.2	526.2	247.1	295.8	363.1	426.8
46.0	412.4	490.4	524.9	544.7	259.8	309.8	379.5	441.8
48.0	427.6	506.3	541.8	562.3	272.2	323.1	393.5	459.9
50.0	441.8	521.6	557.7	578.3	283.7	335.3	406.4	474.8
52.0	455.1	536.0	572.7	593.9	294.7	347.6	418.3	490.3
54.0	466.1	548.0	586.3	607.9	305.0	358.8	430.4	502.7
56.0	477.3	560.7	599.2	620.9	314.5	368.8	440.9	513.0
58.0	488.2	571.6	610.7	632.9	323.4	379.8	449.6	527.1
60.0	496.8	581.2	621.5	644.3	331.8	388.6	460.8	539.1
62.0	507.6	592.2	631.9	654.7	339.8	396.9	469.0	548.2
64.0	516.2	600.5	641.3	664.6	347.2	404.6	477.3	555.8
66.0	526.1	610.8	650.6	673.5	354.0	413.0	485.6	568.3
68.0	530.7	616.2	658.2	682.0	360.1	420.3	491.7	575.2
70.0	538.8	625.0	666.6	690.4	366.1	426.0	498.2	584.5
72.0	546.2	633.2	674.5	698.2	371.6	432.0	504.7	590.4
74.0	551.0	637.9	680.9	705.0	376.7	438.2	511.0	599.0
76.0	558.2	645.7	687.5	711.3	381.5	443.4	516.0	603.5
78.0	565.2	652.3	692.6	716.5	385.8	447.5	521.8	606.2
80.0	569.1	653.4	696.3	720.3	388.6	448.9	519.5	609.0

Table A2.8. Test 7 - Thermocouple Readings (TC41-TC48)

Time (min)	TC41	TC42	TC43	TC44	TC45	TC346	TC47	TC48
0.0	21.7	21.8	21.7	21.7	21.7	21.7	21.7	21.7
2.0	21.7	21.9	21.8	21.9	21.6	21.7	21.8	21.8
4.0	22.5	23.3	23.6	23.9	21.7	21.9	22.5	23.1
6.0	24.6	26.8	27.9	28.7	22.0	22.9	24.6	26.5
8.0	29.4	34.6	37.0	39.0	22.9	25.3	29.2	33.9
10.0	37.7	46.9	51.2	54.5	24.9	29.7	37.5	44.8
12.0	50.2	64.8	71.7	76.8	28.6	36.7	49.5	61.9
14.0	66.8	88.2	97.8	104.8	34.5	46.9	65.7	82.5
16.0	86.1	113.2	125.3	133.6	42.7	59.6	83.5	106.8
18.0	107.4	141.2	155.3	165.5	53.3	74.5	104.2	132.9
20.0	130.0	167.8	184.6	196.4	65.7	90.6	125.4	158.8
22.0	153.5	194.2	214.1	227.8	79.4	107.4	146.6	183.1
24.0	177.0	224.1	245.8	260.8	94.3	125.2	169.8	210.0
26.0	201.7	254.8	277.7	293.1	109.9	143.7	192.4	235.0
28.0	225.8	282.2	306.9	323.1	125.8	161.5	213.2	259.3
30.0	250.0	311.0	337.2	354.4	141.7	179.2	236.5	283.8
32.0	275.1	336.4	364.2	381.5	157.6	197.3	256.7	304.8
34.0	297.0	362.9	392.3	411.4	173.3	214.2	276.3	328.1
36.0	318.8	385.9	416.9	436.6	188.9	231.8	295.6	352.1
38.0	341.3	410.6	441.2	460.0	204.3	248.8	314.6	370.3
40.0	360.7	431.8	464.4	483.8	219.1	264.9	331.5	393.8
42.0	379.2	452.8	486.3	505.7	233.4	281.1	347.8	408.0
44.0	396.6	471.4	506.2	526.2	247.1	295.8	363.1	426.8
46.0	412.4	490.4	524.9	544.7	259.8	309.8	379.5	441.8
48.0	427.6	506.3	541.8	562.3	272.2	323.1	393.5	459.9
50.0	441.8	521.6	557.7	578.3	283.7	335.3	406.4	474.8
52.0	455.1	536.0	572.7	593.9	294.7	347.6	418.3	490.3
54.0	466.1	548.0	586.3	607.9	305.0	358.8	430.4	502.7
56.0	477.3	560.7	599.2	620.9	314.5	368.8	440.9	513.0
58.0	488.2	571.6	610.7	632.9	323.4	379.8	449.6	527.1
60.0	496.8	581.2	621.5	644.3	331.8	388.6	460.8	539.1
62.0	507.6	592.2	631.9	654.7	339.8	396.9	469.0	548.2
64.0	516.2	600.5	641.3	664.6	347.2	404.6	477.3	555.8
66.0	526.1	610.8	650.6	673.5	354.0	413.0	485.6	568.3
68.0	530.7	616.2	658.2	682.0	360.1	420.3	491.7	575.2
70.0	538.8	625.0	666.6	690.4	366.1	426.0	498.2	584.5
72.0	546.2	633.2	674.5	698.2	371.6	432.0	504.7	590.4
74.0	551.0	637.9	680.9	705.0	376.7	438.2	511.0	599.0
76.0	558.2	645.7	687.5	711.3	381.5	443.4	516.0	603.5
78.0	565.2	652.3	692.6	716.5	385.8	447.5	521.8	606.2
80.0	569.1	653.4	696.3	720.3	388.6	448.9	519.5	609.0